21117

NATIONAL LIBRARY
OTTAWA

BIBLIOTHÈQUE NATIONALE
OTTAWA

CANADA

NAME OF AUTHOR WILLIAM PATRICK STEWART

TITLE OF THESIS STABILITY OF THREE ROCK SLOPES

UNIVERSITY UNIVERSITY OF ALBERTA

DEGREE FOR WHICH THESIS WAS PRESENTED M.Sc

YEAR THIS DEGREE GRANTED 1974

Permission is hereby granted to THE NATIONAL LIBRARY OF CANADA to microfilm this thesis and to lend or sell copies of the film.

The author reserves other publication rights, and neither the thesis nor extensive extracts from it may be printed or otherwise reproduced without the author's written permission.

(Signed) W.P. Stewart

PERMANENT ADDRESS:

Dept. of Civil Engineering,
The University of Alberta,
Edmonton, Alta T6G 2G7

DATED April 22 1974

NL-91 (10-68)

THE UNIVERSITY OF ALBERTA

STABILITY OF THREE ROCK SLOPES

by

Ⓒ WILLIAM PATRICK STEWART

A THESIS

SUBMITTED TO THE FACULTY OF GRADUATE STUDIES AND RESEARCH
IN PARTIAL FULFILMENT OF THE REQUIREMENTS FOR THE DEGREE
OF MASTER OF SCIENCE

DEPARTMENT OF CIVIL ENGINEERING

EDMONTON, ALBERTA
SPRING, 1974

THE UNIVERSITY OF ALBERTA

FACULTY OF GRADUATE STUDIES AND RESEARCH

The undersigned certify that they have read, and recommend to the Faculty of Graduate Studies and Research, for acceptance, a thesis entitled STABILITY OF THREE ROCK SLOPES submitted by William Patrick Stewart in partial fulfilment of the requirements for the degree of Master of Science in Civil Engineering.

....
Z. Eisenstein, Supervisor

N. Morgenstern
....
N. R. Morgenstern

....
D. M. Cruden

T. Patching
....
T. H. Patching

Date: April 17, 1974

ABSTRACT

Rock slope stability is a complex problem that is becoming more important as ever higher slopes are being planned. A considerable amount of theoretical work on the topic has been published and a literature review of that work is presented. To gain confidence in the application of the theoretical models to design, case histories are required to confirm the assumptions of the models. The purpose of this thesis is to present in detail three case histories of failures of rock slopes.

The small slides studied were chosen for their simplicity. In two of the cases the failure surface was fully exposed and accessible for measurement and observation.

Details of sampling procedures, sample preparation, and direct shear testing to obtain strength parameters are given. It was found that repeated testing on a single sample and testing of small samples gave consistent, reasonable results so that a large number of tests were conducted on a relatively small amount of sample. It was found also that the test results could be interpreted equally well by a straight line or a power law strength envelope.

As in many case histories in soil mechanics, all of the details of the failures were not known and some assumptions had to be made. One of the case histories had a calculated factor of safety of about 0.9. This value is felt to be reasonably close to the anticipated value of unity, and would indicate that the methods followed and the assumptions made in this case history were reasonable. In particular it indicates that the maximum shear strengths measured in direct shear testing governs the field behaviour, at least at low normal stresses.

The other case histories had calculated factors of safety of about 0.5. It is felt that the pre-failure geometry was probably more complex than had been assumed for these cases. These case histories indicate that back-analyses of slides to obtain strength parameters, in which all of the failure details are not known, may lead to an estimate of strength parameters on the unsafe side.

ACKNOWLEDGEMENTS

The author of this thesis is grateful to Dr. Z. Eisenstein under whose supervision the research for this thesis was conducted. His topic suggestion and continued encouragement were appreciated.

The author is also indebted to Dr. N. R. Morgenstern and Dr. D. M. Cruden for their helpful discussions on various aspects of the thesis.

Appreciation is extended to the technicians and machinists of the Department of Civil Engineering and the Department of Technical Services for their expert assistance and to the keypunch operators of the Department of Computing Services for their assistance in coding and typing this thesis.

The financial assistance provided by the Department of Energy, Mines, and Resources for the research work and the financial support given by the National Research Council of Canada are gratefully acknowledged.

Finally, the author wishes to acknowledge, with many thanks, the continual encouragement, support and editorial assistance given by his wife, Barbara, and the tolerance and acceptance displayed by his daughters.

TABLE OF CONTENTS

Page

Release Form (i)

Title Page (ii)

Approval Sheet (iii)

Abstract (iv)

Acknowledgements (vi)

Table of Contents (vii)

List of Tables (ix)

List of Figures (x)

CHAPTER 1 INTRODUCTION 1

CHAPTER 2 GENERAL CONSIDERATIONS IN ROCK SLOPE STABILITY

2.1 Introduction 3

2.2 Geological factors affecting rock slope stability 5

2.3 Strength of joints 14

2.4 Modes of failure 22

2.5 Methods of analysis of sliding failure 23

2.6 Summary 33

CHAPTER 3 CASE HISTORIES

3.1 Introduction 34

3.2 Brenda Mines case histories 35
3.3 Endako Mines case history 45

CHAPTER 4 SAMPLING AND TESTING

4.1 Sampling of jointed hard rock 51
4.2 Sample preparation 58
4.3 Roughness measurement 60
4.4 Selection of testing apparatus 62
4.5 Selection of testing conditions 63
4.6 Shear testing apparatus 65
4.7 Interpretation of test results 67
4.8 Test results 77
4.9 Variations in results 78
4.10 Testing of large samples 82
4.11 Effect of molybdenite on strength 85
4.12 Joint roughness 87
4.13 Comparison of strengths with data from other sources 87

CHAPTER 5 ANALYSES OF CASE HISTORIES

5.1 General 94
5.2 Discussion 100
CHAPTER 6 SUMMARY 107
LIST OF REFERENCES 110
APPENDIX A SHEAR TEST RESULTS 117

LIST OF TABLES

Table	Description	Page
4.1	Roughness parameters and strengths	88

LIST OF FIGURES

Figure		Page
2.1	Toppling failure, example and conditions of occurence (after de Freitas and Watters, 1973)	24
2.2	Two-dimensional analysis of sliding block (after Jaeger, 1971)	29
2.3	Three-dimensional analysis of sliding wedge (after Jaeger, 1971)	31
3.1	Map of open-pit at Brenda Mines Ltd.	36
3.2	General view of North wall, Brenda Mines Ltd. Slides are between second and third bench above drill rig	38
3.3	Photographs of slide No. 1 at Brenda Mines Ltd.	40
3.4	Geometry of slide No. 1 at Brenda Mines Ltd.	41
3.5	Photographs of slide No. 2 at Brenda Mines Ltd.	42
3.6	Geometry of slide No. 2 at Brenda Mines Ltd.	43
3.7	Map of open-pit at Endako Mines Ltd.	46
3.8	Photograph of slide at Endako Mines Ltd.	47
3.9	Contour map with idealized model of slide at Endako Mines Ltd.	48
3.10	Geometry of slide at Endako Mines Ltd.	49
4.1	Photograph of drilling unit used	53
4.2	Example of core obtained from drilling	56
4.3	Mercury lapidary saw used for cutting samples	59

4.4 Typical roughness plot obtained with roughness measuring device (at true scale) 61

4.5 Shear testing apparatus 66

4.6 Effects of machine friction not directly accounted for in data analysis 68

4.7 Examples of applying geometric correction to test results 71

4.8 Stick-slip in direct shear test (after Coulson, 1970) 73

4.9 Repeatibility of test results on a single sample 76

4.10 Maximum strength envelopes for samples cut from BB14, molybdenite joint from Brenda Mines Ltd. 79

4.11 Maximum strength envelopes for samples cut from BB10, calcite joint from Brenda Mines Ltd. 80

4.12 Maximum strength envelopes for samples cut from EC12, molybdenite joint from Endako Mines Ltd. 81

4.13 Comparison of strength of large molybdenite sample with strength envelopes of smaller samples 83

4.14 Comparison of strength of large calcite sample with strength envelopes of smaller samples 84

4.15 Effect of molybdenite on strength 86

4.16 Roughness plots for Brenda molybdenite samples 89

4.17 Roughness plots for Brenda calcite samples 90

4.18 Roughness plots for Endako molybdenite sample 91

5.1 Equivalent friction angles for analyses of slides 98

5.2 Possible failure conditions in rock slope with computed factor of safety less than unity 101

CHAPTER 1

INTRODUCTION

The stability of natural and cut rock slopes is one of the major problems facing engineers on many mining and construction sites. Loss of life, damage to property and severe financial consequences can result from slope failures, especially with the increasing size of excavated slopes being constructed or planned for the immediate future. Considerable research effort has been applied to the problem of rock slope stability in recent years, and the importance of rock mechanics has been recognized by professional societies throughout the world.

Patton (1966a) indicated that research on rock slope stability has frequently increased after large slides have occured that involved the loss of lives. The disastrous Vaiont slide of 1963 certainly indicated a real need for investigations into all aspects of rock slope stability. Moreover the present research effort will likely be sustained by the added incentive of economics. Development of large equipment is allowing the construction of large-scale open pit mines. Brawner (1971a) indicated open pits are being planned up to 3000 feet deep. With such deep pits, excess excavation costs can be as high as 5 to 15 million dollars per degree of slope.

Much of the recent work that has been published deals primarily with theoretical models. However to have confidence in these theories and their application to real rock slopes, case histories using the theories must be undertaken. Brawner (1971a) stated the situation clearly. "We are desperately in need of case studies and analysis of field failures to test theoretical concepts. Only then will real practical progress be made."

The purpose of this thesis is to attempt to make a contribution to filling this need. Chapter 2 presents a literature review of rock slope stability. The geological settings and geometries of three small slides are given in Chapter 3. Chapter 4 describes the sampling and testing procedures followed to obtain strength parameters for the materials involved in the slides. Analysis of the slides and discussion of the results are given in Chapter 5 and a summary of the thesis is presented in Chapter 6.

CHAPTER 2

GENERAL CONSIDERATIONS IN ROCK SLOPE STABILITY

2.1 Introduction

Slope stability considerations in hard rock first became common in the engineering literature during the early part of the 1960's. Terzaghi (1962) calculated the theoretical critical height of a vertical slope of solid rock to be in the order of 4200 feet. Since such heights are not common in nature it must be inferred that discontinuities control the stability of most rock slopes. Terzaghi mentioned most of the other factors that are important in rock slope stability, i.e. geometry of discontinuities, groundwater pressures, continuity of joints, time effects, and stresses due to excess relief. He did not mention seismic effects or residual stresses and considered strength as purely frictional (except for lack of continuity of joints). (Although the term joint does have a specific meaning in geolgy, it is commonly used to refer to all types of discontinuities in rock in the rock mechanics litreature. Herein joint will be used interchangeably with discontinuity).

About the same time John (1962) introduced the work done in rock mechanics in Central Europe to the English literature. He defined rock mechanics to be, "a mechanics of a discontinuum, that is, a jointed medium," and defined several basic terms such as rock mass, degree of jointing, and extent of joint. He also listed the important engineering features of a rock mass as: "(1) homogeneous zones, (2) rock type, (3) geological separations, (4) orientation of geological planes, (5) width of separations (aperture) (6) joint surfaces, (7) joint fillings, (8) distribution and extent of joints and sets of joints, and (9) water conditions." He recommended that joint orientation be analyzed on an equal-area plot and presented a method of classification for rock based on the compressive strength of the rock substance and the spacing of joints. In their discussion of John's paper Bjerrum and Jorstad (1963) felt "it is most unlikely that it will ever be possible to obtain reliable determinations of the data required for a theoretical calculation," primarily because of the time effects, such as a seasonally fluctuating water table that could lead to irreversible deformations by extension of fractures. Time effects would not appear to be a dominant feature in cut slopes. Open-pit mine slopes are only designed for relatively short life spans. Long-term cut slopes, such as around permenant structures, are designed with a higher factor of safety. Time effect failures are unlikely at the lower stress levels in a slope with a high factor of safety. The abundant work, both in practical design and theoretical research, that has been done recently, indicates a more optimistic view of slope design.

2.2 Geological factors affecting rock slope stability

Geometry of discontinuities

Probably the most important aspect of the discontinuities in a rock mass are their orientation and position in relation to a slope. All discontinuities within a rock mass cannot be measured, therefore extrapolation of measured data is necessary. Measurement of joint orientations can be done most easily in outcrops, excavations or adits. Details of line survey techniques are given by Piteau (1970). For design of new slopes, or for sampling within a slope, borehole techniques are used. To maximize core recovery, triple-wall core barrels are preferred to single- or double-wall barrels. Core recovered from a borehole, and oriented by paint dribbles in an inclined hole or by devices such as the Craelius instrument (Bridges and Best,1971), can be used for fracture measurements. Alternatively, or preferably in conjunction with oriented core, the borehole can be used for joint measurements. Downhole cameras (John, 1958) and borehole periscopes (Trainer and Eddy, 1964) have been used for direct observations while acoustic logging tools have been develcped (Myung and Baltosser, 1972) for indirect measurement. Sampling along a line produces a bias in the data which must be corrected (Terzaghi, 1965). On large projects the amount of data collected in a comprehensive survey can be very large. To handle the data, computer methods have been devised (Robertson, 1970). Most writers indicate that the majority of joints occur in sets in which the joints are sub-parallel. The computer programs can sort data to determine significant patterns. On projects covering large areas there may be variations of the jointing pattern over the area studied. Piteau and Russell (1972) have indicated that a cumulative sums technique is useful for detecting these changes.

Spacing of joints (degree of jointing, intensity) can be important in relation to the size of the cut to be made. Most writers use an average spacing, but Snow (1968,1970), using water loss measurements in packed boreholes, indicated that spacing is skewed, approximately following a Poisson distribution. The sheeting joints formed roughly parallel with the surface of igneous rocks have been found to increase in spacing with depth from the surface (Bjerrum and Jorstad, 1963).

Continuity

If a joint does not form a continuous failure surface through a slope, failure must occur through portions of intact rock. Since joints are inherently much weaker than intact hard rock, discontinuous failure surfaces are much stronger than continuous ones. Continuity is probably the most difficult property of a joint to determine. An indication of continuity can be gained from measurements in adits. Robertson (1970) indicates average joint lengths in homogeneous igneous rocks is in the order of one to six feet, but does not indicate the length of the gaps between joints.

The slides that were considered in this study showed that joint surfaces were continuous over at least a full bench height (about 50 feet). The ores present on joint surfaces were deposited by hydrothermal deposition (Kimura and Drummond, 1969), suggesting that there is some interconnection of joints to considerable depth. Very few cases of design of actual slopes in hard rock are reported in the literature, and the few cases that are reported (eg. Wallace et al, 1969) make no mention of the effects of lack of continuity along the joints. Either the effect is assumed not to be present, i.e. the joints are continuous, or the design is conservative.

Groundwater

Groundwater can exist in three basically different situations in jointed rock masses. The water can be present in voids in the rock substance, in voids in joint fillings, and in open joints (Mueller, 1963). Wittke (1970) reported that work by Louis showed that the permeabiltiy coefficient of intact rock was in the order of 10^{-8} to 10^{-13} cm/s (centimeters per second) and that of jointed rock with one set of plane parallel joints, having openings of 0.1 to 0.6 mm and approximately 1m spacing was in the order of 10^{-4} to 10^{-1} cm/s. Therefore the rock substance can be considered essentially impermeable, and the effects of groundwater in the voids in the rock substance can be considered negligible. Water in the voids in joint fillings can affect the properties of the fillings. These effects can be considered by soil mechanics techniques. However it is the water in open joints that can have the greatest effect on slope stability.

In theory groundwater can affect slope stability in several ways. It could reduce the strength characteristics of the material of the joints, reduce normal stresses across joints, create additional forces on the mass by filling tension cracks, and create seepage forces on the mass. Horn and Deere (1962) found that frictional characteristics of very smooth mineral surfaces were affected considerably by the presence of water, but Coulson (1972) found that for rock surfaces, (as opposed to pure mineral surfaces) coefficients of friction for wet and dry surfaces normally differed by 10% or less, even for surfaces ground with #600 grit. Most natural joint surfaces are rougher than this, so that the effect of water on coefficients of friction should be negligible. Mueller (1963) indicated that seepage forces are relatively unimportant in rock slope stability. Therefore the main effects of groundwater on stability, are the reduction of normal stress (effective stress) and the creation of additional lateral forces on the mass. It must be remembered, however, that these effects are a result of the pressure in the water, not the quantity of flow of water. Flow may be so little that water disappears from the surface by evaporation and gives a false impression that water would not be important in the slope.

It is generally agreed in the literature that a purely theoretical approach to groundwater studies is problematic due to the difficulty of measuring field permeabilities of a jointed rock mass. The general approach has been to measure water pressures within a slope with piezometers and interpolate between the points of measured pressure with an anisotropic theoretical solution fitted to the field measurements (Lyell, 1970). Lyell gave details of installation and testing of porous tip piezometers. Other types of piezometers, such as air, transducer, and vibrating wire types can also be used. The positioning of piezometers depends on geological and groundwater conditions of the area, as well as the position of potential failure zones. This method is mainly applicable to existing slopes. For application to design of slopes, permeability must be measured more directly. Several authors (e.g. Maini et al., 1972) have used flow-rates from pressurized, packer-isolated sections of boreholes to estimate permeability of jointed rock, but interpretation of results is difficult. Morgenstern (1971) listed some of the factors giving rise to problems in the determination of field permeability.

Perched water tables can be encountered in layered sequences or beneath impermeable discontinuities. Those can be accounted for in more complete theoretical models (Lyell, 1970). The permeability of zones of rock may increase due to the opening of joints when the rock mass is unloaded because of the cutting of a slope (Terzaghi, 1962). Bjerrum and Jorstad (1963) indicated that failures are most prevalent during periods of high infiltration, i.e. during periods of snow melt and also periods of high rainfall. In addition, freezing of the slope surface can cause excessive water pressure build-up within a slope. Because of the problems of predicting water pressures in a slope, piezometers should always be installed in a slope to monitor water pressures if it is felt that water pressures might be important.

If groundwater pressures are a factor in the stability of a slope, drainage can improve the stability. A possible additional benefit in blasted slopes is the reduction in the number of wet holes which require more expensive explosives. Several methods of drainage are available. Hoek and Sharp (1970) listed these as:

"(1) Vertical boreholes with pumps
(2) Drainage galleries behind the slope, with or without supplementary boreholes drilled from the gallery, and
(3) Horizontal or near horizontal boreholes drilled from the slope face."

The optimum location and size of drainage galleries has been investigated by Sharp (1970). Brawner and Huculak (1961) provided details of the use of horizontal drains. Hoek and Sharp (1970) also emphasized the importance of control of surface water, to prevent its flow into vertical cracks and joints, which would otherwise create horizontal loads on possible failure blocks.

Time effects

The "time effect" is the reduction of the factor of safety of a slope over time due to gradual deterioration of the slope materials and adjustments towards equilibrium of stresses induced by unloading of the slope. The existence of the time effect was shown in the studies of Bjerrum and Jorstad. However two aspects are most important: (1) the length of time involved, and (2) magnitude of stresses in relation to failure stresses. The failures studied by Bjerrum and Jorstad were on slopes formed by glacial ice, thousands of years ago. It is not reasonable to design slopes on the basis of strength that might exist thousands of years in the future. Secondly, fatigue failures, creep and internal stress readjustments are important only at near failure conditions, and long-term slopes in strategic locations are usually designed with a higher factor of safety, reducing the possibility of time effect failures.

Other factors

Residual stresses are generally felt to be unimportant in slope failures as horizontal stresses are almost totally relieved by relaxation resulting from the slight opening of joints caused by unloading of the slope (Hoek, 1971c). It has been suggested that a quasi-tectonic stress can occur due to the presence of mountains around a pit (Kim and Dimock, 1972), but it is not clear that the effect of this stress differs from an actual tectonic stress. Slope geometry has an obvious effect on stability. A slope concave in plan gives increased lateral constraint, increasing the stability of the slope. Piteau and Jennings (1970) showed that the 'big holes' of Kimberly could sustain higher slope angles if the radius of curvature was smaller. Conversely a convex surface reduces lateral constraint leading to instability. Brawner (1971b) gave details of a slope failure of a promontory that projected out of the slope of an open pit mine. Blasting to create a slope can have two detrimental effects; the increased fracturing of rock, and dynamic effects. Control blasting can reduce the fracturing of final slopes. Bauer and Calder (1971) indicated three methods that can be used; cushion blasting, pre-shearing, and buffer blasting. Pre-shearing the slope is the most expensive but also gives the most satisfactory slope. An important advantage of control blasting is the reduction of costs due to less excavation by the elimination of overbreak. Dynamic effects include the acceleration of the rock mass and high joint air or water pressures. Dynamic effects can be considered in an analysis by statical methods by adding horizontal acceleration forces and possibly pressure increases or by dynamic methods in a finite element analysis (at least in principle) provided the data required is available. Seed et al (1969) indicated the nature of bedrock motions and gave a reference list of applications of dynamic methods in soil.

2.3 Strength of joints

As was indicated in the introduction to this chapter, the stability of most rock slopes is dominated by the joints within the slope. Therefore the strength of the joints are an essential factor in any rational analysis of rock slopes. Natural rock joints can be of various materials, can have several orders of roughness, can have bridges which contain solid rock, and may be infilled with foreign or weathered material. All of these factors cause variations in the strength of joints.

Infillings of gouge and clay can be treated with the methods of soil mechanics. For reasonably rapid rates of failure these materials will be undrained because of their low permeability and their strength can be considered purely cohesive. However model tests reported by Goodman (1970) indicate that thinner layers of infilling, even if they fill a joint completely, may be affected in their strength by the presence of the solid material of the walls of the joint. It is therefore desirable to test such joint materials within a sample containing the joint walls.

In theory at least rock bridges in a joint can increase the strength of a joint considerably. This effect can be treated simply as an effective cohesion as done by Terzaghi (1962) or more completely as a tension-shear phenomena as done by Latjai (1969). However as mentioned in the section on continuity, continuity effects are usually ignored in most cases of design and in the small slides studied by the author there was no evidence of rock bridges, so this effect will not be discussed further.

Flat surfaces

Friction of flat surfaces is usually considered to follow Amonton's law that the shear strength is proportional to normal load. This can be explained for materials having a limited area of contact and plastic behaviour as follows (Jaeger, 1971). If σ_n =normal stress, τ =shear stress, Y=yield strength of material, S=shear strength of material, and Ac=actual area of contact per unit macroscopic area, then

$$\sigma_n = Y\,Ac$$

$$\tau = S\,Ac$$

and therefore $\tau = S\,(\sigma_n/Y) = (S/Y)\sigma_n = k\sigma_n$ where k = constant. This value of $k = \tau/\sigma_n$ constant is called the coefficient of friction and is usually denoted by μ . When the law is applied to experimental data, one usually finds that the best-fit straight line does not pass through the origin but gives an intercept, usually called cohesion (c). This gives rise to the Coulomb failure criterion, $\tau = c + \mu\sigma_n$.

However if the contact points are elastic and brittle, total contact area is no longer proportional to normal force

N, but becomes proportional to $N^{2/3}$ (Coulson, 1972). Coulson reported that Seal found the shear strength of polished diamond to vary as $N^{0.8}$, perhaps indicating partially elastic behaviour.

The coefficient of friction will, of course, vary with material type. Horn and Deere (1962) published friction coefficients of smooth surfaces of pure minerals, but rocks are usually a combination of minerals, so that each type of rock must be tested to determine its shear strength. Horn and Deere and others have found that the presence of water can affect the frictional characteristics of highly polished or cleavage plane surfaces. On these smooth surfaces water generally behaves as an antilubricant on massively structured minerals, and as a lubricant on layered minerals. However these effects decrease with increasing surface roughness. Coulson (1972) gives an average roughness of 70 micro-inches as the approximate upper limit for the water effect, this being the average value of roughness of hard rocks lapped with #600 silicon carbide grit. The roughness of natural joints, unless slicken-sides have been formed on them by movement, will generally greatly exceed this value.

Flat surfaces generally have a lower coefficient of friction when moving (dynamic) than when still (static). This is usually attributed to the time-dependent growth of bonds at points of contact. This difference can give rise to the 'stick-slip' phenomenon during shear testing. The phenomenon can be easily explained by frictional mass-spring models (e.g. Jaeger, 1971).

Considerable work has been devoted to measuring the basic coefficient of friction of flat surfaces of rock. Coulson (1970) concluded that angles of sliding friction varied from 14° to 40°, with the bulk of his tests falling in the range from 26° to 36°, for a wide range of rock types. Highest friction angles were observed on limestones and lowest values were measured on schistose gneiss. Krahn (1974) found values for limestone of about 37°. In addition no surface is perfectly flat, so the roughness differences on a small scale can affect measured strengths. Coulson suggested measurement of a maximum angle on a surface profile as an indication of strength to be expected. Krahn developed several roughness parameters in his study. These are (values of elevation, y, measured at equal intervals, dx)

(1) centre-line average: $\mathrm{CLA} = \frac{1}{N} \sum_{i=1}^{N} |y|$

(2) root mean square: $\mathrm{RMS} = \left[\frac{1}{N} \sum_{i=1}^{N} y^2 \right]^{1/2}$

$$(3)\quad Z_2 = \left[\frac{1}{N} \sum_{i=1}^{N} (dy/dx)^2 \right]^{1/2}$$

$$(4)\quad Z_3 = \left[\frac{1}{N} \sum_{i=1}^{N} (d^2y/dx^2)^2 \right]^{1/2}$$

Roughness parameters (1) and (2) are essentially the same, measuring the average deviation in elevation from a mean plane. Z_2 is a measure of the average slope of the surface and Z_3 is a measure of the roundness of peaks and valleys in the profile. Krahn found the best correlation of strengths with the Z_2 parameter. Coulson found that the maximum i angle measured was never fully developed, suggesting that shearing of asperities occurred even at low normal loads (see next section).

Surface irregularities

If surface irregularities exist along a joint then extra work must be done to lift the upper block of material over the irregularities or to shear through the irregularities (the term asperities is commonly used interchangeably with irregularities). Patton (1966a,b) showed that for regularly spaced, equal sized asperities a bilinear envelope of strength is developed both theoretically and experimentally. At low stresses the angle of inclination (i) can be added directly to the angle of friction ($\phi = \tan^{-1}\mu$), as the upper block rides up the asperities. At higher stresses the asperities are sheared off, giving rise to an effective cohesion intercept. The model can be summarized as:

(1) $\tau = \sigma_n \tan(\phi + i)$, at low stresses
(2) $\tau = c + \sigma_n \tan(\phi)$, at high stresses

The transition point is governed by the friction characteristics of the joint, the geometry of the irregularities, and the strength of the material. However in natural joints the asperities are irregular in geometry at least, and thus change failure mode at different stress levels, giving rise to continuously curved failure envelopes. Such curved envelopes can be expressed as a power law of the form: $\tau = k\sigma_n^m$

Ladanyi and Archambault (1969) developed a more complete theory of joint strength to account for variations in asperities. At low stresses, with no shearing of asperities the total shear force, s, is given by

$s = s^1 + s^2 + s^3$

where s^1= component due to external work done against external force, N

s^2= component due to additional internal work due to dilatancy

s^3= component due to friction if no dilatancy.

and $s^1 = N(dy/dx) = N\dot{v}$

where dy/dx=rate of dilation (= tan i for regular teeth)

and $s^2 = s\,\dot{v}\tan\phi^1$ (due to component of s normal to irregularities)

where ϕ^1= average value of friction mobilized along asperities.

and $s^3 = N\tan\phi$ (for flat surfaces)

A fourth component is introduced by shearing of the aperities:

$$s^4 = As^0 + N\tan\phi^0$$

Along an irregular shear surface, both modes occur simultaneously. If a= portion of area over which shearing of asperities occurs, then:

$$s = (s^1+s^2+s^3)(1-a) + s^4 a$$

and thus the shearing strength, τ, is given by:

$$\tau = \frac{S}{A} = \frac{\sigma(1-a)(\dot{v}+\tan\phi)+a(\sigma_n\tan\phi^0+S^0)}{1-(1-a)\dot{v}\tan\phi^1}$$

However this expression contains several parameters which must be separated and determined individually, and for natural joints with infillings over portions of the surface, it is impossible to accurately measure values of each component separately. Empirical curve-fitting, with due regard for theoretical considerations, is a more practical approach to failure envelopes. Jaeger (1971), for example, suggests a law of the form:

$$\tau = a\{ 1-e^{-\beta\sigma_n}\} + \sigma_n \tan\phi$$

This expression avoids the vertical tangent at the origin as in a power-law and the sharp break in the bilinear strength envelope.

The form of the strength law used in an analysis can affect the results of the analysis. Jaeger (1971) gives several examples for a sliding block type of analysis. Seegmiller (1972) did not give details of how he obtained constants for a power curve strength law for his study, but gave factors of safety of 0.79 to 0.98 for the failures he investigated using a power law. These results give a more satisfactory account of the slides than the c, parameters he fitted to test results, which indicated factors of safety of about 7 (Krahn,1974). Seegmiller indicated that the linear approach was mathematically simpler. However the methods of analysis given by Jaeger (1971) show either strength law to be equally straightforward to apply (see Section 2.5) Pentz (1971) strongly suggested that a non-linear (power curve) law is preferable for rock slope stability studies.

Several authors have proposed that measured laboratory strength values be reduced by the measured laboratory geometric component, then increased by a measured field geometric component. Coulson (1970) suggested a measured instantaneous i correction (where $i = \tan^{-1}(dy/dx)$). Krahn (1974) suggested comparing forward and reverse friction angles, the difference being equal to 2i. However two difficulties arise in applying this field geometric component. The main problem is in obtaining representative field roughness values, due to a lack of adequate exposures (Krahn, 1974). Secondly there is the problem of the order of roughness. Patton (1966a,b) considered two orders of roughness (approximately feet and inches) and concluded from his study that only first-order roughness can be considered as a valid component of strength. In his study of the Frank Slide, Krahn concluded that no geometric field component was acting.

2.4 Modes of failure

The presence of joints within a rock mass allow the possibilities of many modes of failures of rock slopes. The two basic modes are toppling (or overturning) and sliding. De Freitas and Watters (1973) indicate the conditions for the modes to occur.

For regular rock blocks of base width, b, and height, h, and frictional strength ϕ, inclined at a dip α, four conditions exist (see Fig.2.1):

"(1) complete stability, when $b/h > \tan\alpha$ and $\alpha < \phi$

(2) toppling only when $b/h < \tan\alpha$ and $\alpha < \phi$

(3) sliding only when $b/h > \tan\alpha$ and $\alpha > \phi$

(4) sliding and/or toppling when $b/h < \tan\alpha$ and $\alpha > \phi$"

The toppling mode of failure can be important and can involve large areas and volumes of material (up to 180 x 10^7 cubic yards in one example given by de Freitas and Watters). However most of the slides recorded in the literature appear to be sliding failures and methods of avalysis have been developed more extensively for this type of failure.

2.5 Methods of analysis of sliding failures

One of the basic propositions underlying the calculation of the stability of a rock slope is that a reliable model of the rock mass can be constructed (Piteau, 1970). Models can be of two types: (1) physical scale models, or (2) mathematical models.

Physical scale models can be most useful in illustrating the modes of failure that are possible, e.g. Mueller and Hoffman (1970). Details of materials that have been used in physical models are given by Stimpson (1970).

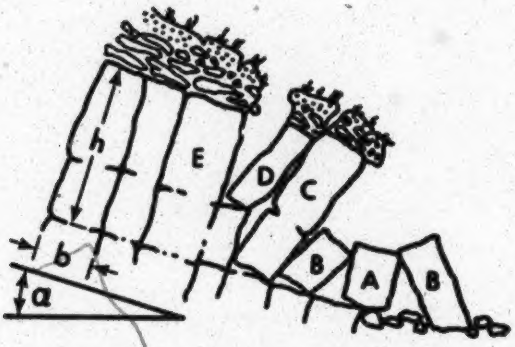

(a) Example of toppling failure. Block A is removed by erosion, blocks B,C,and D topple but E remains because it is wider.

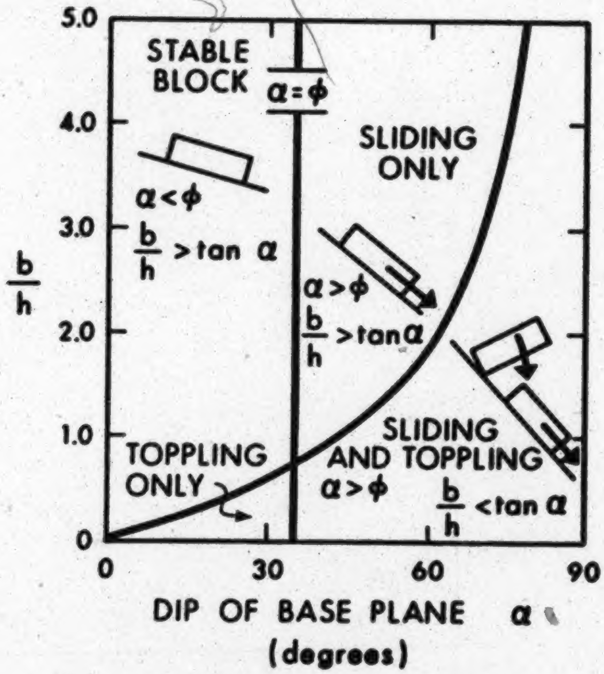

(b) Conditions for sliding and toppling, angle of friction = 35^0

Fig.2.1 Toppling failure, example and conditions of occurence (after de Freitas and Watters,1973)

However, as indicated by Pentz (1971), the building and testing of a scale model is both time consuming and costly, and thus parametric design studies on scale models are an unrealistic procedure.

Mathematical models, on the other hand, can be varied quickly and relatively inexpensively. Two basic approaches are possible: (1) stress analysis, and (2) limit equilibrium. Stress analysis of discontinuous media has only become a reasonable proposition since the introduction of the finite element method. Goodman et al (1968) developed a special one-dimensional joint element for two-dimensional analyses, and Mahtab (1970) extended this concept to three dimensions. However application of the method requires measurement of the joint stiffness. In testing of natural joints any previous movement or slight mis-matching of the sample pieces would introduce errors. Machine stiffness must also be accurately known to correct measured values. Barton (1972) indicated that both normal and shear stiffnesses varied with normal stress, so that an iterative analysis would be required, greatly increasing computing costs. Barton also indicated that "a fundamental requirement of the finite-element method is the conservation of energy....In reality energy is dissipated in friction and aspertity failure along the joints, and should therefore be 'dissipated' in the numerical analyses if they are to be realistic." However this requirement of conservation of energy is applicable only in elastic analyses. The problem can be overcome by formulating the equations governing the model to include energy dissipation. Elastic-plastic analysis is one such formulation, and it was used by Pariseau (1973) to study rock slope stability.

A greater difficulty in use of the finite-element method is the development of a suitable stability index (Pariseau, 1973). A local factor of safety can be found for an element, but is not as practical a stability index as a global factor of safety. Mathematically consistent global collapse criteria have not yet been developed. Pariseau developed the use of a random number generator to assign variable material properties to elements in an analysis, as opposed to assigning average material properties to all elements.

The method gives answers significantly different from limit equilibrium methods only in cases where the rock blocks are deformable to a significant degree (Heuze and Goodman, 1972). This condition would not apply in hard rock slopes.

Cundall (1971) devised a computer program on a 'finite difference' basis (i.e. forces and displacements imposed on blocks as opposed to stresses and strains in elements) to analyze jointed rock slopes. This program can accommodate sliding, toppling, and rotation of multiple discrete block models, and produces diagrams of block positions at given increments of time.

The limit equilibrium approach is generally felt to the most practical, reliable method of slope analysis (Pentz, 1971; Hoek, 1971d; Jaeger, 1971, etc.). The method makes two basic assumptions (after Pentz, 1971):

> "(1) that a failure surface can be postulated with a geometry that will allow sliding to take place - a kinematically possible surface, and
> (2) that the distribution of stresses in equilibrium along the potential failure surface can be computed utilizing a knowledge of density, water pressure, and seismic loading."

In jointed rock, failure is kinematically possible only if the joint or joint intersection daylights on the slope. In addition, for three-dimensional slides, the failure block must not have adjacent faces that are tapered, that is faces which tend to push out the remainder of the slope surface when the block moves out of the slope. For kinematically possible failure surfaces, the shearing resistance required to just prevent movement (at the point of limiting equilibrium) is computed. This computed value is then compared to the available shearing resistance (computed from the strength properties of the joints). The ratio of available shearing resistance to required shearing resistance is known as the Factor of Safety. The forces causing instability are self-weight, thrust of adjacent structures, seismic forces, and water forces. The simplest method of analysis arises when the joints strike parallel to the slope face. In this situation the slope failure can be analyzed as a two-dimensional problem. Jaeger (1971) defines the factor of safety (F) in terms of stresses i.e.

$$F = \frac{\sigma_n}{\tau} \mu^*$$

where τ(at failure) $= \mu^* \sigma_n$ and $\tau = \tau$(required in analysis). Jaeger terms μ^* the variable coefficient of friction. For a slope of inclination i, and height H, undercut by a joint of inclination α, and acted on by self-weight only, the factor of safety, F is given by (see Fig.2.2):

$$F = \mu^* \cot \alpha$$

For the Mohr-Coulomb failure law:

$$\tau = c + \sigma_n \tan \phi \text{ or } \mu^* = \tan \phi + c/\sigma_n$$

$$F = \tan \phi \cot \alpha + (2c \sin i)/(\gamma H \sin (i-\alpha) \sin \alpha)$$

For a power law failure criterion:

$$\tau = k \sigma_n^m \text{ or } \mu^* = k \sigma_n^{m-1}$$

$$F = k \{ 1/2 \gamma H \sin (i-\alpha) \cos \alpha \operatorname{cosec} i \}^{m-1} \cot \alpha$$

An analysis is complicated by introduction of tension cracks, water pressures, and seismic forces. Hoek (1970) presented design charts for analyses including tension cracks and water effects. These charts are for a Mohr-Coulomb failure criterion. Hoek (1971b) suggested these

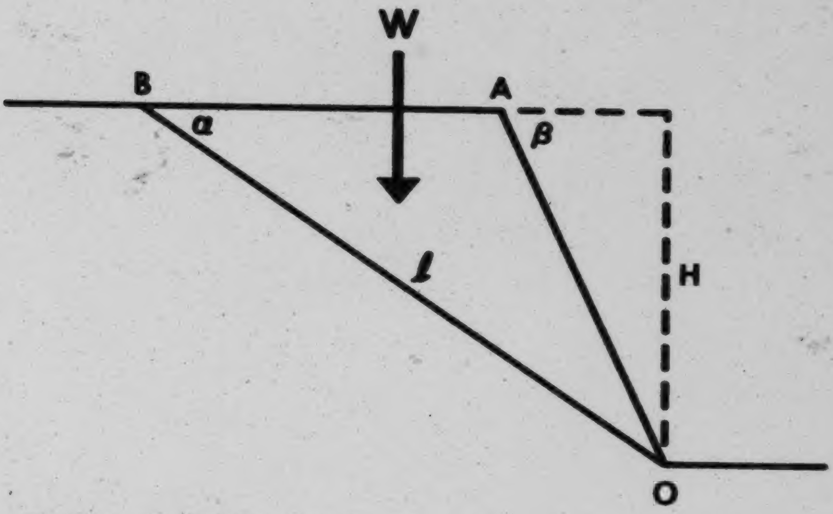

Weight of sliding block

$$W = 0.5\gamma H^2(\cot\alpha - \cot\beta) = 0.5\gamma H^2\sin(\beta - \alpha)\operatorname{cosec}\beta\operatorname{cosec}\alpha.$$

Length of failure surface

$$\iota = H\operatorname{cosec}\alpha.$$

Normal stress

$$\sigma_n = (W/\iota)\cos\alpha = 0.5\gamma H\sin(\beta - \alpha)\operatorname{cosec}\beta\cos\alpha.$$

Shear stress

$$\tau = (W/\iota)\sin\alpha.$$

Factor of safety: $F = (\sigma_n/\tau)\mu^* = \mu^*\cot\alpha.$

in which $\mu^* = (\tau/\sigma_n)$ at failure conditions.

Coulomb Law: $\mu^* = \mu + c/\sigma_n$

then $F = \mu\cot\alpha + (2c\ \sin\beta)/(\gamma H\sin(\beta - \alpha)\sin\alpha.$

Power Law: $\mu^* = k\sigma_n^{m-1}$

then $F = k(0.5\gamma H\sin(\beta - \alpha)\cos\alpha\operatorname{cosec}\beta)^{m-1}\cot\alpha.$

Fig.2.2 Two-dimensional analysis of sliding block (after Jaeger, 1971)

charts could be used for non-linear envelopes by approximating with a series of straight line envelopes. Jennings (1970) developed a theory for complex modes of failure involving different sets of joints and fracture through intact material. The theory requires knowledge of lengths and degrees of continuity of the joint sets, indeed the mode of failure would probably only occur with discontinuous joints. As mentioned previously, the effects of rock bridges across joints are not generally considered in design procedures of actual cases. Morgenstern and Price (1965) developed a computer method of analysis which can handle any shape of failure surface in two-dimensions with a Mohr-Coulomb strength envelope.

The simple two-dimensional failure with the joints striking parallel to the slope will be the exception rather than the rule. Generally the joints will strike at some angle to the slope face and failure will occur of wedges or blocks of rock sliding on two or more surfaces. The simplest case is that of a rock tetrahedron sliding on two intersecting joints illustrated in Fig.2.3.
An approximate analysis of this wedge can be carried out by assuming sliding on an equivalent plane striking parallel to the slope face and dipping at the angle of the line of intersection (Hoek, 1971b). However this type of analysis will always be conservative, and a more correct analysis

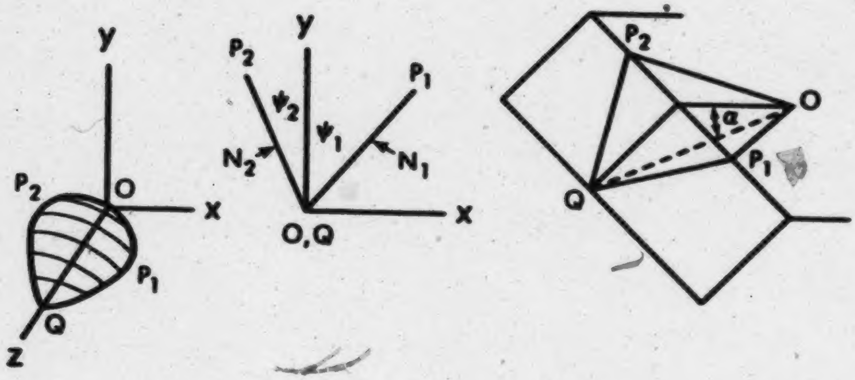

α = dip of line of intersection
OQ = z-axis, Ox horizontal
ψ_1, ψ_2 = apparent dips of planes OP_1, OP_2 viewed along Oz
W = weight of block
μ^*_1, μ^*_2 = variable coefficients of friction

Resolving forces:

$$N_2\cos\psi_2 - N_1\cos\psi_1 = 0$$

$$N_1\sin\psi_1 + N_2\sin\psi_2 - W\cos\alpha = 0$$

$$W\sin\alpha - F^{-1}(N_1\mu^*_1 + N_2\mu^*_2) = 0$$

Hence;

$$N_1 = \frac{W\cos\alpha\cos\psi_2}{\sin(\psi_1 + \psi_2)} \; ; \; N_2 = \frac{W\cos\alpha\cos\psi_1}{\sin(\psi_1 + \psi_2)}$$

$$F = \frac{({}^*_1\cos\psi_2 + {}^*_2\cos\psi_1)\cot}{\sin(\psi_1 + \psi_2)}$$

Fig.2.3 Three-dimensional analysis of sliding wedge (after Jaeger,1971)

must consider the three-dimensional nature of the problem. Jaeger (1971) presented an analysis of this case.

$$F = \frac{(\mu_1^* \cos\psi_2 + \mu_2^* \cos\psi_1)\cot\alpha}{\sin(\psi_1 + \psi_2)}$$

in which:

μ_1^*, μ_2^* = variable coefficients of friction

ψ_1, ψ_2 = inclinations of the joints to the vertical plane containing the line of intersection

α = dip of line of intersection.

In general μ_1^*, μ_2^* are functions of the normal stresses acting on the joints, and are therefore functions of the geometry of the sliding mass. Calculation of the geometry is usually tedious except in simple cases, and computer methods have been devised to simplify this task (eg. Hendron et al, 1971). The computer programs are usually based on vector methods.

John (1968) and Londe et al. (1969) used stereographic projection methods to analyze the three-dimensional problem but the method becomes complex for situations other than the purely frictional case with only gravity loading.

McMahon (1971) and Shuk (1970) have considered a probablistic approach to slope design. Factors affecting slope stability such as geometry of discontinuities and strength are considered to have ranges of values represented by statistical distributions (normal, log-normal, etc.).

These distributions can be used to compute a probability of failure. Slope optimization can be carried out to minimize total cost, which consists of initial costs, maintenance costs and the probable failure cost.

2.6 Summary

From the above literature review it is obvious that rock slope stability is a complex topic. At the risk of oversimplification the chapter will be briefly summarized.

The most significant factors affecting the stability of rock slopes are the geometry of discontinuities, groundwater pressures, and the strength of the discontinuities. The most practical method of analysis is the limit equilibrium method, applied on a two- or three-dimensional basis.

CHAPTER 3

CASE HISTORIES

3.1 Introduction

The previous chapter indicated the many factors affecting rock slope stability and indicated several theoretical methods of analysis. However to confidently incorporate these factors and analyses into a slope design, it is necessary to have case histories which indicate that the methods do work in practice.

Krahn (1974) gave a comprehensive summary of case histories that have been presented. However very few of the case histories were complete with tests on natural joints in hard rock; most tests reported were on prepared surfaces, compacted or broken samples, or in relatively soft materials (shales or coals). Hoek (1971a) reported test results on porphyry that corresponded reasonably well with that of a slide in the Atalaya Open Pit, Spain. Seegmiller (1972) tested clay-filled joints in connection with slides that occurred in the Twin Buttes Mine, Arizona, but found that the strength values measured were higher than those required for stability of the slides. The shear testing that Krahn (1974) conducted for his study of the Frank Slide, Alberta gave results in reasonably good agreement with a stability analysis.

However in comparison with the large numbers of case histories present in the soil mechanics literature, there is a definite shortage of case histories in stability of hard rock slopes. Since there is a lack of case histories available it is desirable to investigate failures that are as simple as possible in terms of geometry and the number of materials involved. For this reason it was decided to study small slides with relatively simple geometry. This chapter gives the geological and geometrical details of three case histories studied.

3.2 Brenda Mines case histories

Brenda Mines Ltd. is located 18 miles west of Peachland, British Columbia and is at approximately 5500 feet elevation. Full production of the copper-molybdenum mine was achieved in early 1970. The expected life of the mine is 20 years. The Brenda ore body occurs within a highly fractured quartz diorite termed the Brenda Stock. The ore minerals occur as secondary infillings in the fractures.

The ore body is elongated in a northeasterly direction and is being mined by open-pit methods. The pit as developed to mid-1973 is shown in Fig.3.1. The benches are 50 feet high and the proposed final slope is of the order of 45

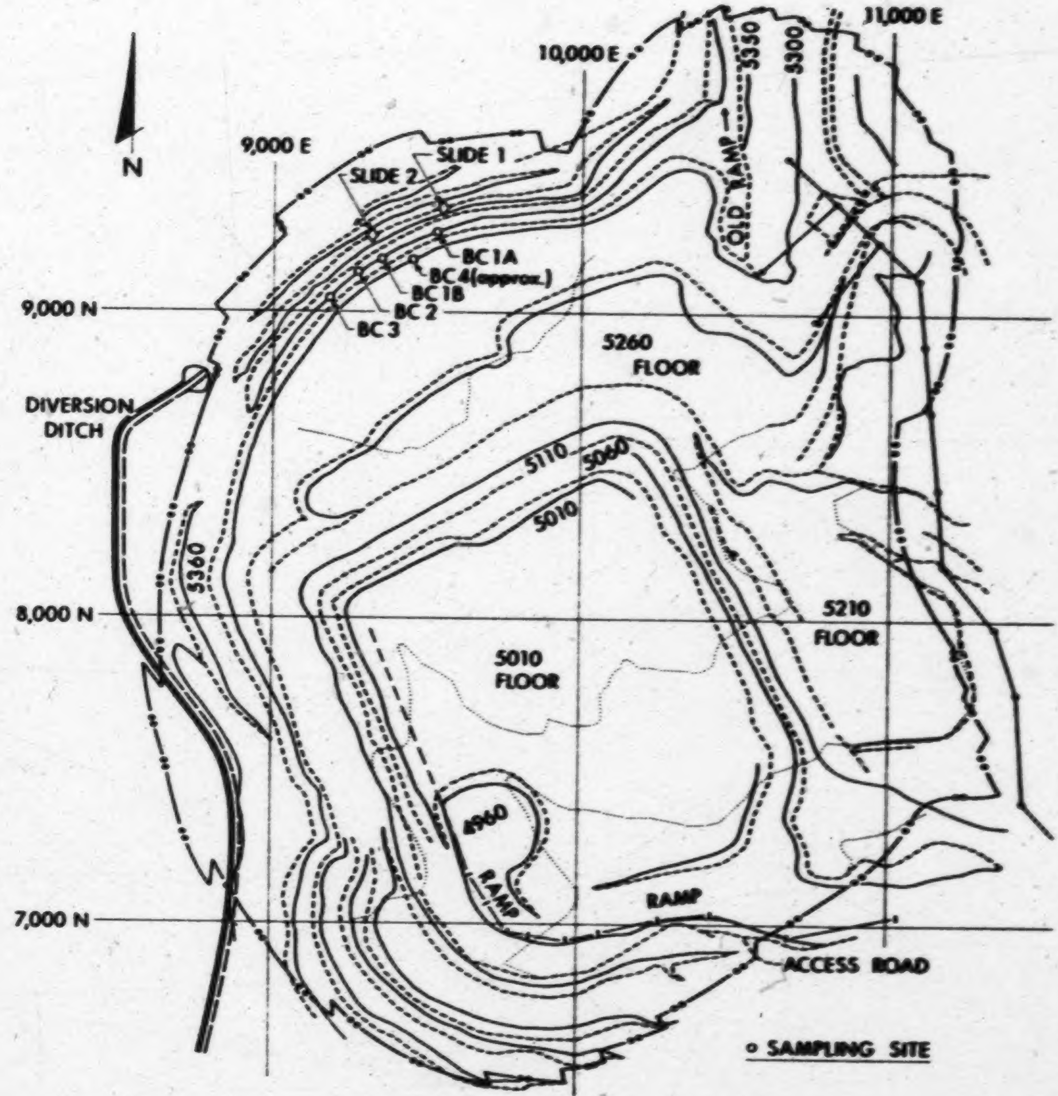
N
9,000 E
10,000 E
11,000 E
SLIDE 1
SLIDE 2
BC 1A
BC 4(approx.)
BC 1B
BC 2
BC 3
9,000 N
8,000 N
7,000 N
DIVERSION DITCH
5350
5300
OLD RAMP
5260 FLOOR
5110
5060
5010
5360
5210 FLOOR
5010 FLOOR
4960
RAMP
RAMP
ACCESS ROAD
o SAMPLING SITE

Fig.3.1 Map of open-pit at Brenda Mines Ltd.

degrees. Cahoon (1973) has back-analyzed three slides in the pit, but no indication of the failure surface materials was given. These analyses were based on Hoek's charts. A bench-size wedge failure was analyzed as a two-dimensional planar failure, and gave strength parameters of $44° < \phi < 48.8°$ and $0 < c < 180$ psf. Two failures were analyzed as "apparent" circular failures and gave strength parameters of $\phi = 47°$ and c approximately equal to 900 psf.

Two small slides occurring in the North wall of the pit were selected for the case histories. An over-all view of the North wall is shown in Fig.3.2. These slides were selected because the surfaces on which sliding occurred were fully exposed for observation and measurement. In addition it was assumed that the pre-failure geometry was defined completely by adjacent wall and floor sections. The slides were accessible from the benches above and below, and the right sides and walls were therefore measured by tape and theodolite survey. Check points on the right sides of the slides indicated an accuracy of about 3%. As can be seen in the photographs in Figs.3.3 and 3.5, the slides have a wedge shape, the right sides being very planar, but the left sides being very broken and rough. It is apparent that sliding in the usual sense could not have occurred on the broken left surfaces. For the left hand sides of the slides, the average inclinations were estimated using a Brunton compass. In

Fig.3.2 General view of North wall, Brenda Mines Ltd. Slides are between second and third bench above drill rig.

considering the kinematics of sliding for both slides it became clear that both slides were close to being in a position where sliding could occur on the right sides only, as opposed to sliding along the lines of intersection of the wedges. It was therefore hypothesized that sliding had occurred on the right sides of the wedges, and after the main slides had occurred the loss of confinement allowed blocks of material to topple out of the left sides of the wedges. For the slide denoted No.1, a minor increase of the dip of the left side (7°) would allow sliding to occur on the right side only. For the slide denoted No.2, an average inclination measured between the large block near the base of the slide and the top of the line of intersection, gave a slide geometry such that sliding could occur on the right side only. On the molybdenite coated surface (slide No.1) faint striations were observed that pointed approximately down dip on average. It was thought that these were an indication of the correctness of the hypothesis. However similar striations were observed on some of the samples obtained for testing, and may be related to the deposition of the molybdenite.

The geometry of slide no.1 is shown in Fig.3.4. The dashed line on the left indicates the approximate average inclination of the left side of the slide as measured in the field. It was assumed that more blocks had toppled from the

Fig.3.3 Photographs of slide no. 1 at Brenda Mines Ltd.

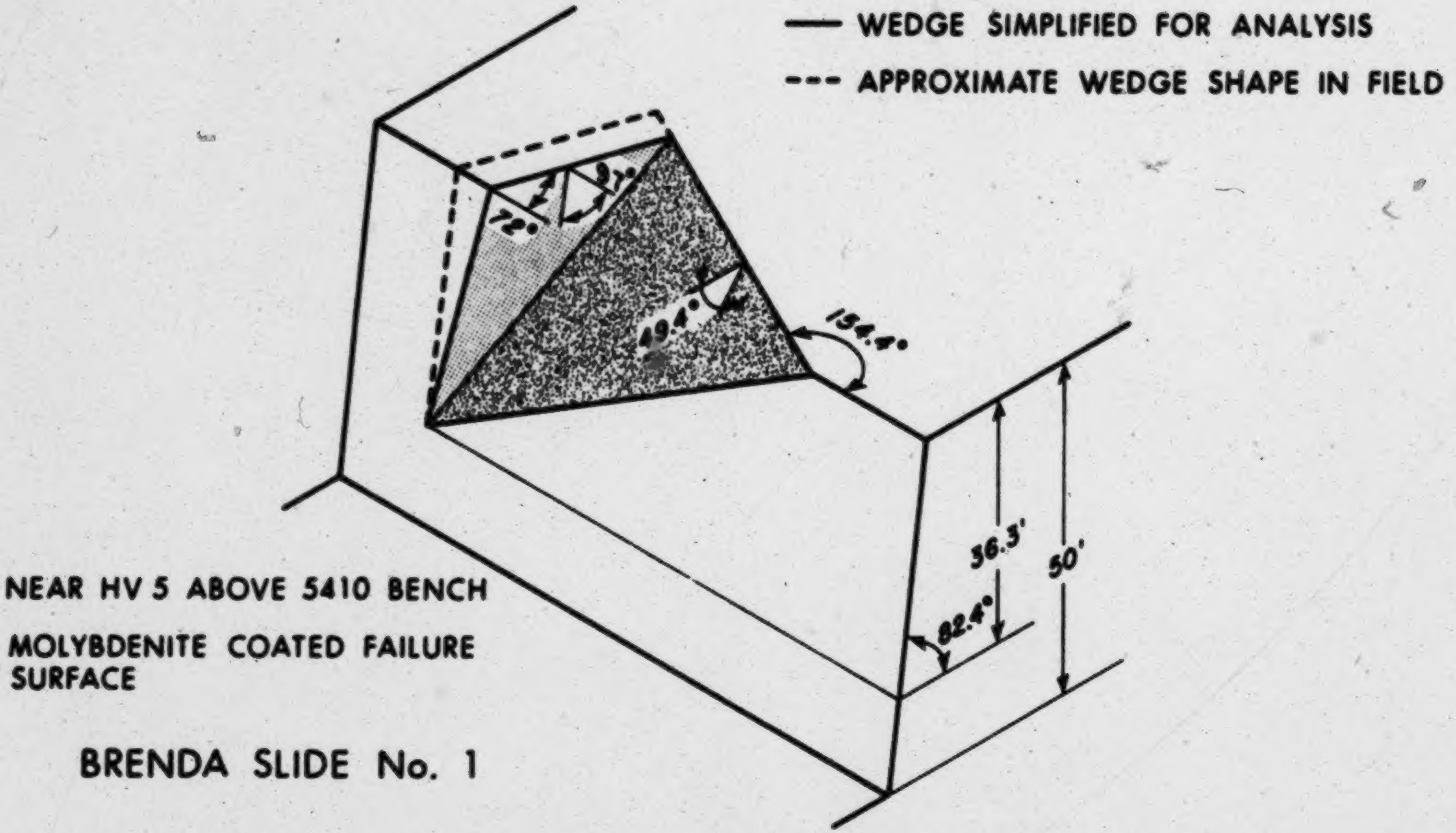
WEDGE SIMPLIFIED FOR ANALYSIS
APPROXIMATE WEDGE SHAPE IN FIELD
72°
97°
49.4°
154.4°
36.3'
50'
82.4°
NEAR HV 5 ABOVE 5410 BENCH
MOLYBDENITE COATED FAILURE SURFACE
BRENDA SLIDE No. 1

Fig.3.4 Geometry of slide no. 1 at Brenda Mines Ltd.

Fig.3.5 Photographs of slide no. 2 at Brenda Mines Ltd.

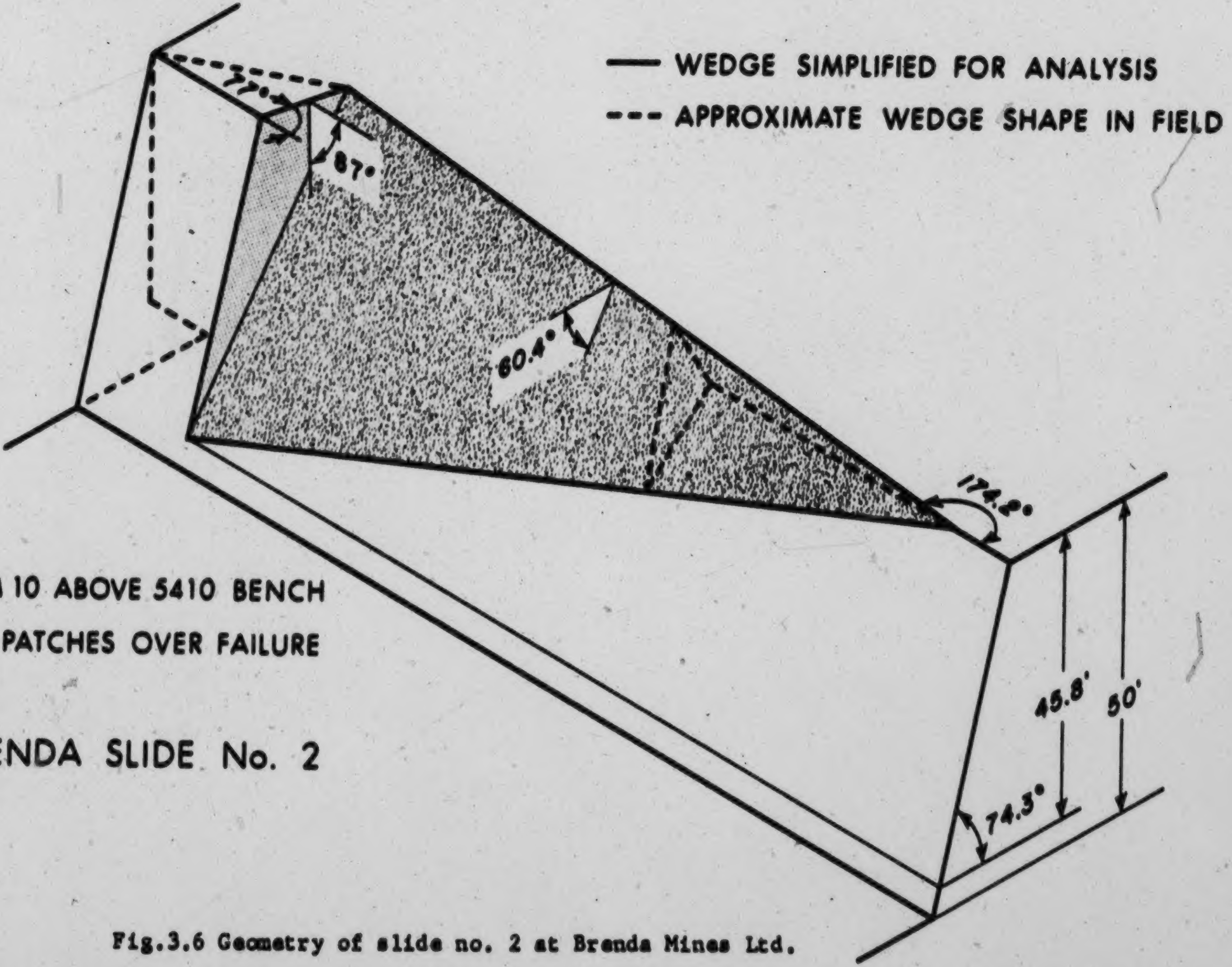
— WEDGE SIMPLIFIED FOR ANALYSIS
--- APPROXIMATE WEDGE SHAPE IN FIELD
77°
87°
60.4°
174.2°
45.8'
50'
74.3°

NEAR PM 10 ABOVE 5410 BENCH

CALCITE PATCHES OVER FAILURE SURFACE

BRENDA SLIDE No. 2

Fig.3.6 Geometry of slide no. 2 at Brenda Mines Ltd.

upper part of this surface than from the lower part to establish a stable surface (see de Freitas and Watters, 1973). For the reasons noted above the measured dip of this surface was increased in the idealization to a point at which sliding occurred on the right base of the slide only and this dip was used in the assumed pre-failure geometry. The right surface was inspected and a piece was taken for identification of the surface minerals. The main mineral forming the surface coating was identified as molybdenite (MoS_2), but contained minor amounts of a variety of secondary minerals.

The geometry of slide no.2 is shown in Fig.3.6. The dashed lines represent the approximate shape of the slide in the field. As mentioned previously the large block at the lower left (visible in the photograph of Fig.3.5) was considered as the edge of the main slide mass. The portion of the right side of the slide that remained in place is discussed in Chapter 5. Again the surface was inspected and the material occurring in patches over the surface was identified as calcite. It was assumed that patches of calcite on the mass that slid corresponded to the "bare" portions of the failure surface that remained on the wall. Samples used for testing had this correspondence of patches of calcite on the two halves of the samples.

3.3 Endako Mines case history

Endako Mines Ltd. is located 6 miles southwest of the village of Endako in central British Columbia and is at approximately 3200 feet elevation. The molybdenum mine was officially opened in June, 1965 and a major mill expansion took place in 1967. The open pit mine has been developed in the predominantly quartz monzonitic Endako pluton of the Topley Intrusives (Kimura and Drummond, 1969). The molybdenite occurs mainly in quartz-molybdenite veins.

The ore body is elongated in an east-west direction and is presently being mined in two adjacent open pits. The east pit as developed to mid-1973 is shown in Fig.3.7. On the south wall the benches are 99 feet high on an overall slope of 49.5 degrees. McLeod (1971) gave some details on some slides that have cccurred at Endako Mines. One of these was a shear plane failure on a quartz-molybdenite vein dipping at 45°. McLeod further states that shear plane failures along quartz-molybdenite veins are very common and that all of these had taken place along veins with dips of more than 34°, suggesting that the friction angle for these veins is about 34°.

The slide chosen for analysis occurred in the east pit and is shown in the photograph in Fig.3.8. Unlike the case histories at Brenda Mines, this slide area was not

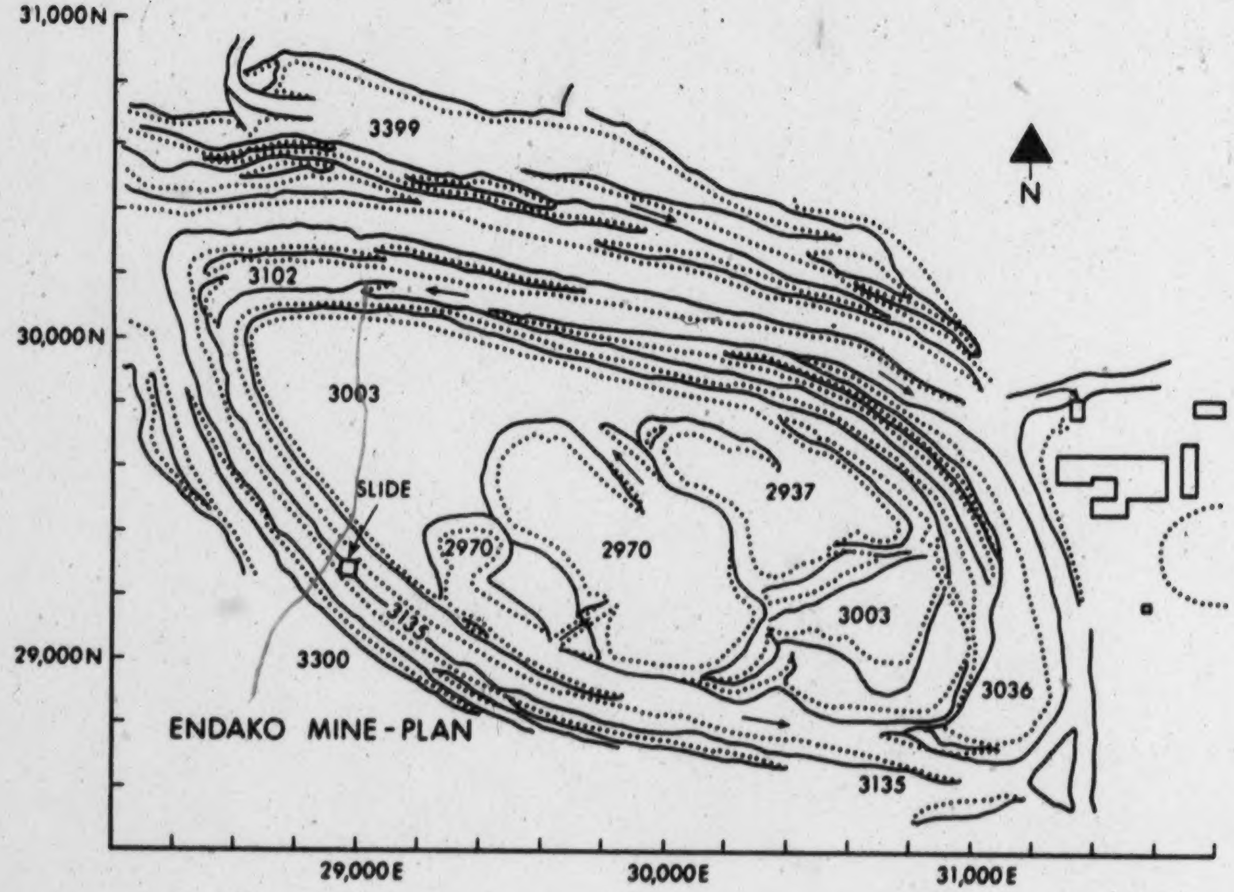
31,000N
30,000N
29,000N
29,000E
30,000E
31,000E
N
3399
3102
3003
SLIDE
2970
2970
2937
3003
3036
3135
3135
3300
ENDAKO MINE-PLAN

Fig.3.7 Map of open-pit at Endako Mines Ltd.

Fig.3.8 Photograph of slide at Endako Mines Ltd.

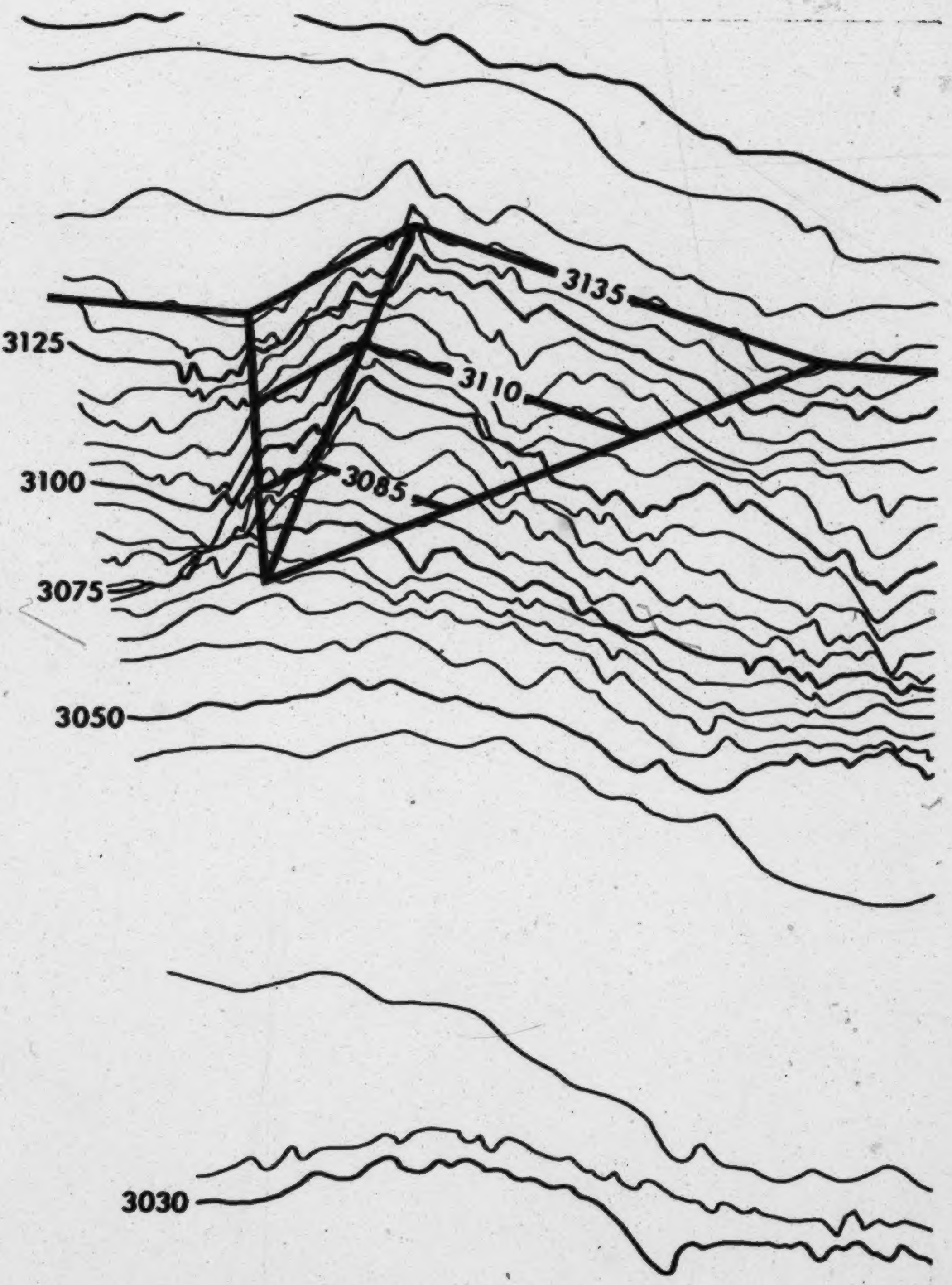
3135
3125
3110
3100
3085
3075
3050
3030

Fig.3.9 Contour map with idealized model of slide at Endako Mines Ltd.

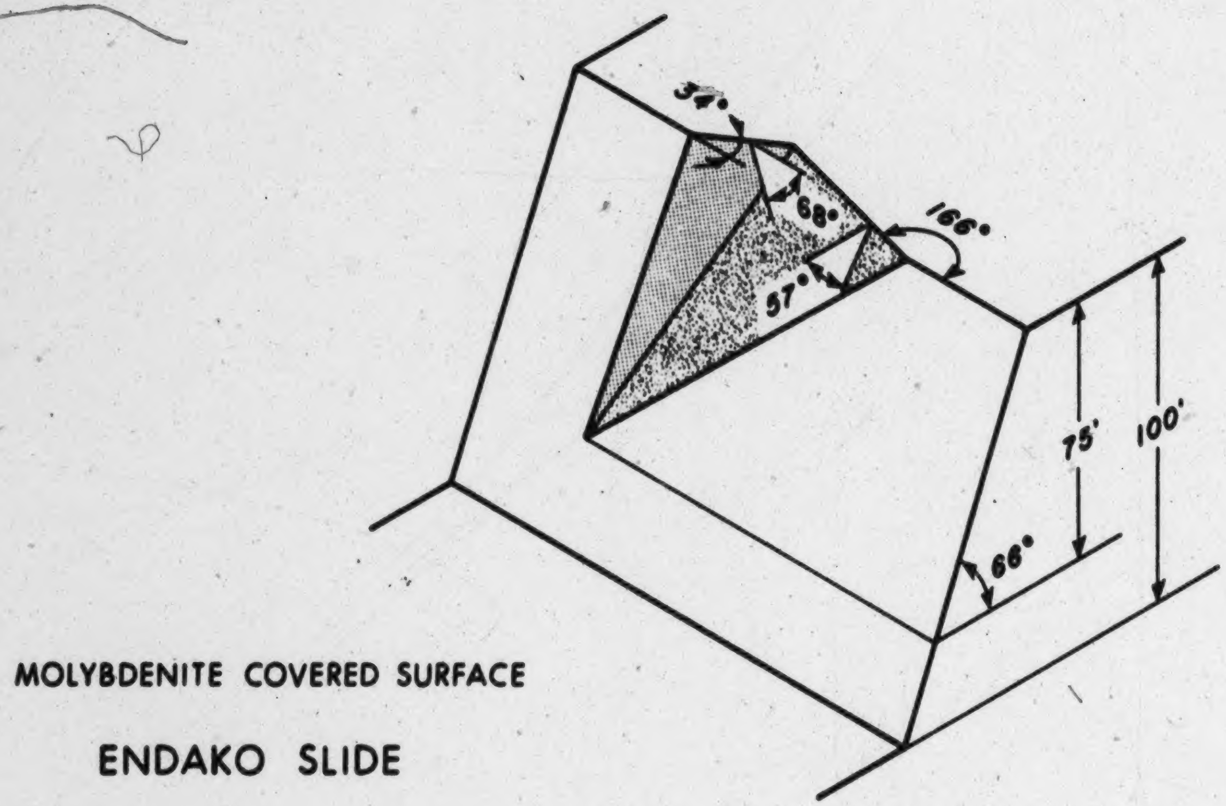
34°
68°
57°
166°
75'
100'
66°
MOLYBDENITE COVERED SURFACE
ENDAKO SLIDE

Fig.3.10 Geometry of slide at Endako Mines Ltd.

accessible and was partially covered with debris from above. A theodolite triangulation survey was carried out, but the results were somewhat suspect because there were not definite points on the slide to survey. A triplet of overlapping photographs of the slide was available and a contour map was prepared from these by Miller Engineering Services Ltd. of Vancouver. A wedge-shaped slide was fitted to this contour map by trial and error and the results are shown in Fig.3.9. The resulting geometry is shown in Fig.3.10. The failure surface on the right side of the wedge was dark in colour, and given the nature of the mine, was assumed to be molybdenite.

Samples were taken at both mines for strength testing. Details of sampling and testing are given in the next chapter and analyses of the slides are carried out and discussed in Chapter 5.

CHAPTER 4

SAMPLING AND TESTING

4.1 Sampling of jointed hard rock

After having recognized the governing type of discontinuities in the slides described in the previous chapter, it was necessary to find representative samples for testing to obtain strength values for comparison with back analyses. It was considered desirable to use the portable coring unit developed by the Department of Civil Engineering, the University of Alberta.

Previous work in the Department had involved an electric concrete coring apparatus used successfully in softer rocks. Similar equipment has been used by others. For example Brawner et al (1972) reported successful sampling in coal formations. However, in hard igneous rocks, drilling rates as slow as 1 in./hr. were encountered. In order to overcome this and other deficiencies modifications were made to the equipment.

The basic modification was the use of a Stihl gasoline motor with a special coring transmission to replace the electric drill. The gasoline motor was rated at 6 h.p., as opposed to 2.3 h.p. for the electric drill. Adaptors and a water jacket were constructed by machinists of the

Department. A small submersible electric pump was used for supplying the water to the drill from a 45 gal. drum via ordinary garden hose. Diamond-tipped core barrels were purchased commercially in 4",6", and 10" diameter single-wall models and a 6" diameter double-wall model. Preliminary tests on concrete indicated that vibration was excessive so that a guide system was mounted on the lower portion of the frame. The guide system consisted of an annular piece of steel plate with three equally spaced adjustable guide wheels. Brass and phenol wheels were tried but tended to jam from the rock dust created by drilling so that rubber-coated wheels with enclosed ball bearings were used. The drilling apparatus is shown in Fig.4.1.

The drilling frame was attached to the rock surface with stove bolts threaded into concrete anchors which had been installed with an electric rotary hammer run by a small generator. Due to the hardness of the rock the anchors would not spread using the electric hammer, and a sledge hammer had to be used to drive the anchors into place. The frame was usually installed manually by two men, but on higher drilling locations an extra anchor and bolt were installed above the drilling location and a come-along hoist was used to assist in holding the frame in place for bolting. Anchor failures were rare as the drilling sites were usually chosen in areas of competent rock. In one case the anchor rotated

Fig.4.1 Photograph of drilling unit used.

with the bolt and could not be tightened by redriving. The other type of anchor failure occurred when the rock broke up around the anchor. This type of failure occurred repeatedly in attempts to sample highly weathered rock. One method to possibly overcome this problem is the use of longer rock-bolts as anchors. This method was attempted but the gas-driven jack hammer to drill the rock-bolt holes failed to operate properly.

Removal of the drilled cores required breaking of the core at the base of drilling. Used core barrels were slipped over the sample and hit with a sledge-hammer. If this was unsuccessful a crow-bar was used to pry on the sample.

Suitable drilling sites required an accessible, reasonably flat area at least two feet square with a desired joint type exposed on the surface. It was desirable to have the joint running roughly perpendicular to the surface but the drilling system could be tilted somewhat by the use of longer bolts and spacers placed under one side of the frame. In this case the anchor installation had to be aligned for this tilt and a thin steel template was used to assist in this alignment. Use of the 4 in. core barrel gave little tolerance in the alignment of drilling with the joint direction and therefore the larger core barrels were used more extensively.

Four samples were obtained from Brenda Mines and five samples were obtained from Endako Mines using this equipment. The sampling sites at Brenda Mines are shown on Fig.3.1. Sample lengths varied from 7 in. to 12 in. and sample diameter varied with the core barrel used. An example is shown in Fig.4.2. Actual drilling rates varied from about 1/2 min. to 5 min. per inch. However anchor installation and core removal were more time-consuming. After most of the problems were solved an average of two samples per day were obtained. The equipment was also used for sampling limestone near Jasper, Alberta and coal near Lake Wabamum, Alberta. As with any sampling technique using a drilling water for cooling and dust removal the system could not sample seams of highly weathered material. This material was washed out of a sample during drilling.

The main problem encountered in this sampling program was the fracturing of samples which prevented the obtaining of large intact samples for testing. It had been hoped that the use of the 6 in. double-wall core barrel would reduce this problem but the cores drilled with this barrel were as fractured as those drilled with the single-wall barrel and drilling took considerably longer because of the increased cutting surface area. Upon examination of the fractures and similar fractures in block samples it was realized that some

Fig.4.2 Example of core obtained from drilling.

of these were mineralized. This indicates that at least some of the fractures existed before the sampling and therefore any sampling technique would give rise to fractured samples. It was felt undesirable to test samples in which the sample had been epoxied together as any misalignment could give a step in the profile of the sample.

However these side fractures associated with the joints did make it easier to remove block samples with hand tools. Several block samples were taken at Brenda Mines using a geological hammer and a crow-bar to pluck the blocks out of the wall. The main problem with this type of sampling is the awkward handling created by the irregular shape and size of samples.

The first samples were transported with the two (or more) pieces of the sample taped together with fiber-reinforced tape. On a few of the samples, rubbing marks created by relative movement during transportation were visible. Consequently on the second trip the samples were transported in separate pieces wedged into boxes to protect the joint surfaces.

It is concluded that the sampling techniques used were as successful as could be expected with the material being sampled.

4.2 Sample preparation

The most time-consuming portion of the testing program was found to be sample preparation. The combination of the hardness of the rock and the crusty nature of the joint coatings created sawing difficulties. Several saws were used with varying success.

A Stihl motor coupled to a cutting wheel was used for rough trimming of block samples but could not be used for accurate cuts. A concrete saw with a power-driven vise was used for some cutting, but the vise required smooth, parallel surfaces. Even with blocking, samples tended to move in the vise and the saw blade would bind. Most success was achieved with a Mercury lapidary saw (Fig.4.3). On this saw the sample is held in position on a cutting table and the blade moves down through the sample. The pressure from the blade helps to hold the sample in position. The maximum size of sample that can be cut is about 6 inches by 6 inches. It would be desirable to have a more powerful motor on the saw as cutting the hard igneous rock was slow, especially on long cuts.

Tap water was used for the cutting fluid to prevent surface contamination with cutting oils. Attempts to keep the water off the joint face with plastic wrapping were not very successful. After the sample was dried minor amounts of

Fig.4.3 Mercury lapidary saw used for cutting samples.

rock dust from the cutting had to be removed by running tap water over the surface and rubbing lightly with a cloth.

Cutting to the exact dimensions of the shear box was impossible so the samples were cut slightly undersize, then cast in a mould with Devcon B Plastic Steel (liquid type). After curing, the sides of the upper block were ground slightly to allow freedom of vertical movement during testing. The samples were then photographed and were ready for roughness measurements and testing.

4.3 Roughness measurement

Surface profiles were measured on all the samples tested with a device developed by Krahn (1974). The device consists of a frame, electric motor, linear variable differential transformer (LVDT), and electronics box. Horizontal distance is measured by the speed of the electric motor and the LVDT measures the vertical movement of a hardened steel tip which slides over the sample surface. Profiles were measured at 1/4, 1/2 and 3/4 of the width of the sample to see if significant differences arose depending on the line of measurement. The profiles were recorded on an x-y recorder. These profiles were digitized for computation of roughness parameters and computer plotting of profiles. An example is shown in Fig.4.4. The device seemed to work well on molybdenite surfaces but left fine scratches on

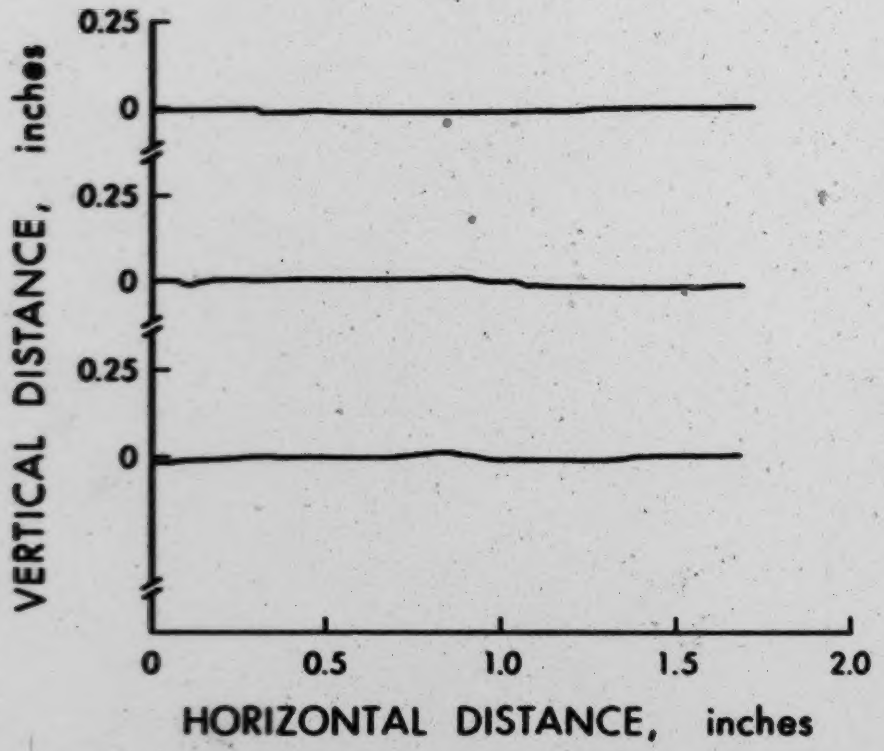

Fig.4.4 Typical roughness plot obtained with roughness measuring device (at true scale).

calcite surfaces. It is felt that these scratches were not enough to negate the measurements and would not have any significant effects on strength testing. A more sophisticated device was used by Coulson (1970), but it is felt that the extra expense probably does not give significantly better results. It would be desirable to compare the type of apparatus used with a more sophisticated surface profile measuring device.

4.4 Selection of testing apparatus

Both triaxial and direct shear devices have been used to study the shear strength of surfaces in rock. In the triaxial test the surface to be tested is oriented at a pre-selected angle to the axis of the specimen, a confining stress is applied and the axial stress is inceased to produce failure. To prevent relative rotation of the samples it is necessary to use spherical seats at both ends of the specimen (Coulson, 1970). However in this case the entire specimen rotates, changing the normal and shear stresses on the failure surface. In addition Goodman (1970) indicates that a finite element analysis of triaxial specimens with an inclined joint gave very uneven stress distributions along the joint if the joint was more compressible than the surrounding rock.

Coulson (1970) lists several advantages of the direct shear method of testing. These are:

> "(1) It allows independent control of normal and tangential forces on the surface of sliding.
> (2) It can be adapted for quite large surface areas.
> (3) Shear displacements several orders of magnitude larger than for the triaxial method can be accommodated.
> (4) When rough surfaces are tested, displacements perpendicular to the surface of sliding can be most readily monitored using the direct shear method."

The chief disadvantage of the direct shear test is the non-uniform stress distribution on the failure surface. Several factors give rise to this situation. The shearing forces on the sample are not co-planar giving rise to moments about a horizontal axis perpendicular to the direction of movement. In addition after some displacement the point of application of the normal force is not over the centre of the contact area increasing the moment mentioned above. Thirdly, for irregular surfaces, rotational tendencies are possible in the horizontal plane. When these are restrained unknown irregular side pressures are created. Despite these drawbacks, direct shear testing was selected because of its several advantages indicated above.

4.5 Selection of testing conditions

Before testing of samples several conditions of testing had to be decided. These were: sample size, moisture conditions, rate of strain, and range of normal loads to be applied. Krahn (1974) has indicated that strength is essentially independent of sample size provided the surface roughness characteristics do not change significantly. Since the samples were essentially the same over their entire area, it was decided to emphasize smaller samples (2"x2") in the testing program, with a check on a few larger samples. Coulson (1970) indicated that a centre line average roughness of about 70 micro-inches was the upper limit for water effects. Since the smoothest surfaces tested had a centre line average roughness of at least 1000 micro-inches it was decided to test the samples dry. In addition Coulson ran tests at speeds varying 0.22 to 0.012 inches per minute (in/min) and found that the rate of shear had no effect on shear strength values (except for very minor changes with dolomite). A constant test rate of 0.05 in/min was therefore chosen. The maximum normal load occurring on the joints in the case histories selected was slightly over 20 pounds per square inch (psi) Therefore it was decided to test the samples at normal loads corresponding to 5,10,20 and 40 psi.

Another consideration in the testing program is the retesting of samples at different normal loads. Since samples are difficult to obtain and prepare, it is desirable to retest if this is possible. However if surface damage changes the surface characteristics of the sample, the strength values will change and the test will be of limited value. Only by attempting retesting of the samples can the validity of retesting be checked.

4.6 Shear testing apparatus

The shear testing apparatus used was built by the Department of Civil Engineering and is shown in Fig.4.5. (Samples of nominal sizes 2"x2" and 4"x5" were tested using different boxes.) The lower half of the shear box is moved by a gear box-chain drive assembly powered by an electric motor. The upper half of the box is restrained by the load cell which measures the shear load. The two halves of the box are separated by teflon strips and the guides on the top box are teflon-coated. The normal load is applied to the upper portion of the sample by a dead weight arrangement. Horizontal and vertical displacements are measured by linear variable differential transformers (LVDTs). Horizontal movement and the shear load were recorded continuously on an x-y recorder and all three measurements were monitored continually by a digital printer which gave a series of three readings about every 8 seconds. The digital printout was punched onto data cards for computer computation and plotting.

A friction correction of 0.5 to 1.5 pounds (depending on the shear box used) was applied to all readings. This friction is a result of the sliding of the box contact along

Fig.4.5 Shear testing apparatus.

teflon strips. Two other sources of friction are present in this shear arrangement. Lateral movement tendencies would cause side-friction on the guides. This was reduced by the use of a teflon coating, but could still exist. Use of side load cells could account for this, but they were felt to be too expensive to be worthwhile, and this effect was ignored. In addition friction could exist between the sample and the top half of the shear box. (In the apparatus vertical movement is accommodated by allowing the sample to move within the top box.) Friction tests were run on Devcon-on-steel surfaces and indicated a coefficient of friction ~~of~~ the order of 0.1. Spray lubricants were used to attempt to reduce this value, but were not effective. However it is not clear that this friction would necessarily be fully mobilized. An attempt to measure the effect of this friction was carried out by attaching a sample that had previously been tested (1-BB14) to the upper half of the shear box with epoxy. The strengths measured with this arrangement fell within the range of those measured in the standard testing arrangement (see Fig.4.6) and therefore the effect was ignored.

4.7 Interpretation of test results

Generally the test results consisted of a rather irregular shear load versus horizontal displacement curve

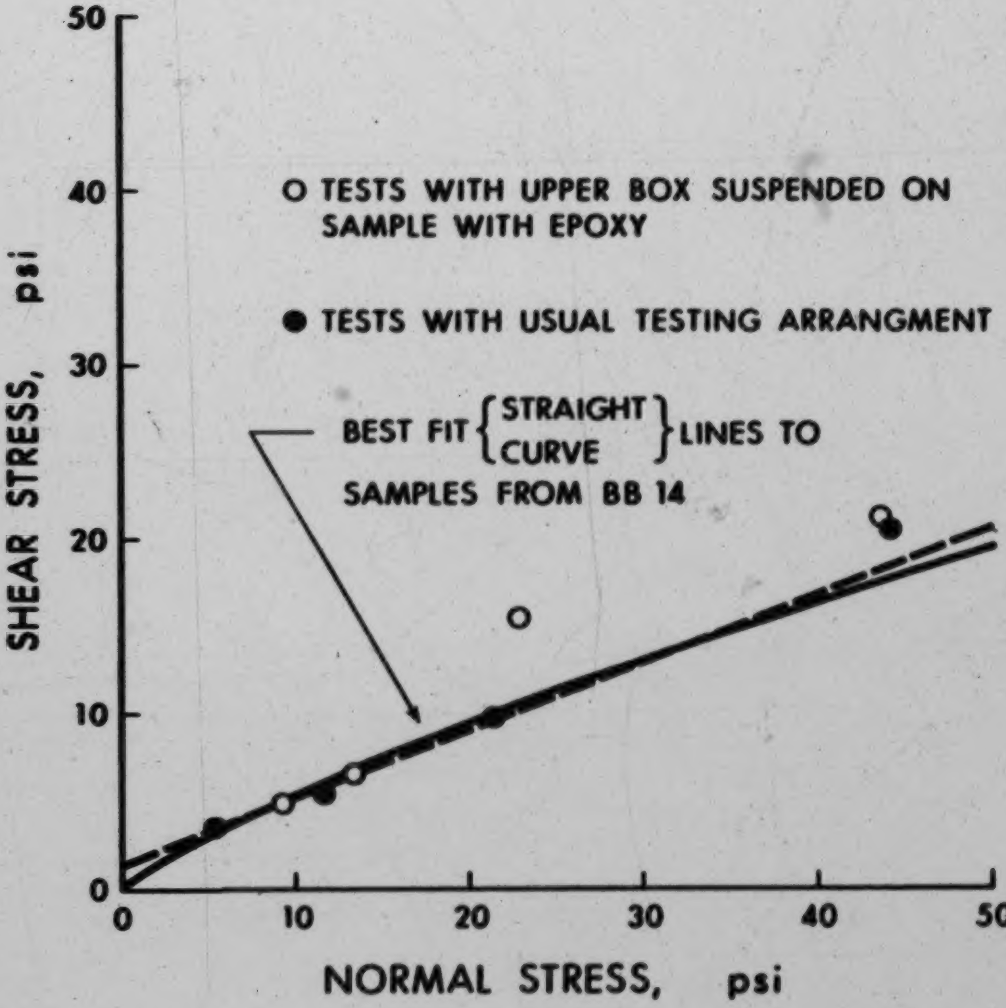

Fig.4.6 Effects of machine friction not directly accounted for in data analysis.

and a fairly smoothly changing vertical deformation versus horizontal deformation curve. The vertical deformations were generally small. There was not any peak-residual type of shear strength behaviour as reported by many authors. The maximum shear load occurred essentially randomly over the half-inch of movement during testing,but usually occurred at the same position for repeated tests on a sample. The type of results are probably partially a result of testing at low normal stresses.Plots of many of the test results are shown in Appendix A.

There are three possible sources for the irregularities in the shear load curves;these are: irregularities in the slope and size of asperities,variations of surface materials over the samples, and stick-slip.

For four tests an attempt was made to separate the geometric component of strength in the manner suggested by Coulson (1970). Tests at a high normal stress and a low normal stress on both a calcite-coated and a molybdenite-coated joint were analyzed. If we let:

$\Phi = \tan^{-1}$ (shear load/normal load)

$i = \tan^{-1}$ (dy/dx)

then: $\varphi = \Phi - i$

where φ is equal to the basic strength friction angle corrected for dilation effects caused by movement over asperities. Basically the same curves resulted at both high and low normal stresses. The resulting curves for the tests at low normal stresses are shown in Fig.4.7. The corrections were rather small but smoothed out the curves slightly. For the calcite sample in particular the resulting curve of φ versus horizontal displacement is a reasonably regularly oscillating line, varying over a fairly narrow band (±3°).

The curves are not as regular or of as short a period as those usually shown for prepared surfaces, but might be partially caused by stick-slip of a natural surface. A simple mechanical model for stick-slip is that given by Coulson (1970). Consider a surface on which the coefficient of dynamic friction (μ_k) is constant and less than that of static friction (μ_s), tested in a shear box. (see Fig.4.8). The lower portion of the sample moves at a velocity V and the upper portion is restrained by a spring of stiffness K developing a shear force S. If no stick-slip occurs, then

$$S = Kx = N\mu_k$$

where x is the extension of the spring required to develop the force S . However if stick-slip occurs the two halves of the sample move together until S is great enough to overcome static friction when

$$S = Kx' = N\mu_s$$

When sliding is initiated the spring force is greater than that required to balance sliding and the top half of the

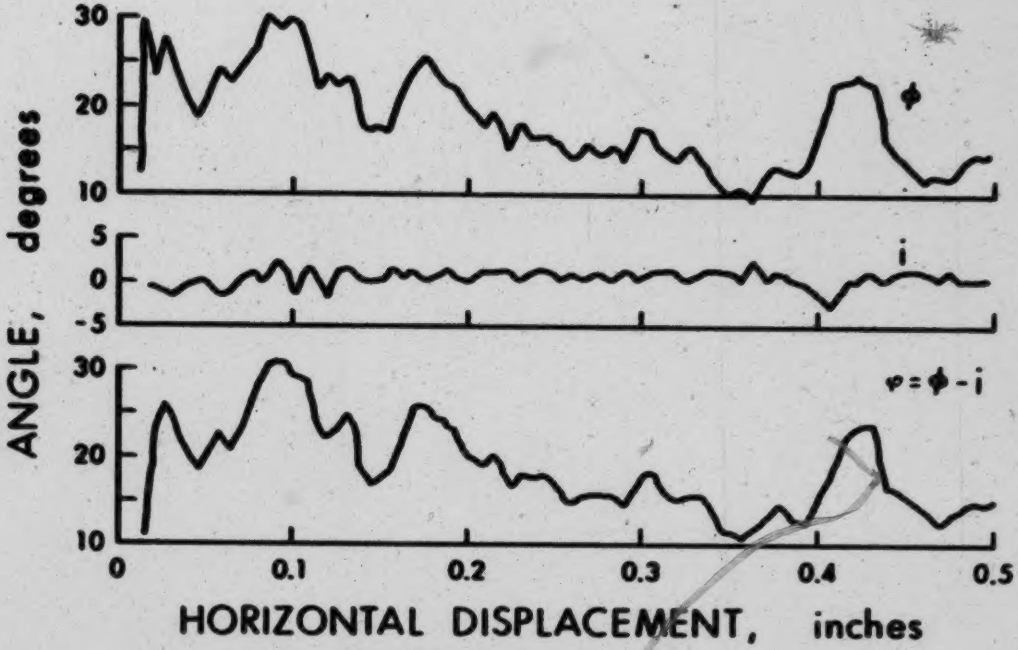

(a) Molybdenite sample.

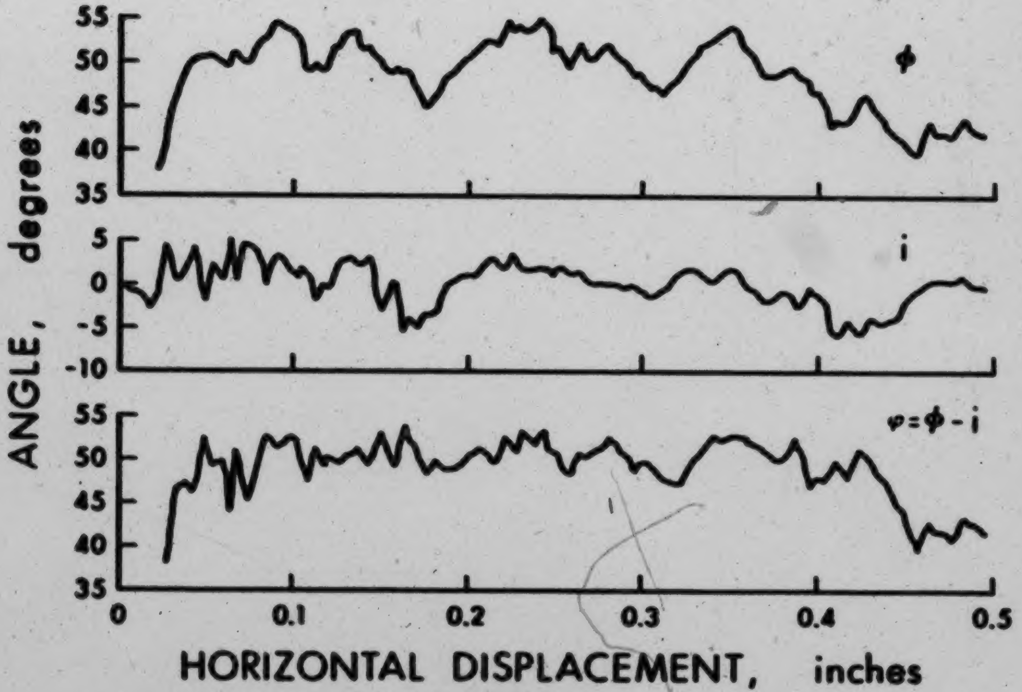

(b) Calcite sample.

Fig.4.7 Examples of applying geometric correction to test results.

sample accelerates towards the spring. The top half of the sample will accelerate until the net force on the sample is zero (i.e. $S = N\mu_K = Kx$) then it will decelerate to zero velocity over the same distance (i.e. $x^1 - x$) at which point the force in the spring will be

$$S = K(x - (x^1 - x)) = K(2x - x^1) = N(2\mu_K - \mu_s).$$

At this point the two halves of the sample will again stick until static friction is again overcome. Note that in this discussion the static coefficient of friction corresponds to the maximum shear load. In addition the limit equilibrium analysis is a static analysis so that the static coefficient of friction is applicable.

To apply the stick-slip equations it is necessary to know the 'spring' stiffness. The stiffness was measured with a dial gauge measuring the displacement of the top box and the load cell was used for reccrding the load. These measurements gave a stiffness of $0.8x(10^4)$ pounds per inch(lb./in.). Regular stick-slip was observed during a test on a flat surface of Devcon-on-steel and interpretation of this test indicated a stiffness of $1.7x(10^4)$ lb./in. Using a stiffness of 10^4 lb./in. and the shear loads measured in the tests would indicate a period $(2(x^1 - x))$ of about $2x(10^{-4})$ to $3x(10^{-3})$ inches. The digital printer only gives values at about $7x(10^{-3})$ inche intervals and therefore regular stick-slip would be hidden in an analysis of the data from the

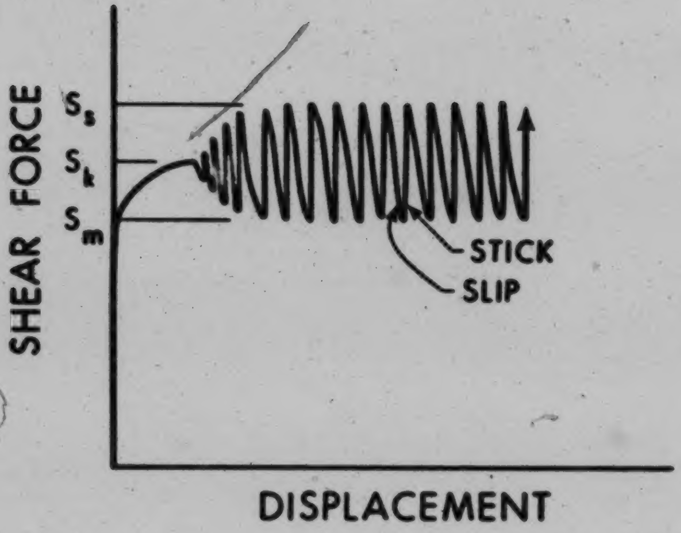

(a) Typical stick-slip curve.

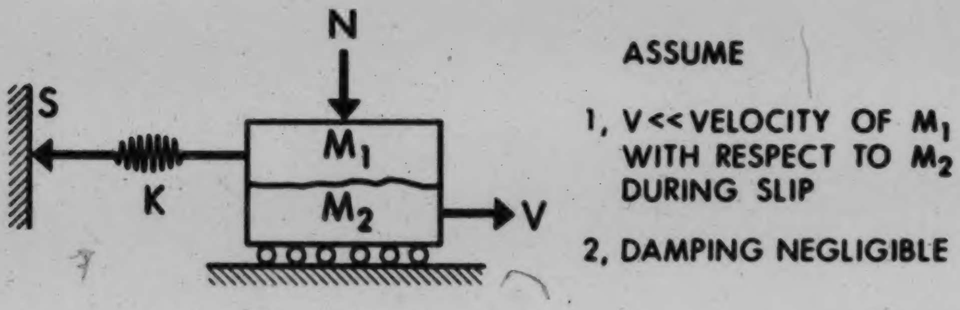
N
S
K
M_1
M_2
V
ASSUME
1, V<< VELOCITY OF M_1 WITH RESPECT TO M_2 DURING SLIP
2, DAMPING NEGLIGIBLE

(b) Idealized model of stick-slip parameters.

Fig.4.8 Stick-slip in direct shear test (after Coulson, 1970).

printer. The x-y recorder plots showed small 'jogs' during the tests but vertical measurements were taken only on the printer and therefore the geometric correction cannot be applied to the recorder plots. Thus it was not possible to fully separate any stick-slip effects that occurred during the tests.

If the irregularities in shear load are primarily due to variations of surface material over the sample, then perhaps some average value of shear load should be considered. There is a higher average around the maximum than over the rest of the test; that is, the maximum is not an isolated phenomenon during the test. It is somewhat difficult to estimate an average shear load accurately, but estimates of the average shear load occurring throughout the inital tests on all samples were made. The average to maximum shear load ratios were approximately 60% for tests on samples from BB-14, 85% for samples from BB-10, and 50% for samples from EC-12. These differences are very significant and it must be decided which measure of strength is applicable.

The best method of deciding whether to use maximum or average shear strength based on test results is by analyzing field failures and determining which strength governed. However it is desirable to have a working hypothesis as to which strength should be used. The samples tested are nominally 2 inches square. If the maximum strength measured on each sample correlates well with that measured on all of the other samples it could be assumed that this strength is mobilized over at least most 2 inch square sections of the joint. If this is the case, then, on average, the maximum strength measured during testing should govern the behaviour of the joint as a whole. If the hypothesis is not correct, it would be expected that factors of safety in excess of unity would be computed if failures were analyzed using the maximum strength. Analyses of three case histories are presented in Chapter 5. On the basis of the working hypothesis the test results given the next section are based on the maximum shear loads occurring during the tests.

During testing of the samples, repeated testing at various normal loads was carried out. It was found that shear load versus displacement curves were generally similar (see Fig.4.9). In addition the initial tests on various samples at different normal loads fell within the range of values for repeated tests. For these reasons it is felt that strength values measured on repeated tests were valid, and these values were included in deriving strength envelopes of the joints.

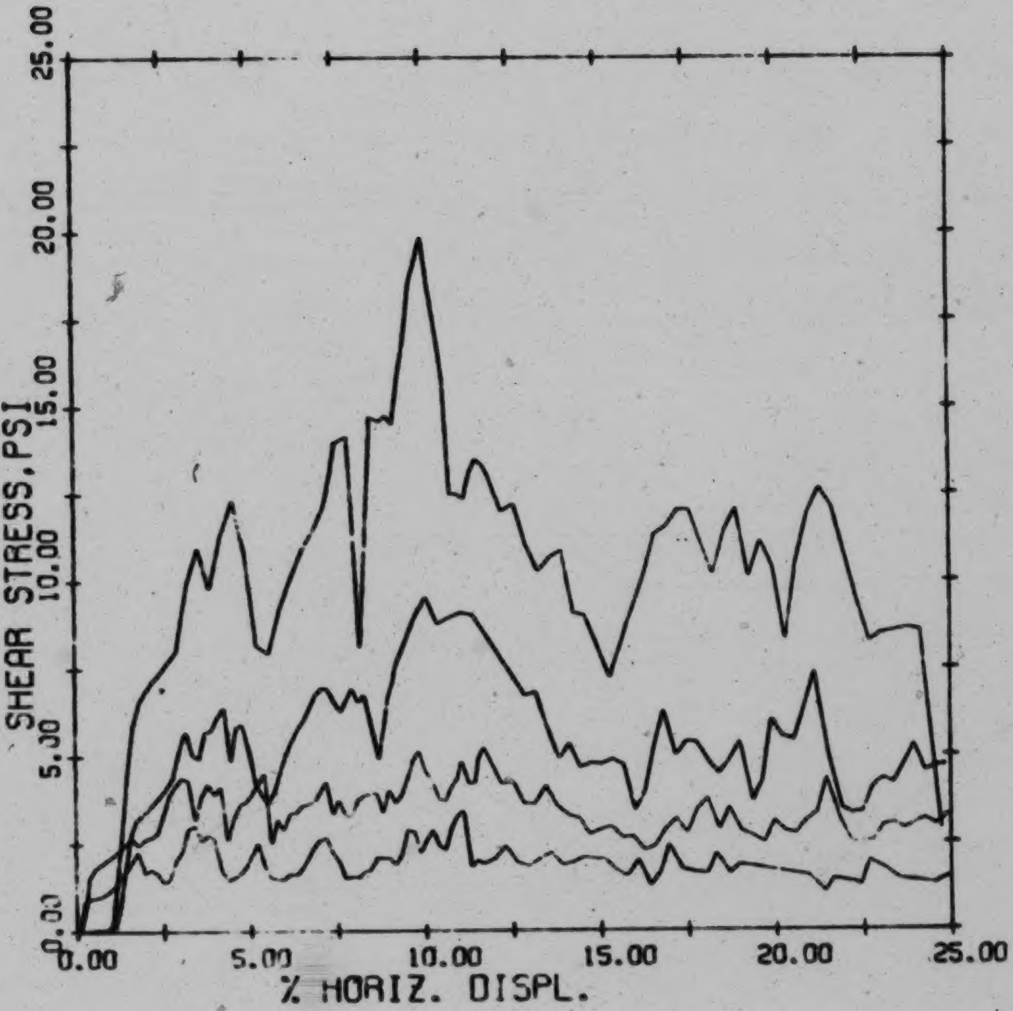

TESTS ON 1-BB14 @ 5,10,20,40PSI NORMAL STRESSES

Fig.4.9 Repeatibility of test results on a single sample.

4.8 Test results

The test data from all the small samples tested was considered in deriving the strength envelopes. When plotted as a Mohr failure envelope (shear stress vs normal stress) the data could be interpreted equally well by a straight line (Coulomb law)

$$\tau = c + \mu \sigma_n$$

or by a power law

$$\tau = k \sigma_n^m .$$

These curves were fitted by a least-squares regression analysis. The data was replotted as ϕ ($= \tan^{-1} \tau/\sigma_n$) versus normal stress and this plot gives an indication that the friction decreased with normal stress. Since the two halves of the samples were separated before testing it is difficult to assign any physical meaning to the intercept (c) in the straight line failure envelope, but it is equally difficult to give physical meaning to the coefficients in the power law curve. Therefore it is felt that either failure envelope could be applied over the stress range tested.

The strength envelopes for the three types of discontinuities tested are (units of psi (pounds per square inch))

(1) Brenda molybdenite joints

(a) Coulomb law $\tau = 1.27 + 0.385\sigma_n = 1.27 + \sigma_n \tan 21^{\circ}$

(b) Power law $\tau = 0.822\ \sigma_n^{0.806}$

The correlation coefficients for (a) and (b) are 0.965 and 0.966 respectively.

(2) Brenda calcite joints

(a) Coulomb law $\tau = 2.81 + 0.89\sigma_n = 2.81 + \sigma_n \tan 41.7°$

(b) Power law $\tau = 1.913\ \sigma_n^{0.803}$

The correlation coefficients for (a) and (b) are 0.966 and 0.972 respectively.

(3) Endako joints

(a) Coulomb law $\tau = 2.86 + 0.442\sigma_n = 2.86 + \sigma_n \tan 23.8°$

(b) Power law $\tau = 1.229\ \sigma_n^{0.746}$

The correlation coefficients for (a) and (b) are 0.898 for both cases.

The data points and best fit lines and power curves are shown in Figs. 4.10, 4.11, and 4.12. As noted in the previous section, these values are based on the maximum shear load measured during the test.

4.9 Variations in results

For the Brenda joints studied, the correlation coefficients are so high as to indicate that there is essentially no difference between the samples. The correlation coefficient is high for the Endako joints as well, but the differences between strengths are higher than for the joints from Brenda Mines. This variability

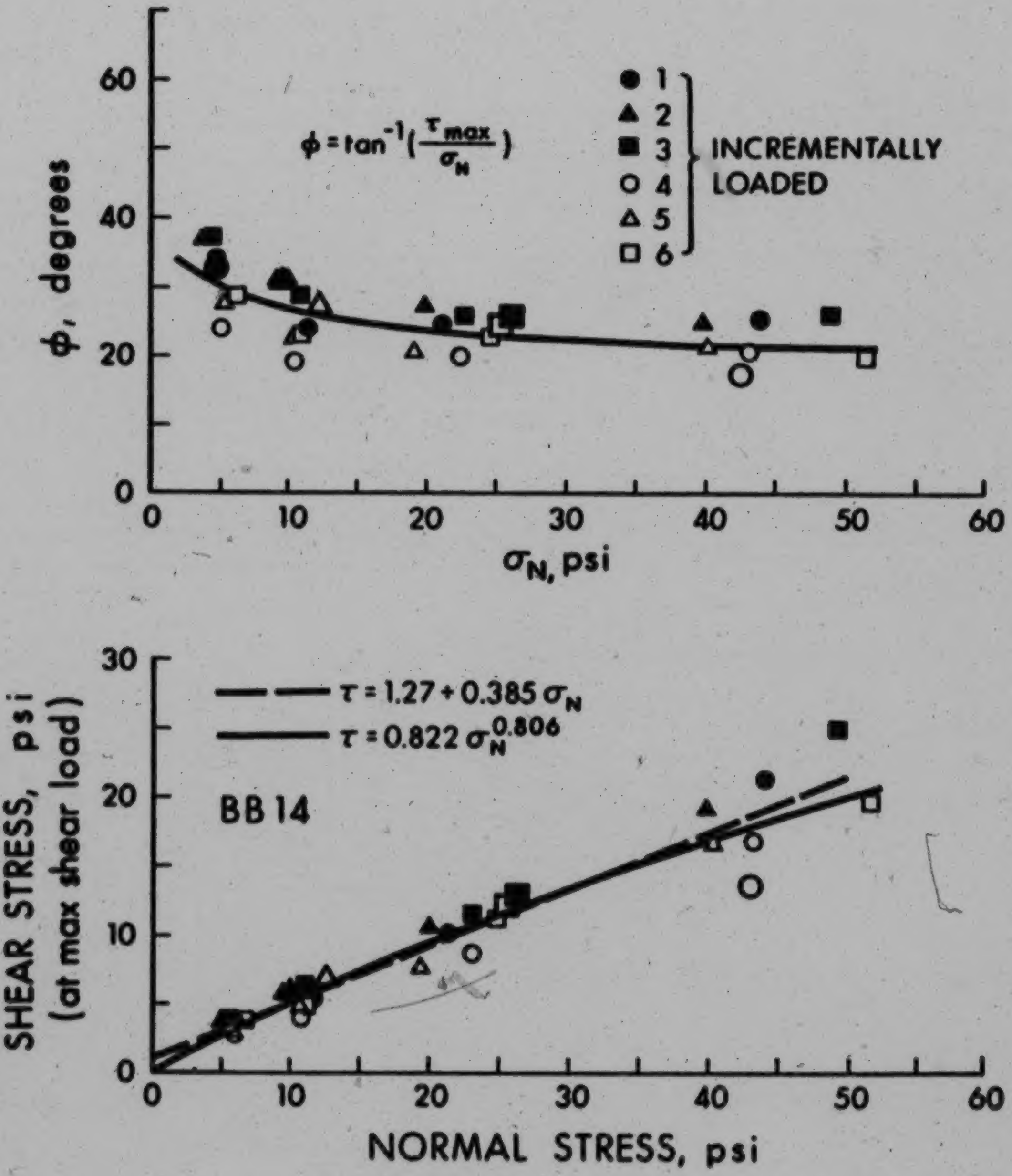

Fig.4.10 Maximum strength envelopes for samples cut from BB14,molybdenite joint from Brenda Mines Ltd.

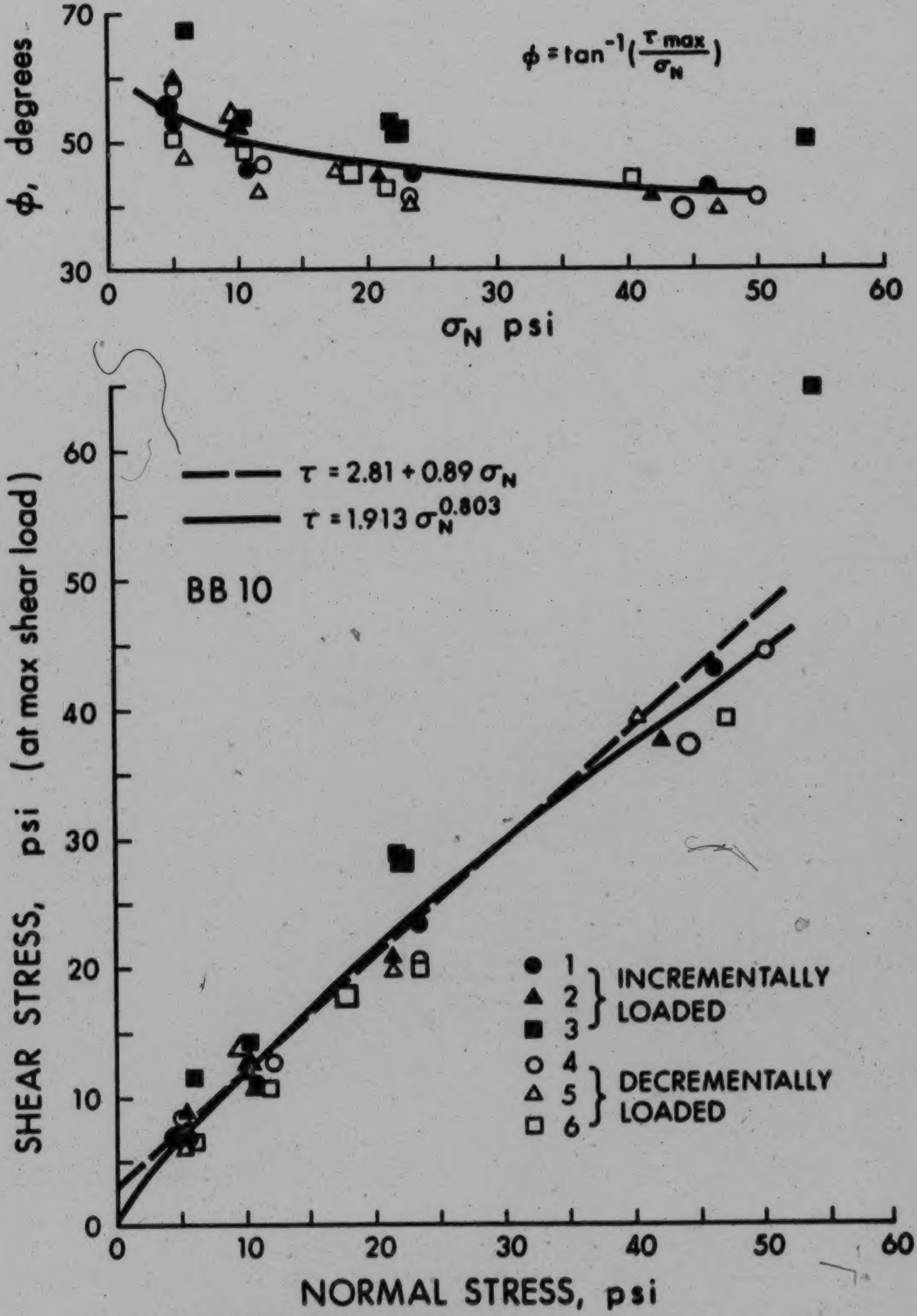

Fig.4.11 Maximum strength envelopes for samples cut from BB10, calcite joint from Brenda Mines Ltd.

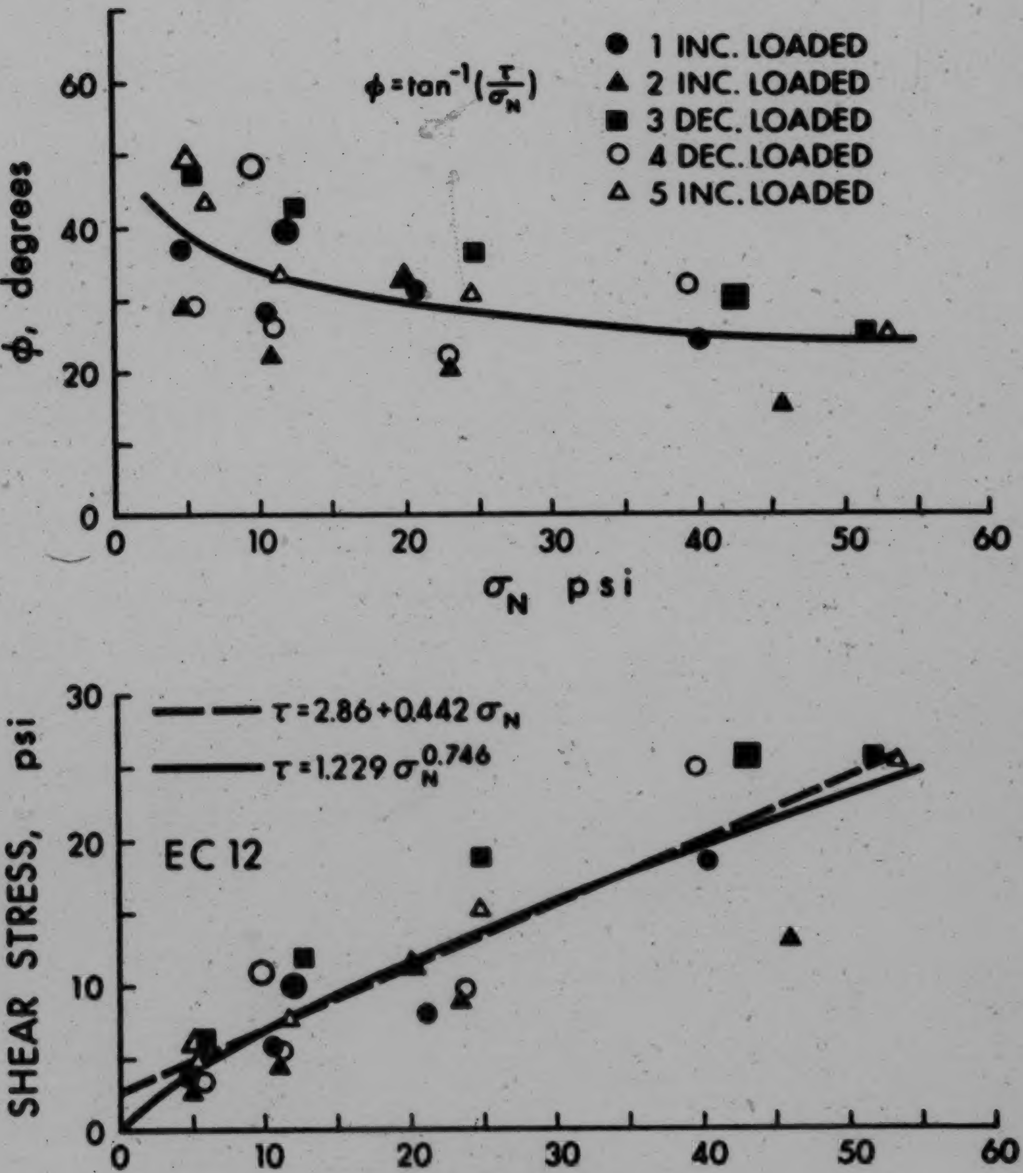

Fig.4.12 Maximum strength envelopes for samples cut from EC12, molybdenite joint from Endako Mines Ltd.

is probably caused by the variable thickness of the thin, partially weathered molybdenite layer. Goodman (1970) indicated that the host material can affect joint strength if the joint infilling covers all the asperities but not to a great thickness. The differences between molybdenite and calcite surfaces were substantial but not surprising. Molybdenite is a natural lubricant, consisting of sheets that are linked by weak bonds between the sulphur atoms of adjacent sheets. On the other hand calcite is massive-structured, consisting of trigonal crystals. These structural differences account for much of the differences measured in the strength values of the joints.

4.10 Testing of large samples

To confirm the test results on the small samples and to check on Krahn's statement that size effects did not exist if the scale of roughness does not change, tests on three larger samples were conducted. One sample of a Brenda molybdenite joint (BB12-4"x4") and two samples of Brenda calcite joints (BC3 and BB5, both 4"x5") were prepared. Unfortunately misalignment of the new larger shear box arrangement negated initial test results. However the equipment was repaired and repeat tests were run on the samples. The results are shown in

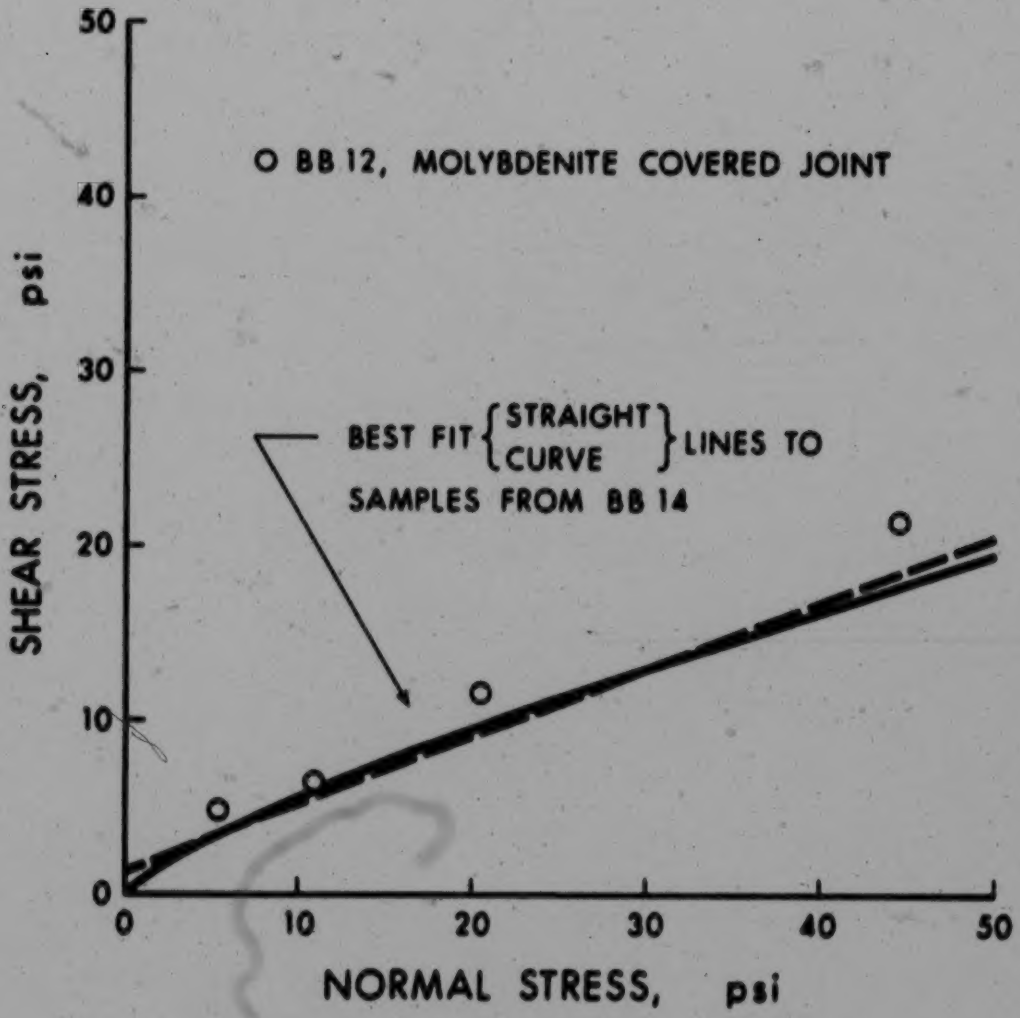

Fig.4.13 Comparison of strength of large molybdenite sample with strength envelopes of smaller samples.

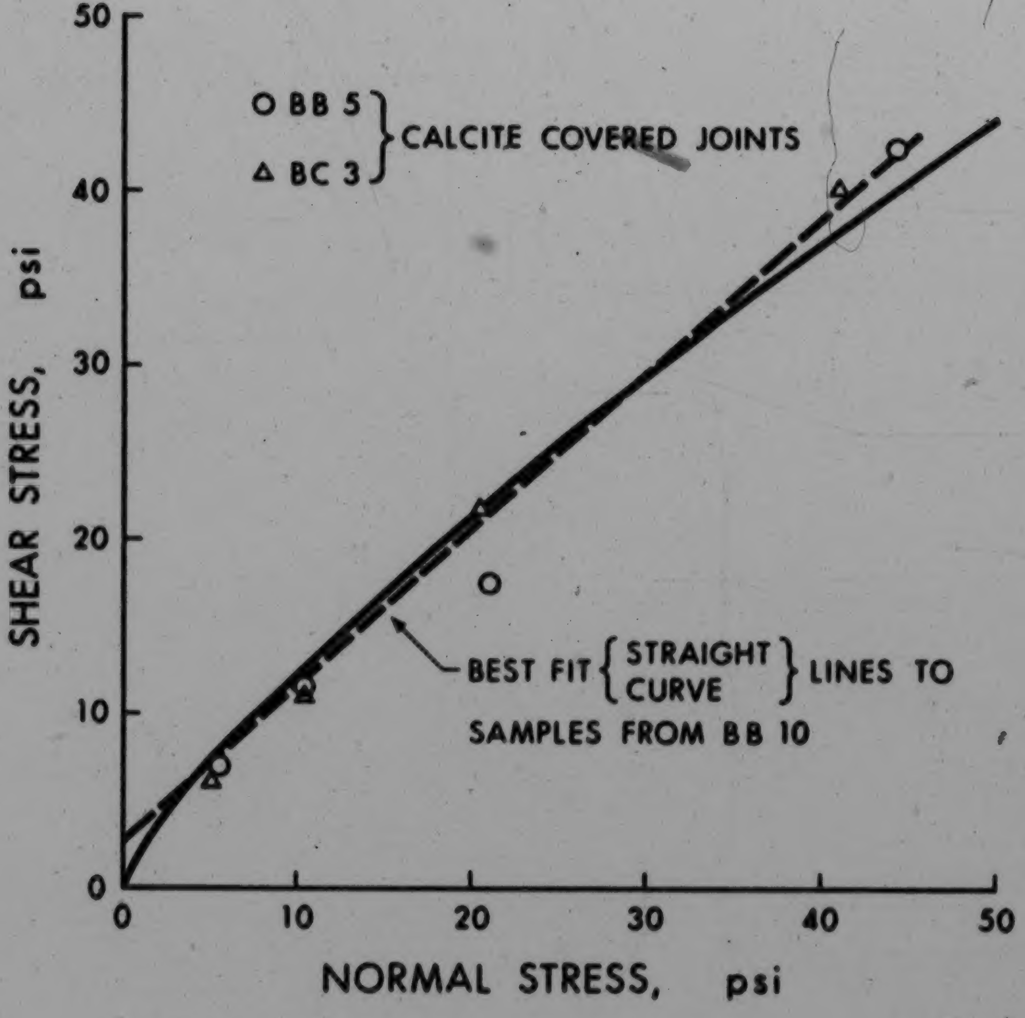

Fig.4.14 Comparison of strength of large calcite samples with strength envelopes of smaller samples.

Figs.4.13 and 4.14. The strengths measured on the large samples fell well within the range of strengths measured on the small samples.

4.11 Effect of molybdenite on joint strength

In order to obtain a measure of the effect of the molybdenite coating on joint strength, the molybdenite was dissolved off the surface of one of the samples (2-BB14) using nitric acid and the sample was retested. The surface profile was measured before testing and the calculated surface parameters remained essentially unchanged from those obtained before the initial testing. After testing the sample did not show the characteristic fine blue-gray streaks exhibited by all the molybdenite samples so it is felt that most, if not all, of the molybdenite was removed. As can be seen in Fig.4.15, considerably higher strengths were measured after the molybdenite was removed. The exposed material that had been under the molybdenite was a phyllosilicate, probably mainly chlorite. Chlorite has a sheet like structure but there is electrical bonding between the sheets, as opposed to the weak intermolecular bonds between molybdenite sheets (Berry and Mason, 1959).

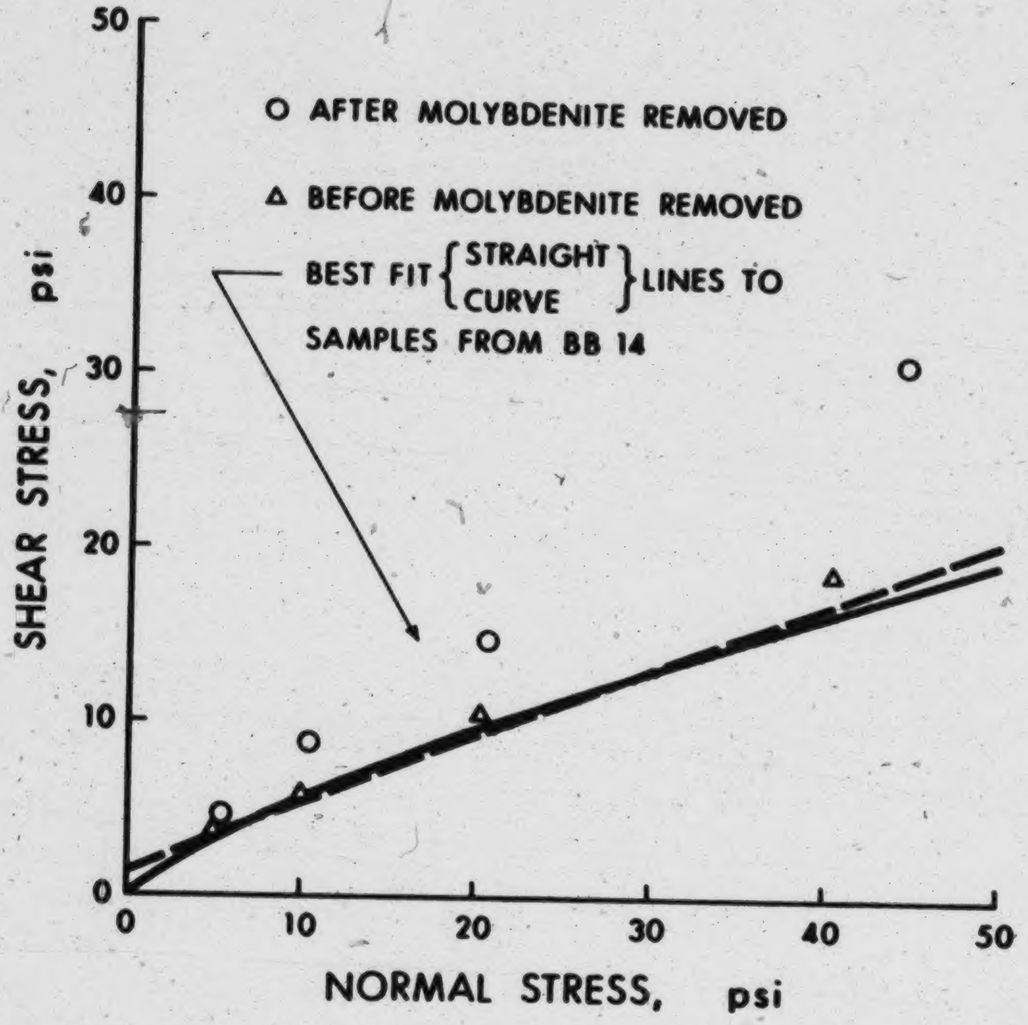

Fig.4.15 Effect of molybdenite on strength.

4.12 Joint roughness

Some typical values of joint roughness parameters and strengths are given in Table 4.1. The main conclusion from this table is that it is the joint material, not the roughness which dominates the strength values. A factor of 2 to 3 in roughness parameters gave very little difference in strength, but a similarly rough surface in different materials gave very different strengths. Some typical surface profiles drawn at a natural scale are given in Figs.4.16 to 4.18.

Comparison of profiles along different lines on the same samples gave maximum deviations from the average of 66% for RMS, 32% for Z_2, and 40% for Z_3. Considering the discussion above these differences are not considered significant and a single profile would adequately represent the sample.

4.13 Comparison of strengths with data from other sources

(a) Calcite joints

The only comparable data found was given by Coulson (1970) who tested joints in siltstone, most of which were covered with a thin layer of calcite. An analysis of his data on calcite surfaces tested at or below 50

TABLE 4.1

Roughness parameters and strengths

Sample Number	Size (in.)	RMS	Z_2	Z_3	ϕ at σ_n = 10psi
Molybdenite coated joints					
1-BB14	2x2	0.00290	0.04947	10.96	24.3°
2-BB14	2x2	0.00812	0.10845	19.62	31.3°
BB12	4x4	0.01745	0.18500	13.68	29.7°
Calcite coated joints					
1-BB10	2x2	0.01163	0.08443	13.41	45.6°
BC3	4x5	0.02550	0.16075	12.12	47.6°
BB5	4x5	0.03809	0.15494	12.93	47.8°
Endako molybdenite joint					
1-EC12	2x2	0/01395	0.22256	67.35	28.0°
Effect of molybdenite on strength Sample 2-BB14 2x2					
Before 1st tests		0.00812	0.10845	19.62	31.3°
After 1st tests		0.00842	0.08383	6.72	
After 'moly' removed		0.00717	0.10494	7.84	40.3°

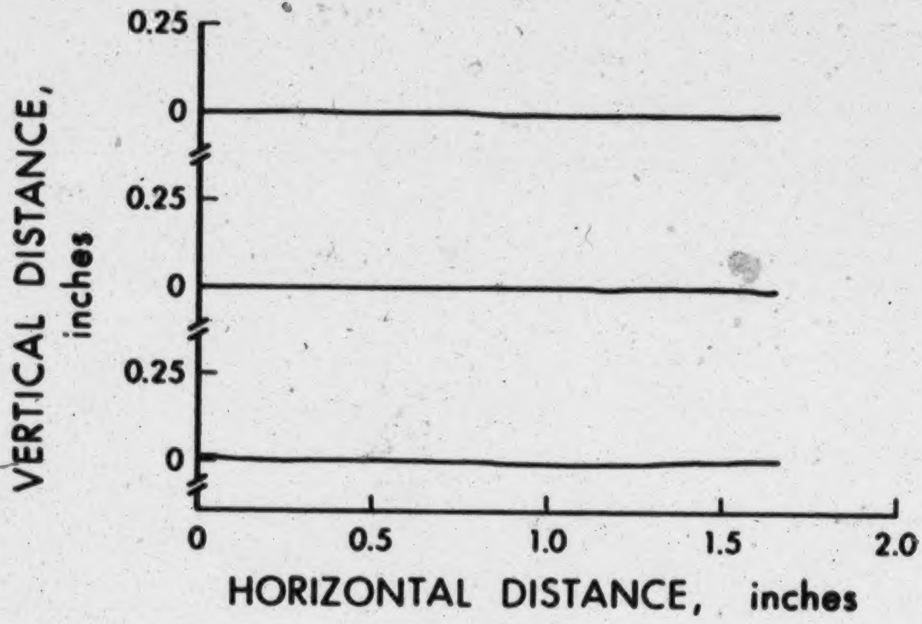

(a) Small sample.

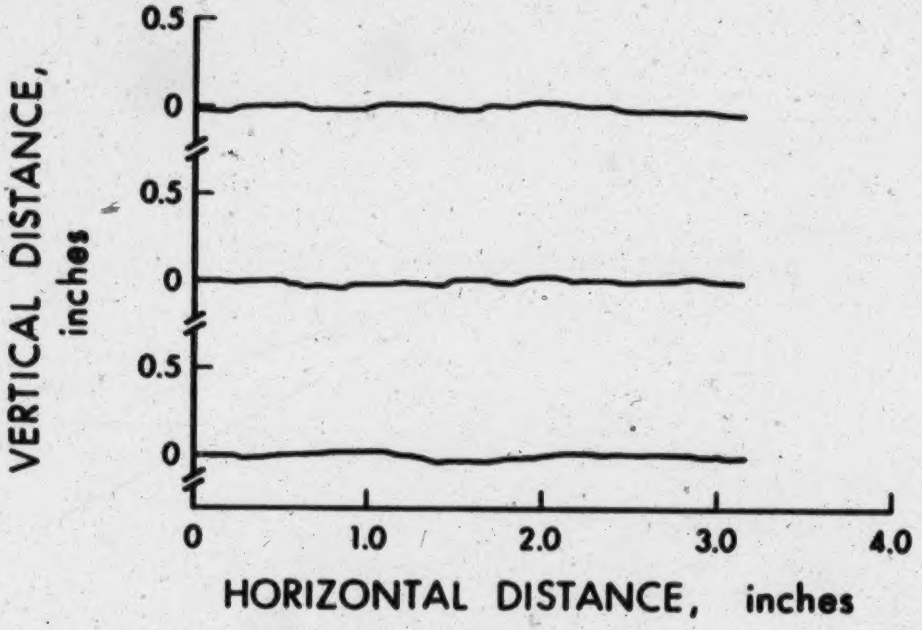

(b) Large sample.

Fig.4.16 Roughness plots for Brenda molybdenite samples.

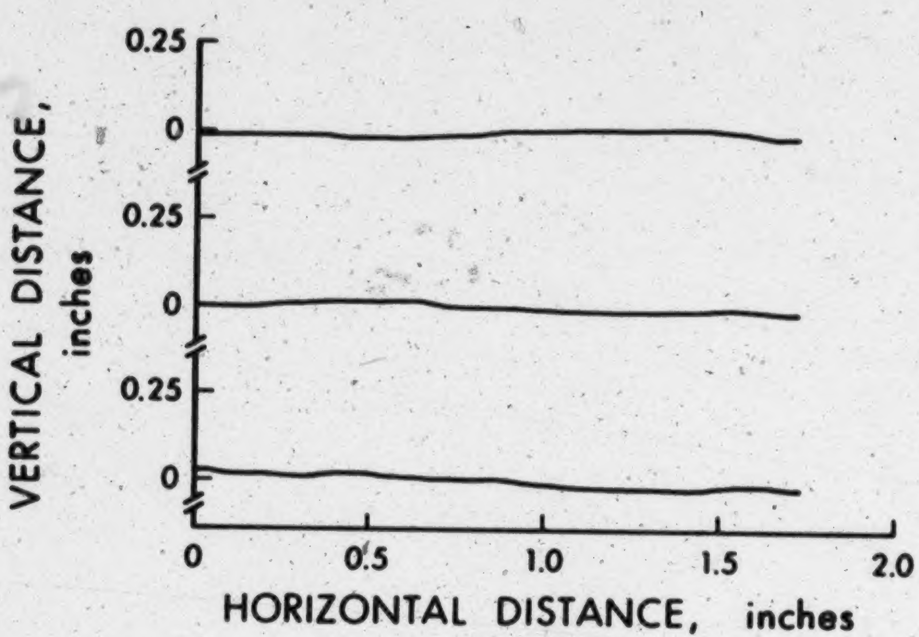

(a) Small sample.

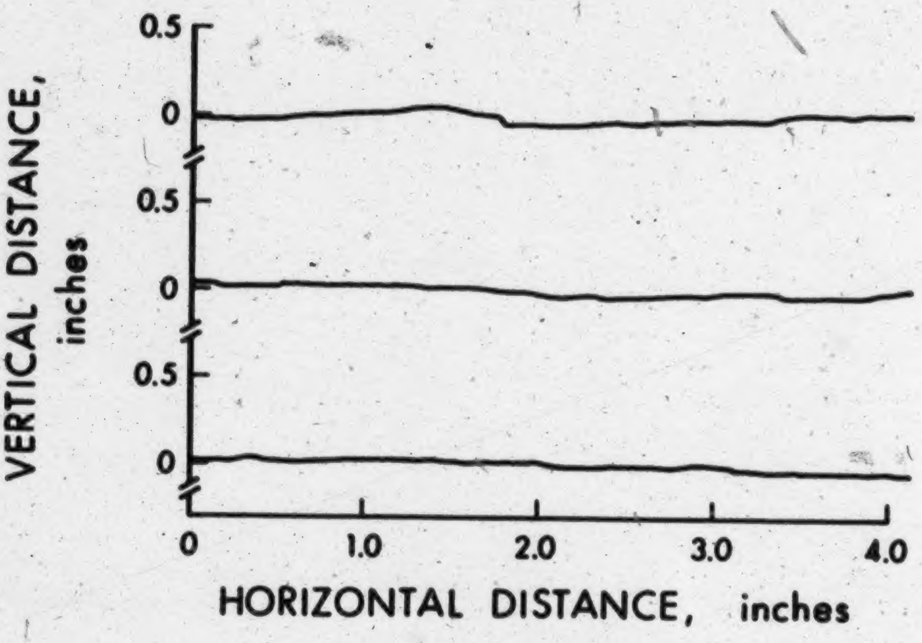

(b) Large sample.

Fig.4.17 Roughness plots for Brenda calcite samples.

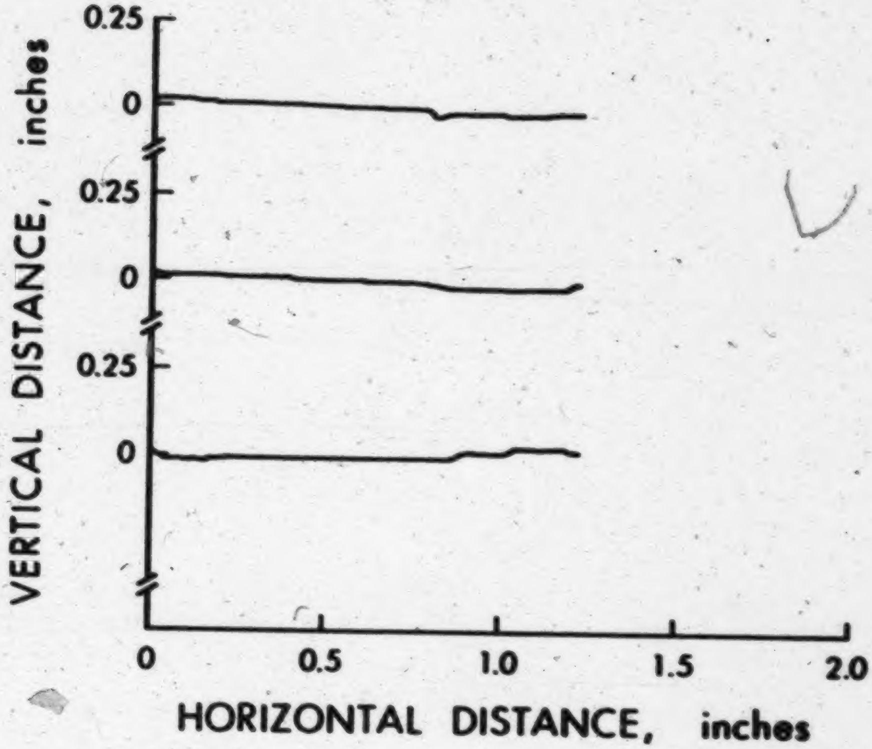

Fig.4.18 Roughness plot for Endako molybdenite sample.

psi gave an average initial ϕ of 55° and an average ultimate ϕ of 36.6°. However geometric effects were considerable with i-angles varying from 5.7° to 34.0° at initial strengths. The average values corrected for the geometric component gave initial (ϕ-i) values of 37.3°. The calculated i-angles for several tests run by the author ranged from -0.2° to 7.2°. If a value of 3° to 4° were added to Coulson's (ϕ-i) values, this would give a friction angle of 41°, just slightly less than that reported by the author.

Horn and Deere (1962) studied the friction of very smooth surfaces in minerals. For oven-dried/air-equilibrated sample they found a coefficient of static friction of 0.12-0.14 for calcite and 0.35 for chlorite. However these values would not apply to natural surfaces with variable roughness and contamination with secondary minerals.

(b) Molybdenite joints

The only data found that might be comparable is that given by Brawner (1970). For the proposed Valley Copper pit in British Columbia he reported strength parameters of a "quartz vein molybdenum slip", over a normal stress range of 130 to 350 psi, to be c= 10 psi, and ϕ = 35°. No details are given but it is quite possible that the veins tested were 'healed' and intact, as opposed to the open joints tested by the author. If this were the case, higher strength values would be expected for Brawner's tests. For similar tests to those of Horn and Deere, Bowden and Tabor (1973) reported a value of about 0.2 for the coefficient of friction of molybdenite crystals, but again this value is for very smooth surfaces. A study of shear plane failures at Endako Mines mentioned previously indicated a friction angle of about 34° for quartz-molybdenite veins.

CHAPTER 5

ANALYSES OF CASE HISTORIES

5.1 General

Except for discussion the final step of a case history is to use the strength parameters obtained from a testing program in an analysis of a failure and to compute the factor of safety. If the computed factor of safety is close to unity, the case history in general confirms the assumptions made and verifies the methods followed. However, even if the factor of safety is close to one, several aspects of the case history may be incorrect but compensating. If the computed factor of safety differs significantly from one, some aspect (or aspects) has (have) been incorrectly interpreted or some assumption regarding details of the failure is incorrect. If the nature of the slide is basically simple it may be possible to quantitatively estimate the errors involved in obtaining a factor of safety other than unity. The aspects of the case history which are important are: (1) the geometry and kinematics of the problem, (2) external factors (water pressures, seismic loading), (3) strength parameters and (4) the method of analysis.

Details on obtaining the strength parameters for these case histories have been given in the previous chapter and it is felt that these strength parameters should reasonably represent the strength of the mass in the field.

The external factors for these case histories are not known and must be assumed. These relatively small slides did not affect mining operations and therefore were not recorded by the mine personnel. Fairly long sections of the wall are blasted at once and it would seem reasonable that blasting of adjacent sections of wall would not induce high seismic loadings unless the wedges happened to occur near the end of a previous section. For the analyses it is assumed that seismic loading is zero.

The joints forming the bases of the wedges of all these slides are shallow, open, continuous, and daylight on the slopes. Under these conditions it seems unlikely that water pressures would build up along the joints. It is possible that the slides could have occurred in the spring with the wall surface frozen while free water existed within the slope. In this case the resisting force on the sliding mass would have been reduced by about one-third if static water pressure built up to the top surface. However it is not clear that this situation necessarily arose. It was assumed that water pressures did not exist in the slopes.

The third factor to be considered is the kinematics of the failure. For the wedge shape slides to be analyzed sliding could possibly occur on either of the basal planes or on both simultaneously (in which case, sliding must occur along the line of intersection of the two planes). If sliding can occur on one plane it will do so in preference to sliding on both planes as the sliding on both planes must overcome resistance on both planes and must occur at a shallower dip than the down-dip direction of one plane. For sliding to be possible on one plane sliding down the dip-direction of the plane must not wedge the block against the other plane (see Hendron et al., 1971). If the only force acting on the wedge is self-weight this can be interpreted visually. When looking along the line of intersection the apparent dip of the plane on which sliding occurs is away from the line of intersection. For the three slides considered, sliding is possible on the right sides of the wedges.

The method of analysis selected is a conventional limit equilibrium analysis. The planes on which sliding occurs are not parallel to the slopes so that a conventional infinite slope analysis cannot be used. The widths of the planes increases up slope so that the areas over which a cohesion intercept would act change over the slopes (if a Coulomb type failure envelope is used). However if the strength is considered purely frictional both the driving force and resisting force will vary directly with the weight of the mass and will "cancel out" in computation of the factor of safety, i.e.

$$F.S. = \frac{\text{resisting force}}{\text{driving force}} = \frac{N\tan\phi'}{S} = \frac{(W\cos\alpha)\tan\phi'}{W\sin\alpha} = \frac{\tan\phi'}{\tan\alpha}$$

In this formula, α is equal to the dip of the right side of the wedge, and ϕ' is an "equivalent friction angle." For the Mohr-Coulomb failure criterion:

$$\phi' = \tan^{-1}(\tau/\sigma_n) = \tan^{-1}((c/\sigma_n)+\tan\phi)$$

For a power law strength envelope:

$$\phi' = \tan^{-1}(\tau/\sigma_n) = \tan^{-1}(k\,\sigma_n^{m}/\sigma_n) = \tan^{-1}(k\,\sigma_n^{m-1})$$

These equivalent friction angles depend on the normal stress level. For the slides considered the average normal stresses on the sliding surfaces were computed on the assumption that the bulk density was 160 pounds per cubic foot,and inserted in the above formulae with the strength parameters obtained from testing, and the average $\tan\phi'$ from the two formulae was computed to give working values. These are:

(1) Brenda Slide no. 1, $\phi' = 28.1°$

(2) Brenda Slide no. 2, $\phi' = 56.4°$

(3) Endako Slide, $\phi' = 40.2°$

The differences in $\tan\phi'$ calculated from the two formulae were 2% to 14% of the average. Values of ϕ' are shown together with strength envelopes in Fig.5.1

Placing these values into the formula for the factor of

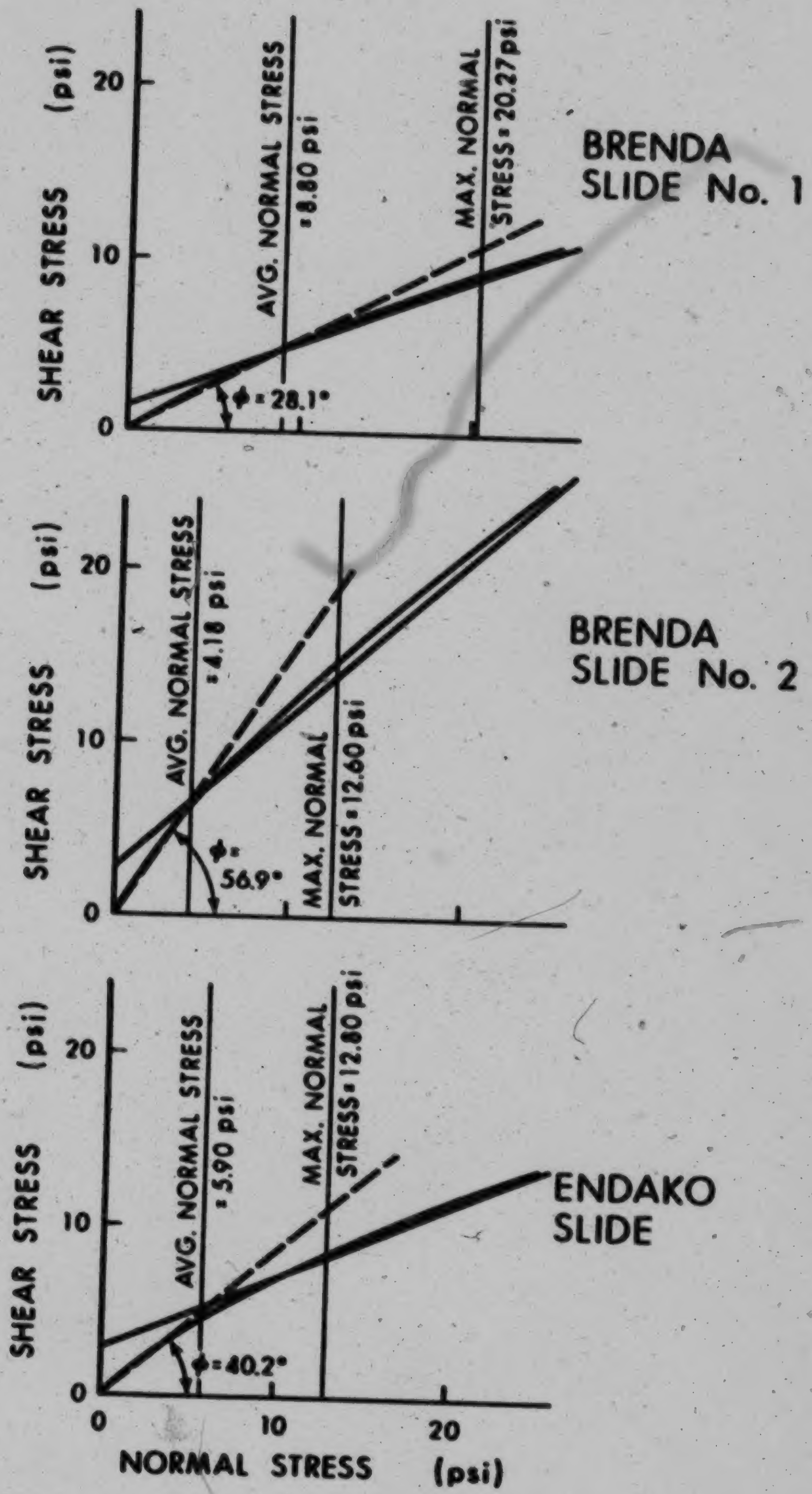

Fig 5.1 Equivalent friction angles for analyses of slides.

safety we obtain:

(1) Brenda Slide no. 1

$$F.S. = \frac{\tan 28.1^\circ}{\tan 49.4^\circ} = 0.46$$

(2) Brenda Slide no. 2

$$F.S. = \frac{\tan 56.4^\circ}{\tan 60.4^\circ} = 0.86$$

(3) Endako Slide

$$F.S. = \frac{\tan 40.2^\circ}{\tan 57^\circ} = 0.55$$

5.2 Discussion

(a) Brenda Slide no. 2

As was mentioned in Chapter 3 one of the reasons for choosing to study these slides was their simplicity. All three slides occurred as rigid block failures on one plane covered with one material. However a number of assumptions had to be made in all three case histories and the effect of possibly incorrect assumptions will vary for each failure.

The calculated factor of safety for this slide is 0.86. This value is felt to be reasonably close to the anticipated value of unity. Since the maximum normal stress that does occur is 12.6 psi, the data was re-evaluated using the tests for which the normal stress was less than 12.6 psi. If this is done the average equivalent friction angle rises to 58.6° giving a factor of safety of 0.94. The small block of rock that remained on the right side of the failure plane (see Fig.3.6) was not measured, but its height was judged to be about one-third of the height of the failed portion. This assumption would give an average normal stress under the block of about 100 psf or 0.7 psi. To extrapolate data to this low value would be dangerous, but an equivalent friction angle would certainly be in excess of 60°, indicating that the block is stable. Thus the presence of the small block would indicate that the method and assumptions of the analysis are basically correct.

(b) Brenda Slide no.1 and Endako Slide.

The relatively low factors of safety computed for these two slides indicate that some aspect (or aspects) of the case histories is (are) incorrect.

In order to expect a factor of safety of unity in a back analysis it is implicitly assumed that a slide was at the point of equilibrium when failure occurred. Consider the proposed cut shown in Fig.5.2(a). Before the cut is made the area is stable because of the complete confinement provided by the material in the proposed cut. If the cut were made instantaneously failure would occur immediately (Fig.5.2(b)). The slope has 'passed through' the point of limit equilibrium.

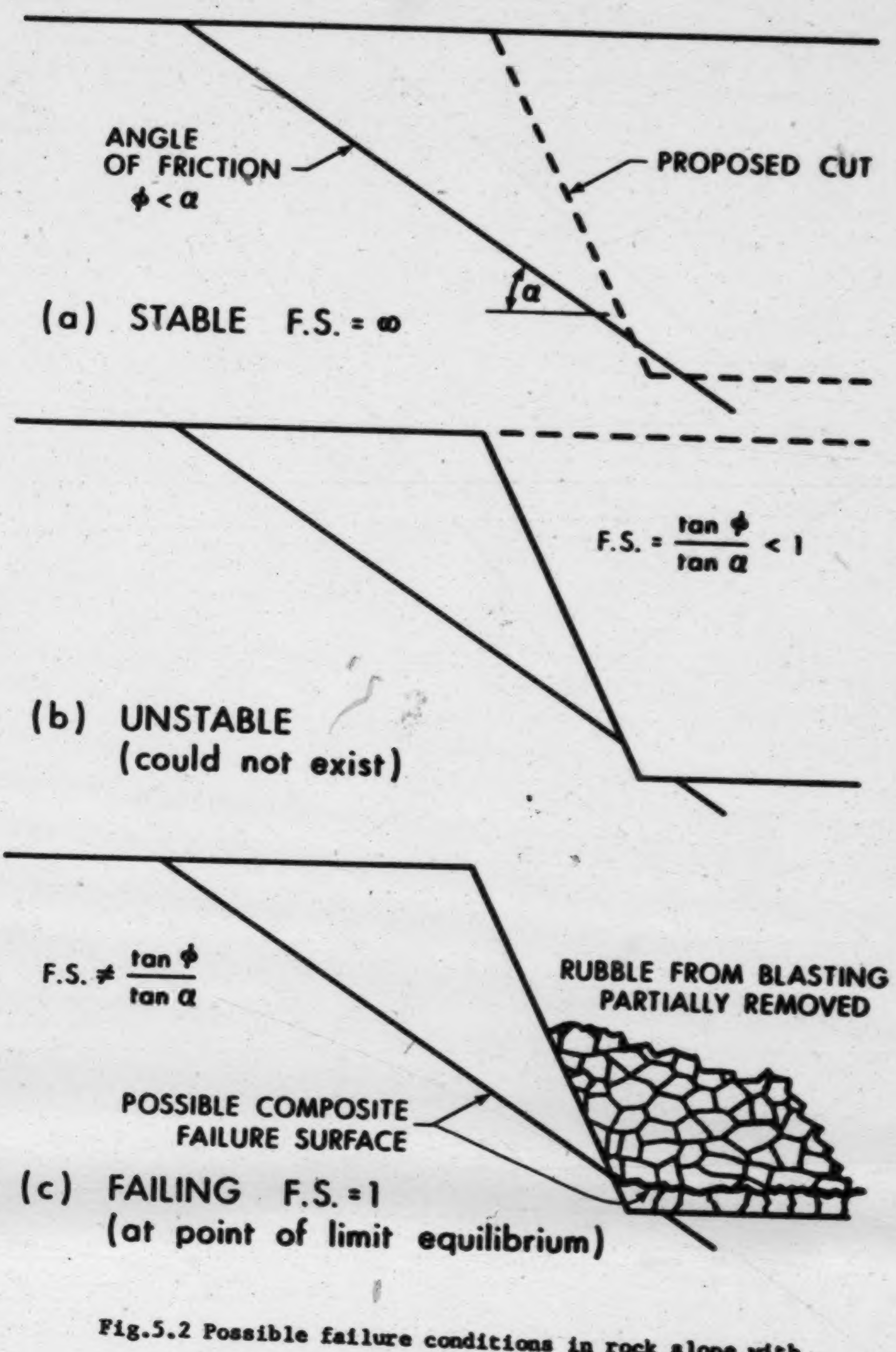
ANGLE
OF FRICTION
$\phi < \alpha$
PROPOSED CUT
α
(a) STABLE F.S. = ∞
F.S. = $\frac{\tan \phi}{\tan \alpha} < 1$
(b) UNSTABLE
(could not exist)
F.S. ≠ $\frac{\tan \phi}{\tan \alpha}$
RUBBLE FROM BLASTING
PARTIALLY REMOVED
POSSIBLE COMPOSITE
FAILURE SURFACE
(c) FAILING F.S. = 1
(at point of limit equilibrium)

Fig.5.2 Possible failure conditions in rock slope with computed factor of safety less than unity.

In practice the cut is made gradually by blasting the cut, then hauling the rubble away. Part of the resistance to sliding of the slope is provided by the rubble, and this resistance will decrease as portions of the rubble are removed. At some point before all of the rubble is removed, the factor of safety will drop to unity, at which point failure will occur (Fig.5.2(c)).

There are other possible reasons for obtaining a factor of safety less than unity for these slides. The surfaces forming the left sides of the wedges may not have been open, continuous joints as assumed. Some smaller blocks beneath the assumed left surfaces may have been integral parts of the main slide masses and might have been carried down with the main slide masses, if they were favourably oriented. As these smaller blocks were pulled out of the left sides of the walls, shearing resistance would have been developed along the edges of the blocks, increasing the factor of safety. Alternately the contacts between these small blocks and the main masses may have failed in tension or shear.

For the slide at Endako the failure surface was not accessible and was partially covered with debris. It is possible that the slide surface was not continuous but contained bridges of solid rock that gave an "effective cohesion" strength component to the surface. However the surfaces of sliding at Brenda were fully exposed and there was no evidence of rock bridges.

For Brenda Slide no. 1 approximate analyses were carried out to determine the magnitude of restraints required to give a factor of safety of unity. Assuming a density of 160 pounds per cubic foot(pcf) the weight of the sliding mass was calculated to be $2.48(10^6)$ pounds or about 1250 tons. Resolving the weight normal and parallel to the dip-direction and considering the frictional resistance leaves an unbalanced force down the plane of about $7.5(10^5)$ pounds.

If small rock rock bridges existed along the left side of the wedge, these would have to fail for the mass to slide. The direction of movement (down-dip) has a small component away from the line of intersection. As a rough approximation it could be assumed that the rock bridges failed in shear under zero normal stress. Using the strength law for intact rock proposed by McClintock and Walsh (1962) the shear strength would be equal to twice the tensile strength. Assuming a tensile strength of 1000 pounds per square inch, approximately that measured in Brazilian tests on granite (Peng and Johnson,1972), would give a required contact area of:

$$A = \frac{7.5(10^5)}{2(10^3)} = 375 \text{ in.}^2 = 2.6 \text{ ft.}^2 \text{(square feet)}$$

The area of the left side of the failure mass was calculated to be 880 ft.^{2}, so the required degree of discontinuity of the joint forming the left side would only be about 0.3%. This is so small that it would be essentially impossible to realize that it existed if the joint had been sampled by borehole techniques.

Resistance to sliding might have been provided by rubble at the toe of the slide. If we consider a horizontal force, R, applied perpendicular to the strike of the failure plane, we can resolve this force parallel and perpendicular to the dip-direction. The parallel component will act up the plane and will be equal to R $\cos\alpha$, where α is the dip. The normal component will also increase the resistance to sliding by increasing the normal force on the plane. This increased frictional resistance will be equal R $\sin\alpha \tan\phi$. Equating the sum of the increased resisting forces to the excess driving force gives a required horizontal force of $7(10^5)$ pounds.

To obtain an estimate of the amount of rubble required to provide this horizontal force, it was assumed that the rubble surface was horizontal and the shear strength of the rubble was given by a friction angle, ϕ, of 45°. To analyze the problem as a two-dimensional passive resistance situation, it was necessary to consider an equivalent force per foot width of the slide. The slide would push as a triangular shape into the rubble. For the same height and area as the triangle, it was calculated that the width of an equivalent rectangle would be 0.77h, where h is the height of the rubble above the toe of the slide necessary to provide the required horizontal resistance. Therefore an equivalent force per foot would be given by R/(0.77h).

This equivalent force per foot can then be compared to the classical passive force, P, given by:

$$P=0.5\gamma Kh^2$$

where γ = density of the rubble

K = coefficent of passive earth pressure

Considering a porosity of about 20% for the rubble the density of the rubble would be 130 pounds per cubic foot. The coefficient of passive earth pressure is given by:

$$K = \tan^2(45^\circ+\phi/2) = 5.8, \text{ for } \phi = 45^\circ$$

Therefore:

$$\frac{P}{0.77h} = 0.5\gamma Kh^2$$

or:

$$h^3 = \frac{2R}{0.77\gamma K}$$

Solving for h gives a required height of rubble above the toe of about 8.5 feet. To satisfy the passive failure assumptions the horizontal rubble would have to extend about

20 feet out the wall.

It is felt that the most likely cause of the low factors of safety obtained was the presence of blasted rubble at the toes of the slopes, that was not accounted for in the analyses. It should be noted that if the slides had been back analyzed, using the same assumptions, to obtain shear strength parameters, the calculated strength parameters would be higher than the actual parameters. This indicates that strength values obtained from back analyses of slides may be considerably in error, on the unsafe side, if the complete history of failure is not known.

The fact that no factors of safety greater than unity were computed indicates that the working hypothesis was probably correct, or at least does not prove that the hypothesis is incorrect. Thus it can at least tenatively be assumed that the maximum shear strength measured in direct shear tests on joints at low normal stresses governs field behaviour.

CHAPTER 6

SUMMARY

Rock slope stability is a complex problem, but a considerable amount of theoretical work has been done on the subject. Case histories to give confidence to these theoretical solutions are now needed. Three case histories were studied in an attempt to contribute to fufilling the need for case histories. In studying these case histories several interesting points were developed.

The drilling procedure used and described was reasonably successful in obtaining samples. Block sampling was also found to be successful on exposures.

During the testing portion of the work it was found that repeated testing on natural joints at low normal stresses gave reliable strengths. It was also found that testing of small samples gave strengths comparable to those obtained on larger samples. These two factors allowed a large number of tests to be conducted on a relatively small amount of sample.

Over the range of normal stresses used during testing it was found that the data could be fitted equally well to a straight line or a power curve.However the straight line had a "cohesion" intercept. Since the samples were originally separate blocks and repeated testing indicated that no significant surface damage occurred during testing, it is difficult to assign any physical meaning to a cohesion intercept. Thus it is felt that a power curve fitted to the data gives a more reasonable representation of the decrease of friction with increasing normal stress.

The molybdenite joints tested had a relatively low shear strength compared to the calcite joints tested. This finding was expected as molybdenite is a natural lubricant.

The three case histories studied were small, bench-size failures chosen for their simplicity. Unfortunately, as in most case histories, all of the details of the three failures were not known and assumptions had to made. In one case history, the results indicated that the assumptions were reasonable, but in the other cases it appears that the pre-failure geometry was more complex than had been assumed.

The case history of Brenda slide no. 1 would indicate that the methods followed presented a reasonable approach to evaluating the stability of rock slopes, at least for small failures occurring on continuous, relatively planar joints. This type of failure can be important in cut slopes around civil engineering works or on access roads in open pit mines. This case history indicates also that the maximum strength measured in testing, at least at low normal stresses, governs the field behaviour.

The two case histories that gave low factors of safety indicate that back-analyses of slides to obtain shear strength parameters may give results higher than the actual strength parameters if all of the details of the slides are not known.

It is hoped that future similar contributions will be forthcoming with more details of the failure history available. Increased co-operation between researchers and mine personnel could result in the recording of these details. In addition studies of larger slides might give better results as effects of boundary conditions should generally be less.

Finally it is hoped that some of the principles described in this thesis will be applied in field situations. Black and Hoek (1967) stated the results of failure to apply the principles of rock mechanics as follows: "The penalty for the practical engineer for attempting to defy the known laws of strata behaviour is inexorably exacted in hard economic terms and sometimes in blood."

REFERENCES

Barton, N.R. 1972. A model study of rock-joint deformation. Int. Jnl. Rock Mech. & Min. Sci. vol. 9, p. 579-602.

Bauer, A., and Calder, P.N. 1971. The influence and evaluation of blasting on stability. Stability in Open Pit Mining. Procs. 1st Int. Conf. on Stability in Open Pit Mining. p. 83-94.

Berry, L.G., and Mason, B. 1959. Mineralogy Concepts Descriptions Determinations. W. H. Freeman and Company, San Francisco. 630 p.

Bjerrum, L., and Jorstad, F. 1963. Discussion on: An approach to rock mechanics, by K.W. John. Procs. Am. Soc. Civil Engrs., vol. 89, no. sm1, p. 300-302.

Black, R.A.L., and Hoek, E. 1967. Status of rock mechanics as applied to mining. Status of Practical Rock Mech. 9th Symp. on Rock Mech., Golden, Colorado. p. 5-26

Bowden, F.P., and Tabor, D. 1973. Friction -an Introduction to Tribology. Anchor Press/Doubleday. Garden City, New York. 178p.

Brawner, C.O., and Huculak, N.A. 1961. The use of horizontal drains in landslide stabilization. 42nd Conf., Canadian Good Roads Association, Banff. p. 383-400.

Brawner, C.O. 1970. Stability investigations of rock slopes in Canadian mining projects. Procs. 2nd Cong. Int. Soc. Rock Mech., Belgrade. vol. 3, p. 7-8.

Brawner, C.O. 1971a. Introduction. Stability in Open Pit Mining. Procs. 1st Int. Conf. on Stability in Open Pit Mining., Vancouver. p. 1-3.

Brawner, C.O. 1971b. Case studies of stability on mining projects. Stability in Open Pit Mining. Procs. 1st Int. Conf. on Stability in Open Pit Mining, Vancouver. p. 205-226.

Brawner, C.O., Pentz, D.L., and Sharp, J.C. 1972. Stability studies of a footwall slope in layered coal deposit.

Stability of Rock Slopes. 13th Symp. on Rock Mech., University of Illinois, Urbana, Illinois. p. 329-365.

Bridges, M.C. and Best, E.J. 1971. Application of oriented drill core in structural geology at Mount Isa. Procs. 1st Australia - New Zealand Conf. on Geomechanics, Melbourne. p. 211-216.

Cahoon, J.A. 1973. Pit wall stability - Brenda. Internal Paper. Unpublished.

Coulson, J.H. 1970. The effects of surface roughness on the shear strength of joints in rock. Ph. D. Thesis, University of Illinois, Urbana, Illinois.

Coulson, J.H. 1972. Shear strength of flat surfaces in rock. Stability of Rock Slopes. 13th Symp. on Rock Mech., University of Illinois, Urbana, Illinois. p. 77-105.

Cundall, P.A. 1971 The measurement and analysis of accelerations in rock slopes. Ph. D. Thesis, University of London.

De Freitas, M.H., and Watters, R.J. 1973. Some field examples of toppling failure. Geotechnique, vol. 23, no. 4, p. 495-514.

Goodman, R.E. 1970. The deformability of joints. Determination of the In-situ Modulus of Deformation. ASTM Special Tech. Publ. No. 477. p. 174-196.

Goodman, R.E., Taylor, R.C., and Brekke, T. 1968. A model for the mechanics of jointed rock. Procs. Am. Soc. Civil Engrs., vol. 94, no. sm3, p. 637-659.

Hendron, A.J. Jr., Cording, E.J. and Aiyer, A.K. 1971. Analytical and graphical methods for the analysis of slopes in rocks. U.S. Army Engineer Waterways Experiment Station, Vicksburg. Tech. Rept. No. 36.

Heuze, F.E., and Goodman, R.E. 1972. Three-dimensional approach for design of cuts in jointed rock. Stability of Rock Slopes. 13th Symp. on Rock Mech., University of Illinois, Urbana, Illinois. p. 397-441.

Hoek, E., and Sharp, J.C. 1970. Improving the stability of rock slopes by drainage. Procs. Symp. Planning Open Pit Mines. S.A. Inst. Min. & Met. p. 193-198.

Hoek, E. 1970. Estimating the stability of excavated slopes in opencast mines. Mining Industries Transactions, Inst. Min. & Metall. vol. 79, p. A109-A132.

Hoek, E. 1971a. Discussion of: Estimating the stability of excavated slopes in opencast mines. Mining Industries Transactions, Inst. Min. & Metall. vol. 80, p. A72.

Hoek, E. 1971b. Influence of rock structure on stability of rock slopes. Stability in Open Pit Mining. Procs. 1st Int. Conf. on Stability in Open Pit Mining, Vancouver. p. 49-63.

Hoek, E. 1971c. Discussion. Stability in Open Pit Mining. Procs. 1st Int. Conf. on Stability in Open Pit Mining, Vancouver. p. 235.

Hoek, E. 1971d. Rock slope stability -how far away are reliable design methods? Procs. 1st Australia - New Zealand Conf. on Geomechanics, Melbourne. p. 307-313.

Horn, H.M., and Deere, D.U. 1962. Frictional characteristics of minerals. Geotechnique. vol. 12, no. 4, p. 319-335.

Jaeger, J.C. 1971. Friction of rocks and stability of rock slopes. Geotechnique. vol. 21, no. 2, p. 97-134.

Jennings, J.E. 1970. A mathematical theory for the calculation of the stability of slopes in open-cast mines. Procs. Symp. Planning Open Pit Mines. S.A. Inst. Min. & Metall. p. 87-102.

John, K.W. 1958. Electronic borehole camera for TV projection. Civil Engineering. A.S.C.E. vol. 28, p. 197.

John, K.W. 1962. An approach to rock mechanics. Procs. Am. Soc. Civil Engrs., vol. 88, no. sm4, p. 1-30.

John, K.W. 1968. Graphical stability analysis of slopes in jointed rock. Procs. Am. Soc. Civil Engrs., vol. 94, no. sm2, p. 497-526.

Kim, Y.S., and Dimock, R.R., Jr. 1972. Model study on the slope stability around an open pit. Stability of Rock Slopes. 13th Symp. on Rock Mech., University of Illinois, Urbana, Illinois. p. 201-225.

Kimura, E.T., and Drummond, A.D. 1969. Geology of the Endako molybdenum deposit. Can. Min. & Metall. Bull., July, 1969. p. 1-10.

Krahn, J. 1974. Rock slope stability with emphasis on the Frank slide. Ph. D. Thesis, University of Alberta, Edmonton.

Ladanyi, B., and Archambault, G. 1969. Simulation of shear behaviour of a jointed rock mass. Rock Mechanics - Theory and Practice. 11th Symp. on Rock Mech, Berkeley. p. 461-500.

Latjai, E.Z. 1969. Shear strength of weakness planes in rock. Int. Jnl. Rock Mech. & Min. Sci. vol. 6, p. 499-515.

Londe, P., Vigier, G., and Vormeringer, R. 1969. Stability of rock slopes, a three-dimensional study. Procs. Am. Soc. Civil Engrs. vol. 95, no. sm1, p. 235-262.

Lyell, K.A. 1970. The interpretation of water pressure factors for use in the slope theory. Proc. Symp. Planning Open Pit Mines, S.A. Inst. Min. & Metall. p. 73-85.

Mahtab, M.A. 1970. Three-dimensional finite element analysis of jointed rock slopes. Ph. D. Thesis, University of California, Berkeley.

Maini, Y.N.T., Noorishad, J. and Sharp, J.C. 1972. Theoretical and field considerations on the determination of insitu hydraulic parameters in fractured rock. Procs. Symp. Percolation through Fissured Rock, Stuttgart. Int. Soc. Rock Mech., Int. Assoc. Eng. Geol. p. T1-E,1-8.

McClintock, F.A., and Walsh, J.B. 1962. Friction on Griffith cracks under pressure. Procs. 4th National Congress on Applied Mechanics, Berkeley. p. 1015-1021.

McLeod, H.N. 1971. Slope stability investigations at Endako Mines Limited. Unpublished.

McMahon, B.K. 1971. A statistical method for the design of rock slopes. Procs. 1st Australia - New Zealand Conf. on Geomechanics, Melbourne. p. 314-321.

Morgenstern, N.R. 1971. The influence of groundwater on stability. Stability in Open Pit Mining. Procs. 1st Int. Conf. on Stability in Open Pit Mining, Vancouver. p. 65-82.

Morgenstern, N.R., and Price, V.E. 1965. The analysis of the stability of general slip surfaces. Geotechnique. vol. 15, no. 1, p. 79-93.

Mueller, L. 1963. Application of rock mechanics in the design of rock slopes. Procs. Int. Conf. on State of Stress in the Earth's Crust, Santa Monica, California. p. 575-605.

Mueller, L., and Hofmann, H. 1970. Selection, compilation, and assessment of geological data for the slope problem. Procs. Symp. Planning Open Pit Mines. S.A. Inst. Min. & Metall. p. 153-170.

Myung, J.I., and Boltosser, R.W. 1972. Fracture evaluation by the borehole logging method. Stability of Rock Slopes. 13th Symp. on Rock Mech. University of Illinois, Urbana, Illinois, p. 31-56.

Pariseau, W.G. 1973. Influence of rock properties variability on mine opening stability analysis. Preprint paper for 9th Can. Symp. Rock Mech., Montreal.

Patton, F.D. 1966a. Multiple modes of shear failure in rock and related materials. Ph. D. Thesis, Univ. of Illinois, Urbana.

Patton, F.D. 1966b. Multiple modes of shear failure in rock. Procs. 1st Cong. Int. Soc. Rock Mech., Lisbon. vol. 1, p. 509-513.

Peng, S., and Johnson, A.M. 1972. Crack growth and faulting in cylindrical specimens of Chelmsford granite. Int. Jnl. Rock Mech. & Min. Sci. vol. 9,p. 37-86.

Pentz, D.L. 1971. Methods of analysis of stability of rock slopes. Stability in Open Pit Mining. Procs. 1st Conf. on Stability in Open Pit Mining, Vancouver. p. 119-141.

Piteau, D.R. 1970. Geological factors significant to the stability of slopes cut in rock. Procs. Symp. Planning Open Pit Mines, S.A. Inst. Min. & Metall. p. 33-53.

Piteau, D.R., and Jennings, J.E. 1970. The effects of plan geometry on the stability of natural slopes in rock in the Kimberley area. Procs. 2nd Cong. Int. Soc. Rock Mech., Belgrade. vol. 3, p. 289-295.

Piteau, D.R., and Russell, L. 1972. Cumulative sums technique: a new approach to analyzing joints in rock. Stability of Rock Slopes. 13th Symp. on Rock Mech., University of Illinois, Urbana, Illinois. p. 1-30.

Robertson, A. MacG. 1970. The interpretation of geological factors for use in slope theory. Proc. Symp. Planning Open Pit Mines, S.A. Inst. Min. & Metall., p. 55-71.

Seed, H.B., Idriss, I.M., and Kiefer, F.W. 1969. Characteristics of rock motions during earthquakes. Proc. Am. Soc. Civil Engrs. vol. 95, no. sm5, p. 1199-1218.

Seegmiller, B.L. 1972. Rock stability analysis at Twin Buttes. Stability of Rock Slopes. 13th Symp. on Rock Mech, University of illinois, Urbana, Illinois. p. 511-536.

Sharp, J.C. 1970. Drainage characteristics of subsurface galleries. Proc. 2nd Cong. Int. Soc. Rock Mech., Belgrade. vol. 3, p. 197.

Shuk, T. 1970. Optimization of slopes designed in rock. Procs. 2nd Int. Cong. Int. Soc. Rock Mech., Belgrade. vol. 3, p. 275-280.

Snow, D.T. 1968. Rock fracture spacings, openings, and porosities. Procs. Am. Soc. Civil Engrs. vol. 94, no. sm1, p. 73-91.

Snow, D.T. 1970. The frequency and apertures of fractures in rock. Int. Jnl. Rock Mech. & Min. Sci. vol. 7, p. 23-40.

Stimpson, B. 1970. Modelling materials for engineering rock mechanics. Int. Jnl. Rock Mech. & Min. Sci. vol. 7, p. 77-121.

Terzaghi, K. 1962. Stability of steep slopes on hard unweathered rock. Geotechnique, vol. 12, no. 4, p. 251-270.

Terzaghi, R.D. 1965. Sources of error in joint surveys. Geotechnique, vol. 15, no. 3, p. 287-304.

Trainer, F.W., and Eddy, J.E. 1964. A periscope for the study of borehole walls, and its use in ground-water studies in Niagra county, New York. U.S. Geol. Survey Prof. paper 501-D, p. D203-D206.

Wallace, G.B., Slebir, E.J., and Anderson, F.A. 1969. Foundation testing for Auburn dam. Rock Mechanics -

Theory and Practice. 11th Symp. on Rock Mech., Berkeley. p. 461-500.

Wittke, W. 1970. Three-dimensional percolation of fissured rock. Procs. Symp. Planning Open Pit Mines. S.A. Inst. Min. & Metall. p. 181-191.

APPENDIX A

SHEAR TEST RESULTS

Tables A-1 to A-4 summarize all the strength testing done for this thesis. The shear strength, τ, for each test is based on the maximum shear load measured in that test as recorded by the x-y recorder. These values of τ will not coincide exactly with those shown on the following pages which are based on the recording done by the digital printer. Generally the strength based on the digital printer recordings is 5% to 10% lower. The angle shown on the tables is equal to $\tan^{1}(\tau/\sigma_n)$.

The remaining pages of the appendix give typical test results. At least one test on every sample tested is given, and a complete series of tests on one sample from each field sample used for the small tests is given. The identification of each test is of the form k-llmm-n, where k= lab sample number from field sample llmm and n= repeat test number, i.e. if n is blank, this indicates the initial test on the sample,, if n= 1, this indicates the first repeated test on the sample etc. The normal load is given for each test and the sample area at the start of the test (AO) is indicated.

TABLE A-1

TEST RESULTS FOR SAMPLE BB14

Speci-men No.		1st Testing	2nd Testing	3rd Testing	4th Testing	5th Testing
1	τ	3.46	3.62	5.33	9.96	20.8
	σ_N	5.23	5.30	11.80	21.5	44.3
	ϕ	33.5	34.3	24.3	24.9	25.2
2	τ	5.90	3.82	5.80	10.55	18.7
	σ_N	9.91	4.97	9.55	20.2	40.1
	ϕ	30.8	37.5	31.3	27.6	25.0
3	τ	12.29	3.87	6.28	11.23	24.3
	σ_N	26.21	5.02	11.3	23.2	49.4
	ϕ	25.1	37.6	29.1	25.8	26.2
4	τ	13.47	2.52	3.73	8.35	16.4
	σ_N	42.95	5.60	10.8	22.9	43.5
	ϕ	17.4	24.2	19.1	20.0	20.7
5	τ	6.68	2.99	4.58	7.5	16.1
	σ_N	12.72	5.65	10.9	19.5	40.4
	ϕ	27.7	27.9	22.8	21.0	21.7
6	τ	11.97	3.81	4.75	10.6	18.85
	σ_N	25.73	6.88	11.1	25.0	51.8
	ϕ	24.9	29.0	23.2	23.0	20.0

Best Fit Strength Envelopes:

Straight Line $\tau = 1.27 + 0.385\ \sigma_N$ (psi)

Power Curve $\tau = 0.822\ \sigma_N^{0.806}$ (psi)

TABLE A-2

TEST RESULTS FOR SAMPLE BB10

Speci-men No.		1st Testing	2nd Testing	3rd Testing	4th Testing	5th Testing
1	τ	6.97	6.88	11.1	23.8	43.3
	σ_N	4.80	5.20	10.86	23.7	46.5
	ϕ	55.5	53.0	45.6	45.0	43.0
2	τ	12.95	8.8	12.1	21.0	37.6
	σ_N	10.1	5.2	10.0	21.2	42.1
	ϕ	52.1	59.4	50.4	44.7	41.8
3	τ	28.2	11.29	13.8	28.7	64.8
	σ_N	22.2	6.09	10.12	22.0	54.0
	ϕ	51.9	67.4	53.8	52.3	50.2
4	τ	37.2	44.7	20.7	12.9	8.25
	σ_N	44.5	50.1	23.5	12.1	5.16
	ϕ	39.9	41.7	41.4	46.6	58.0
5	τ	13.75	39.5	19.9	11.0	6.11
	σ_N	9.78	40.6	21.6	10.75	5.07
	ϕ	54	44.2	42.8	48.4	50.4
6	τ	17.95	39.2	20.2	10.58	6.56
	σ_N	17.90	47.4	23.5	11.78	6.04
	ϕ	45.1	39.7	40.8	42	47.4

Best Fit Strength Envelopes:

Straight Line $\tau = 2.81 + 0.89\,\sigma_N$ (psi)

Power Curve $\tau = 1.913\,\sigma_N^{0.803}$ (psi)

TABLE A-3

TEST RESULTS FOR SAMPLE EC 12

Specimen No.		1st Testing	2nd Testing	3rd Testing	4th Testing	5th Testing
1	τ	9.97	3.65	5.7	12.9	18.4
	σ_N	12.1	4.85	10.7	21.0	40.3
	ϕ	39.5	37.0	28.0	31.5	24.6
2	τ	11.55	2.75	4.45	8.86	12.9
	σ_N	20.2	4.95	11.0	23.4	46.0
	ϕ	32.8	29.1	22.1	20.8	15.8
3	τ	25.6	25.4	18.7	11.8	6.13
	σ_N	43.2	51.7	25.0	12.75	5.70
	ϕ	30.4	26.2	36.8	42.8	47.2
4	τ	11.0	24.8	9.75	5.52	3.26
	σ_N	9.8	39.7	23.8	11.2	5.83
	ϕ	48.4	32.0	22.3	26.2	29.2
5	τ	6.06	4.91	7.65	15.15	25.2
	σ_N	5.20	5.16	11.56	24.8	53.3
	ϕ	49.4	43.6	33.5	31.0	25.7

Best Fit Strength Envelopes:

Straight Line $\tau = 2.86 + 0.442\ \sigma_N$ (psi)

Power Curve $\tau = 1.229\ \sigma_N^{0.746}$ (psi)

TABLE A-4

TEST RESULTS FOR SAMPLES BC3, BB5, B12 and BB14 (Auxilliary Series)

		σ_N	τ	ϕ
BB5	1	10.4	11.48	47.8
	2	21.0	17.4	39.6
	3	5.48	7.00	52.0
	4	44.2	42.5	44.0
BB12	1	20.5	11.6	29.5
	2	44.7	21.4	25.6
	3	5.40	4.85	42.0
	4	11.0	6.29	29.7
BC3	1	10.3	11.15	47.6
	2	5.1	6.05	49.5
	3	20.5	21.8	47.0
	4	41.0	40.2	44.4
BB14-2	Molybdenite Removed			
	1	10.45	8.85	40.3
	2	20.8	14.86	35.4
	3	5.35	4.72	41.4
	4	44.8	30.9	34.7
	Before Molybdenite Removed			
	1	4.97	3.82	37.5
	2	9.55	5.80	31.3
	3	20.2	10.55	27.6
	4	40.1	18.7	25.0

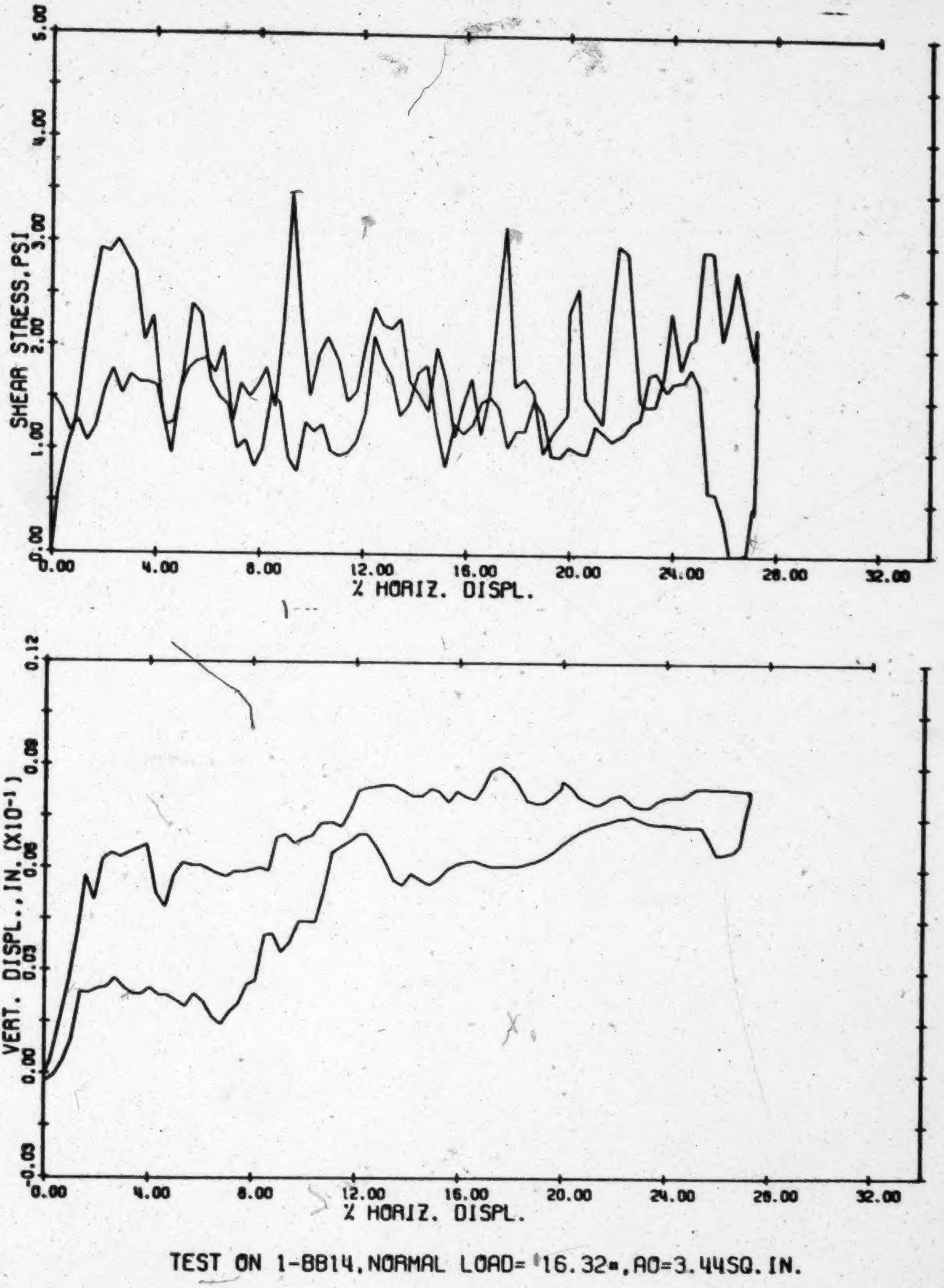

TEST ON 1-BB14, NORMAL LOAD= 16.32*, AO=3.44SQ.IN.

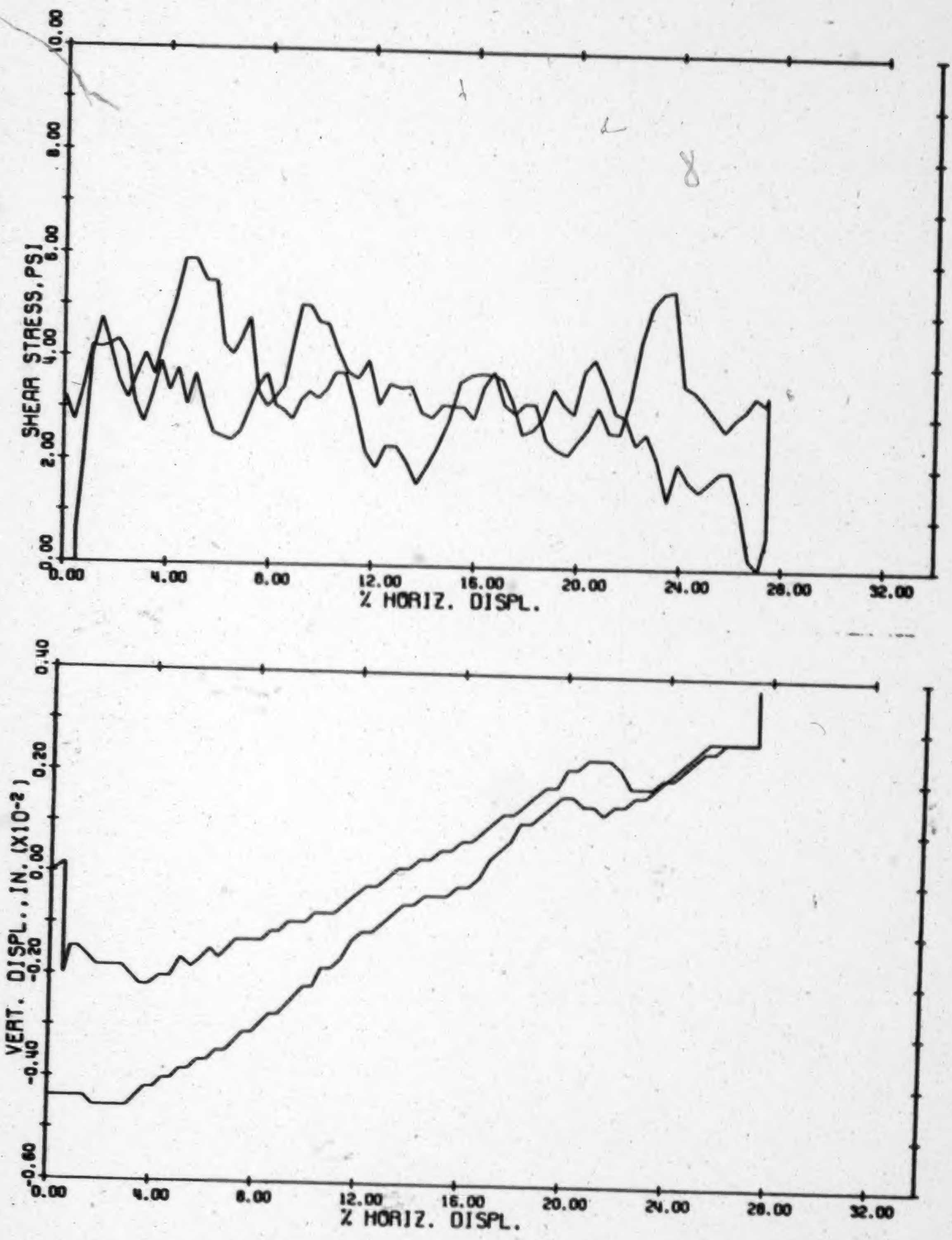

TEST ON 2-BB14, NORMAL LOAD= 31.31*, AO=3.33SQ.IN.

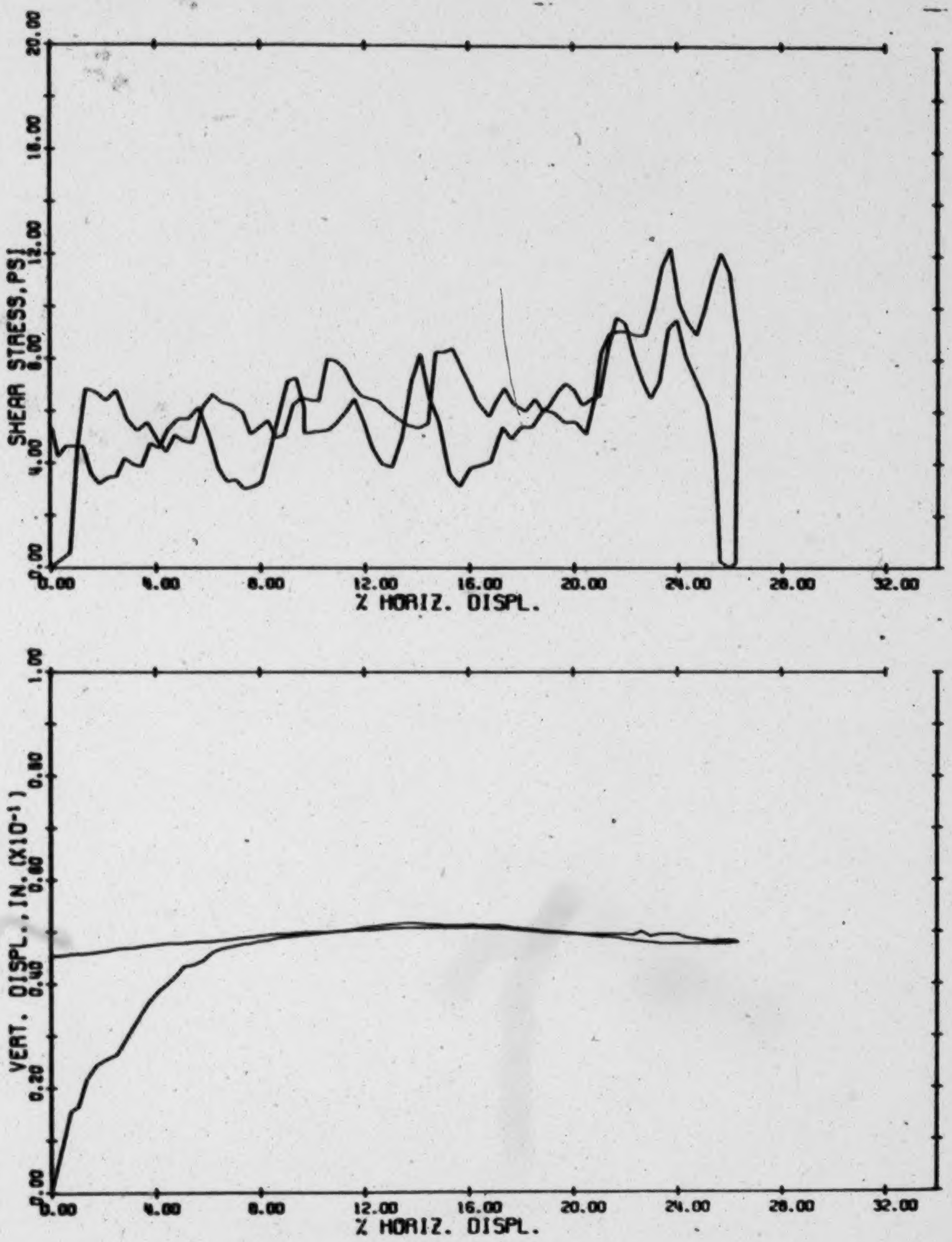

TEST ON 3-BB14, NORMAL LOAD= 71.30#, AO=3.57SQ. IN.

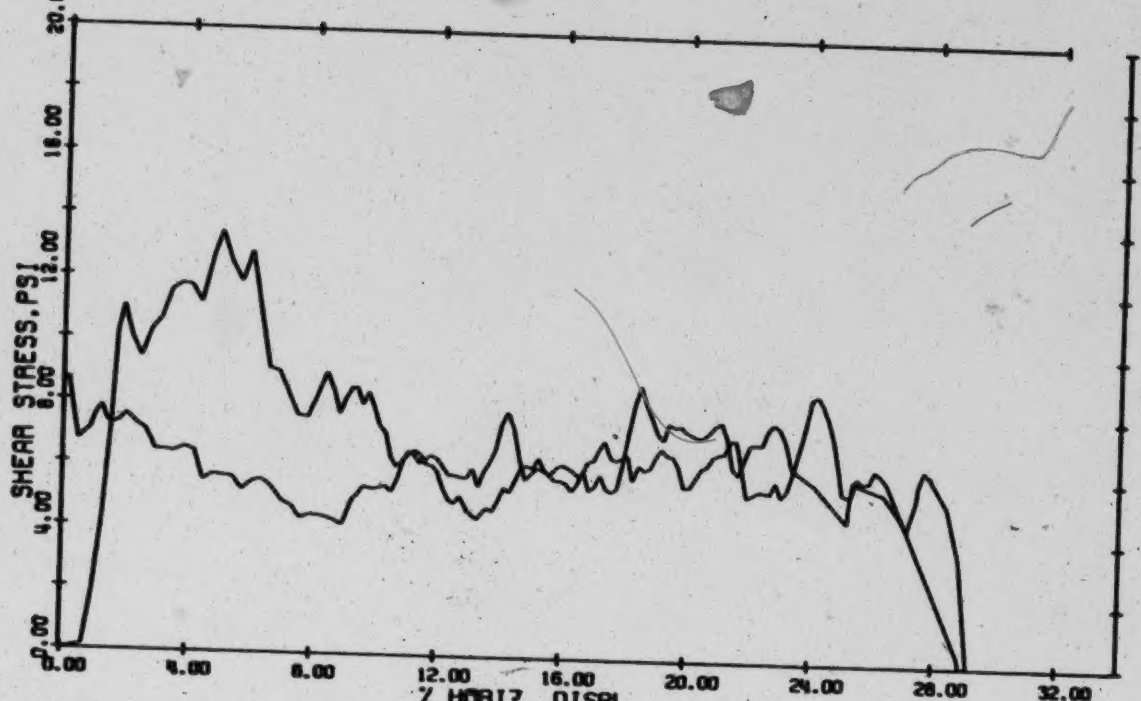

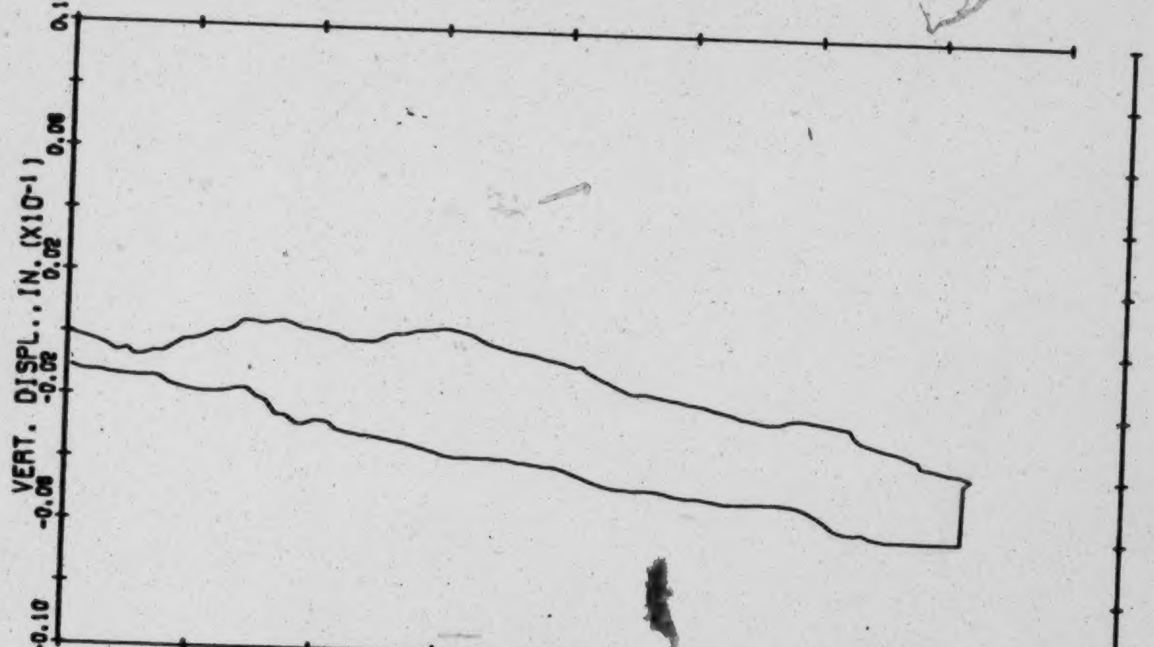

TEST ON 4-8814,NORMAL LOAD=126.28*,AO=3.19SQ.IN.

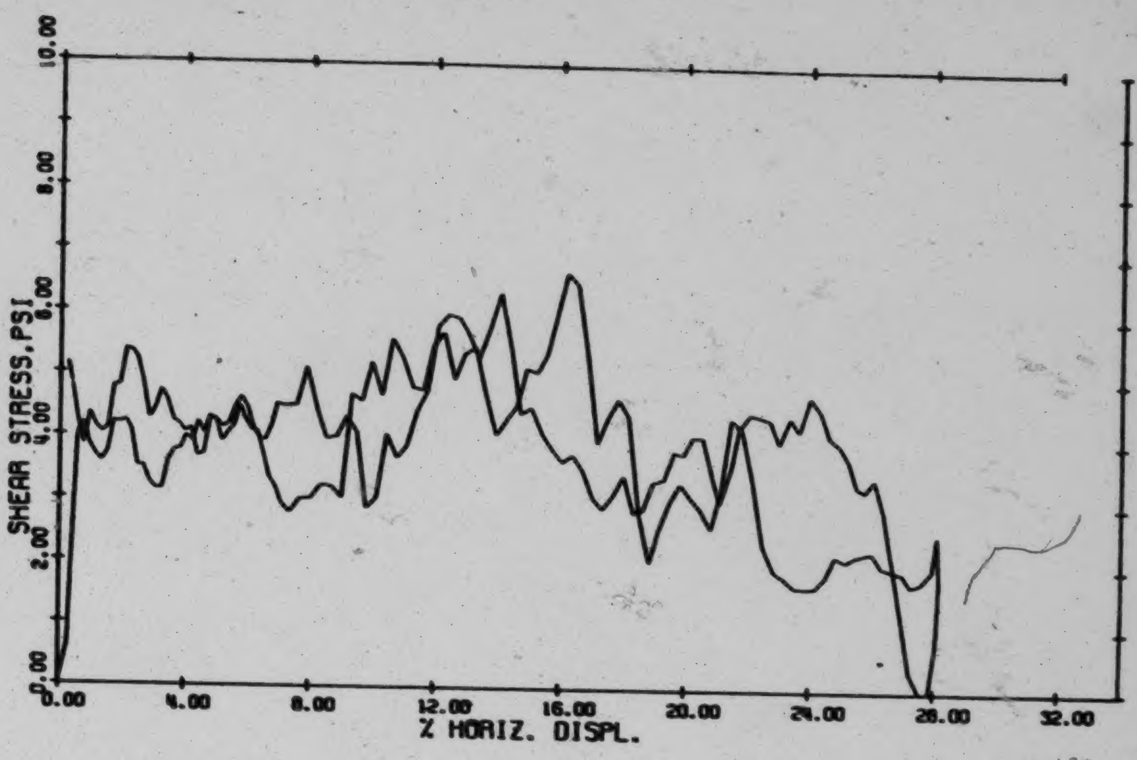

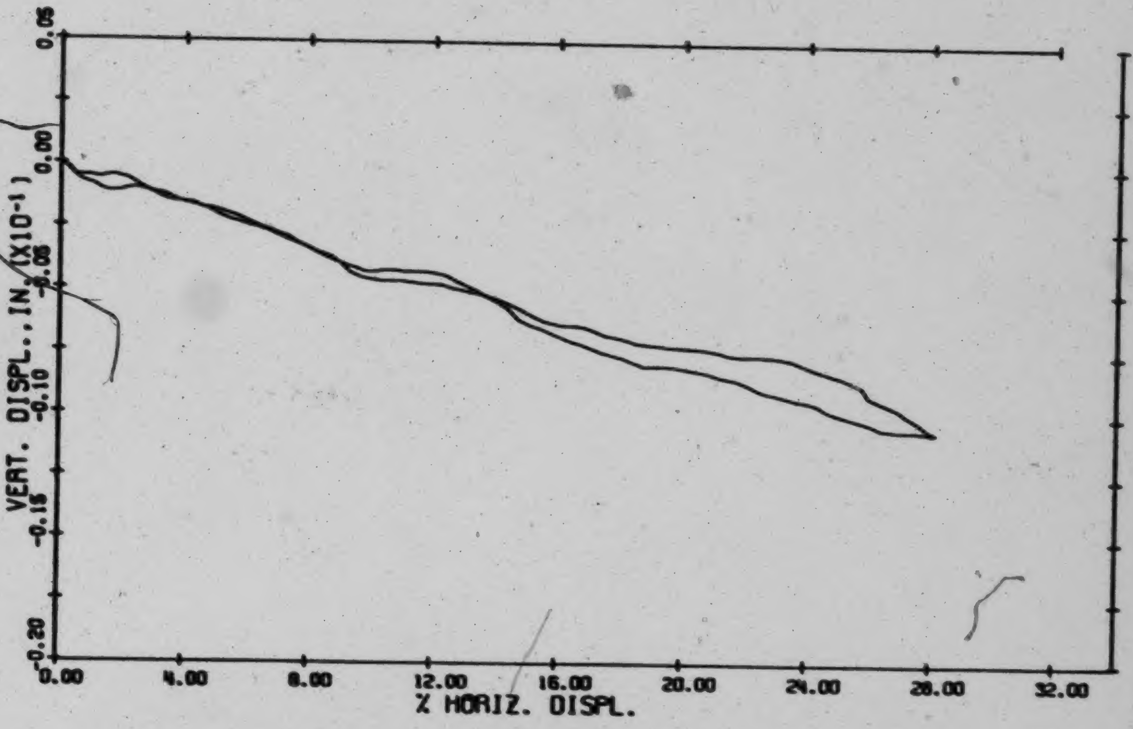

TEST ON 5-BB14,NORMAL LOAD= 31.30*,AO=2.94SQ.IN.

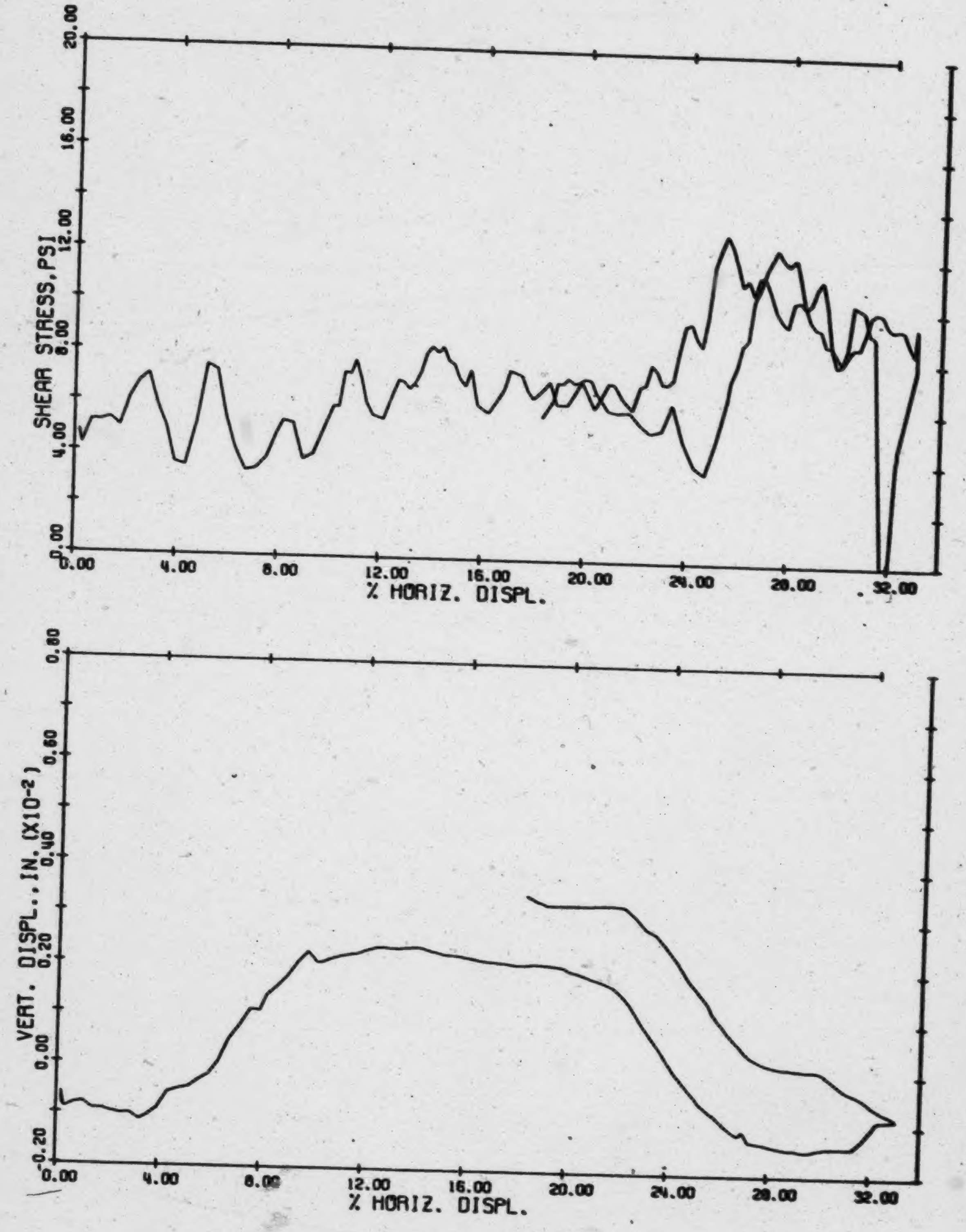

TEST ON 6-BB14,NORMAL LOAD= 61.25#,A0=2.46SQ.IN.

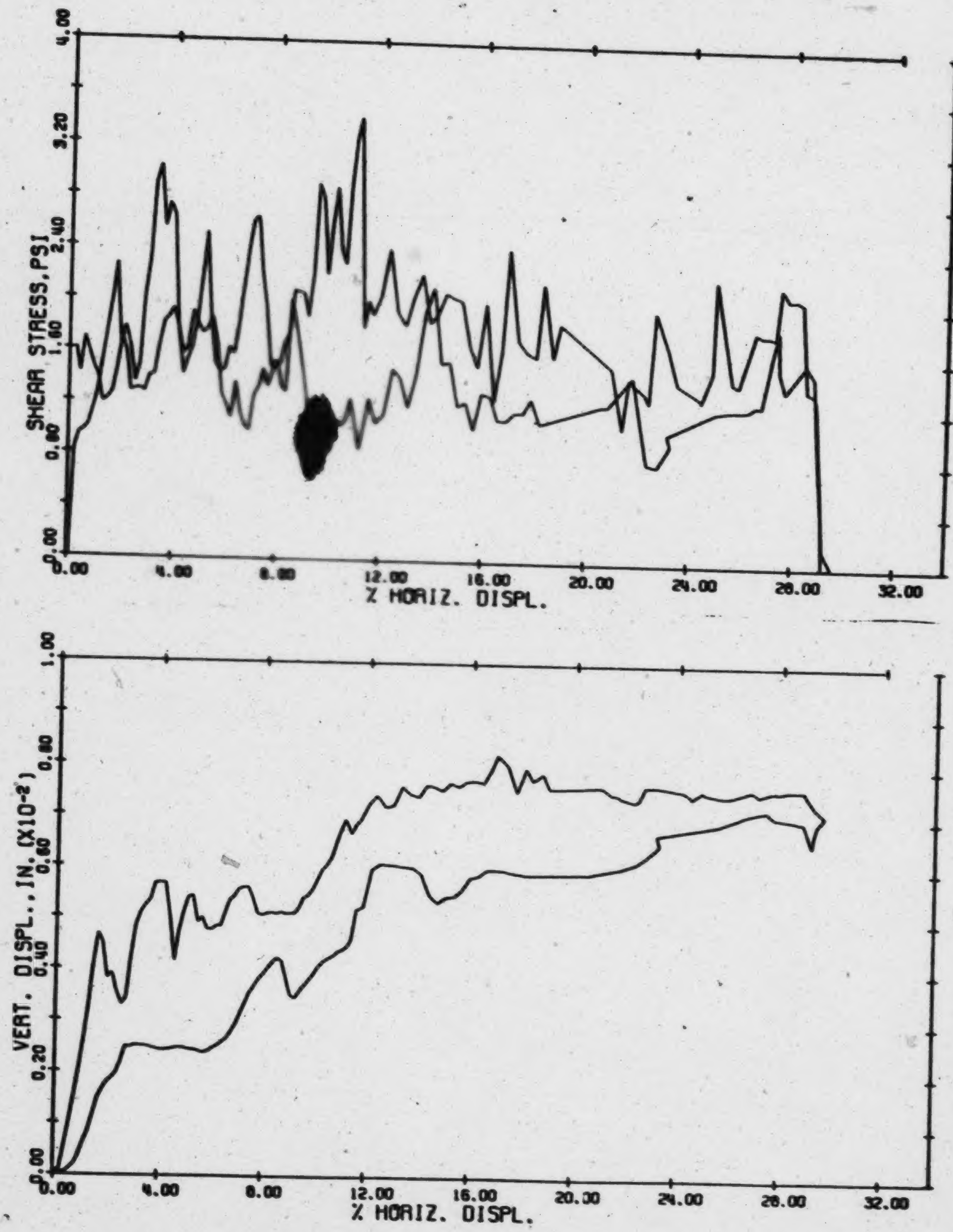

TEST 1-BB14-1,VERT. LOAD= 16.32#,A0=3.44SQ. INS.

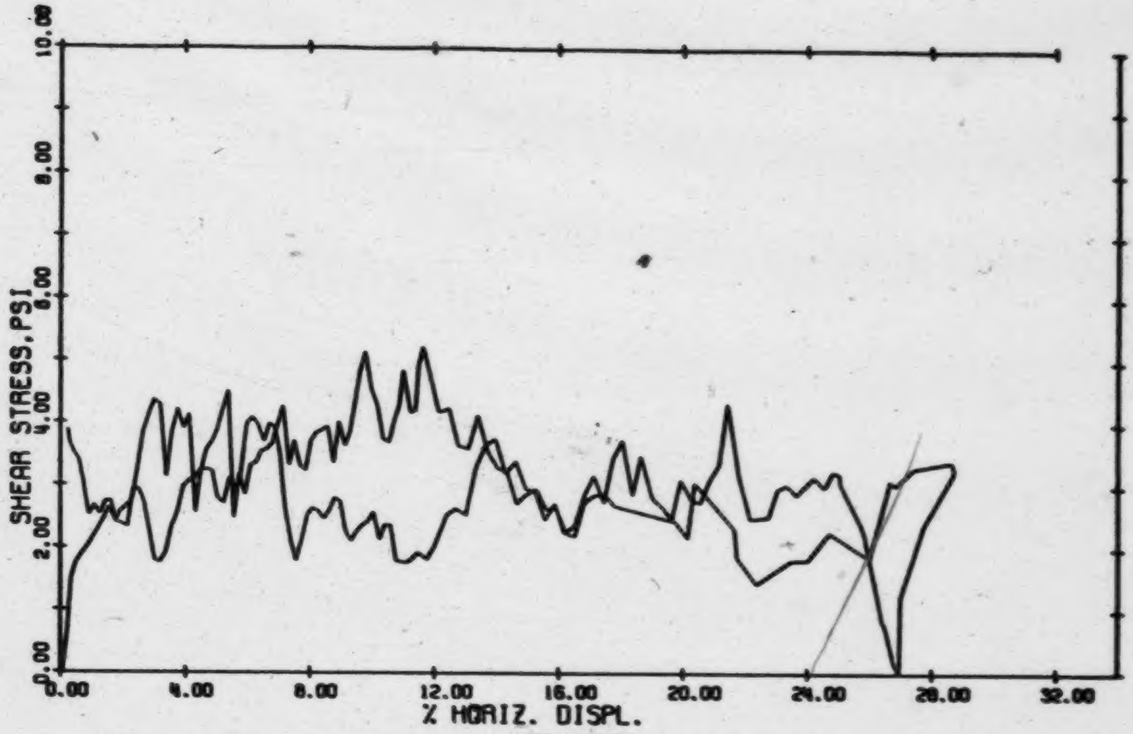

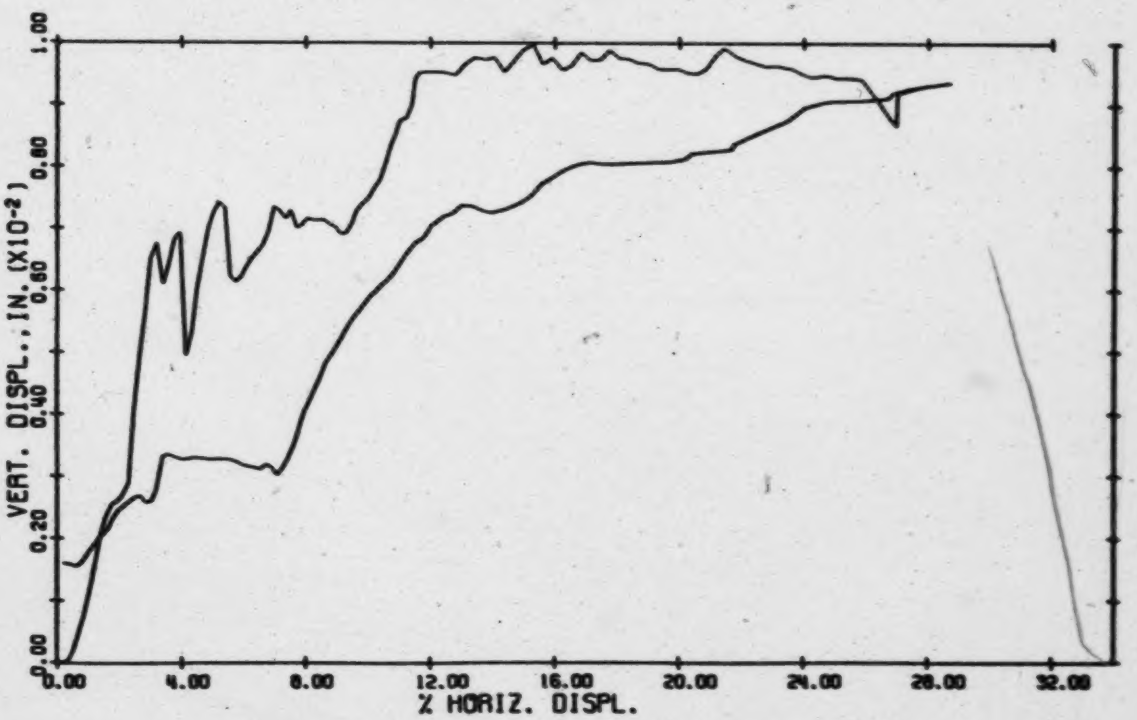

TEST 1-BB14-2, VERT. LOAD= 36.32#, AO=3.44SQ. INS.

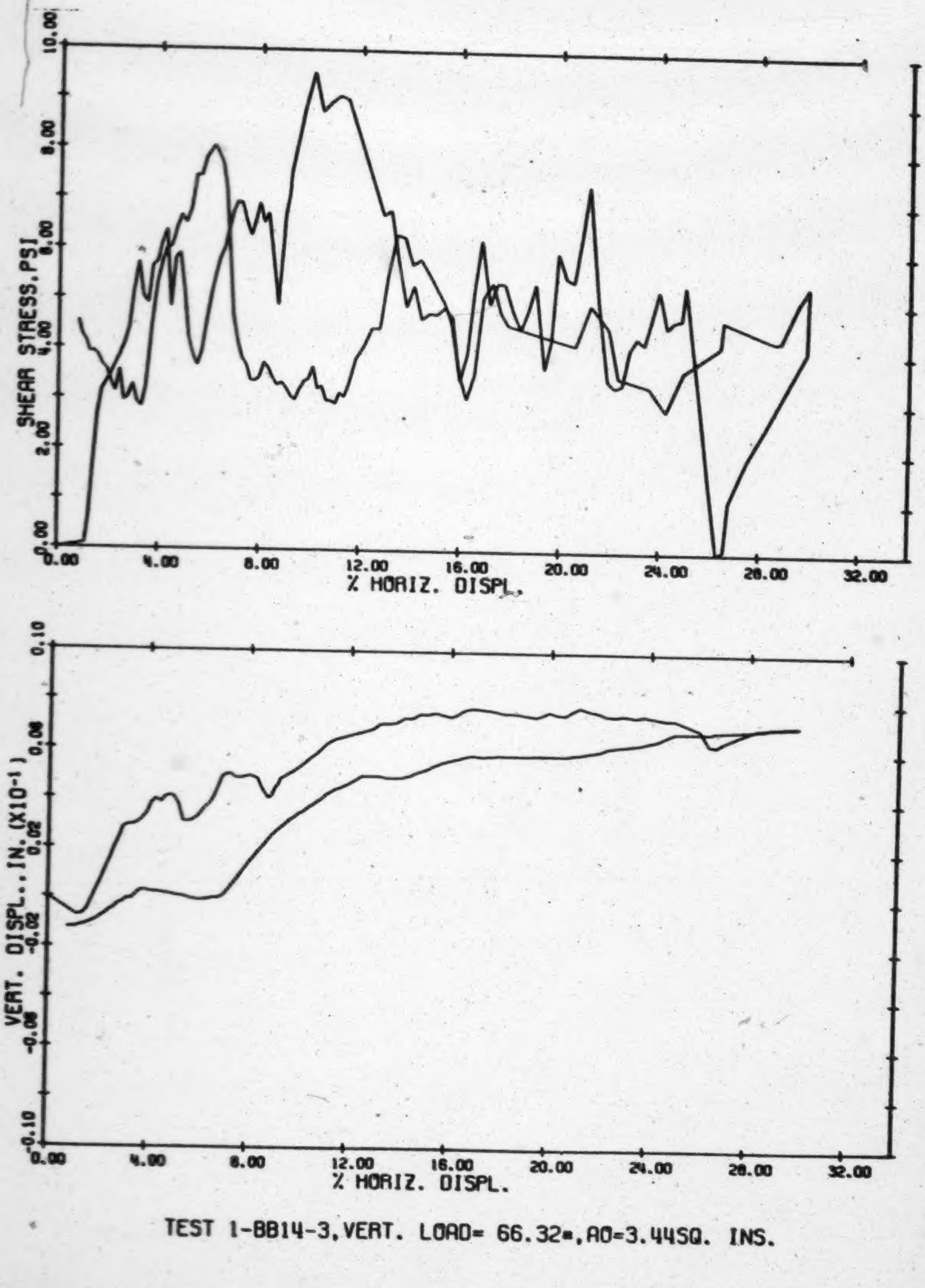

TEST 1-BB14-3, VERT. LOAD= 66.32*, AO=3.44SQ. INS.

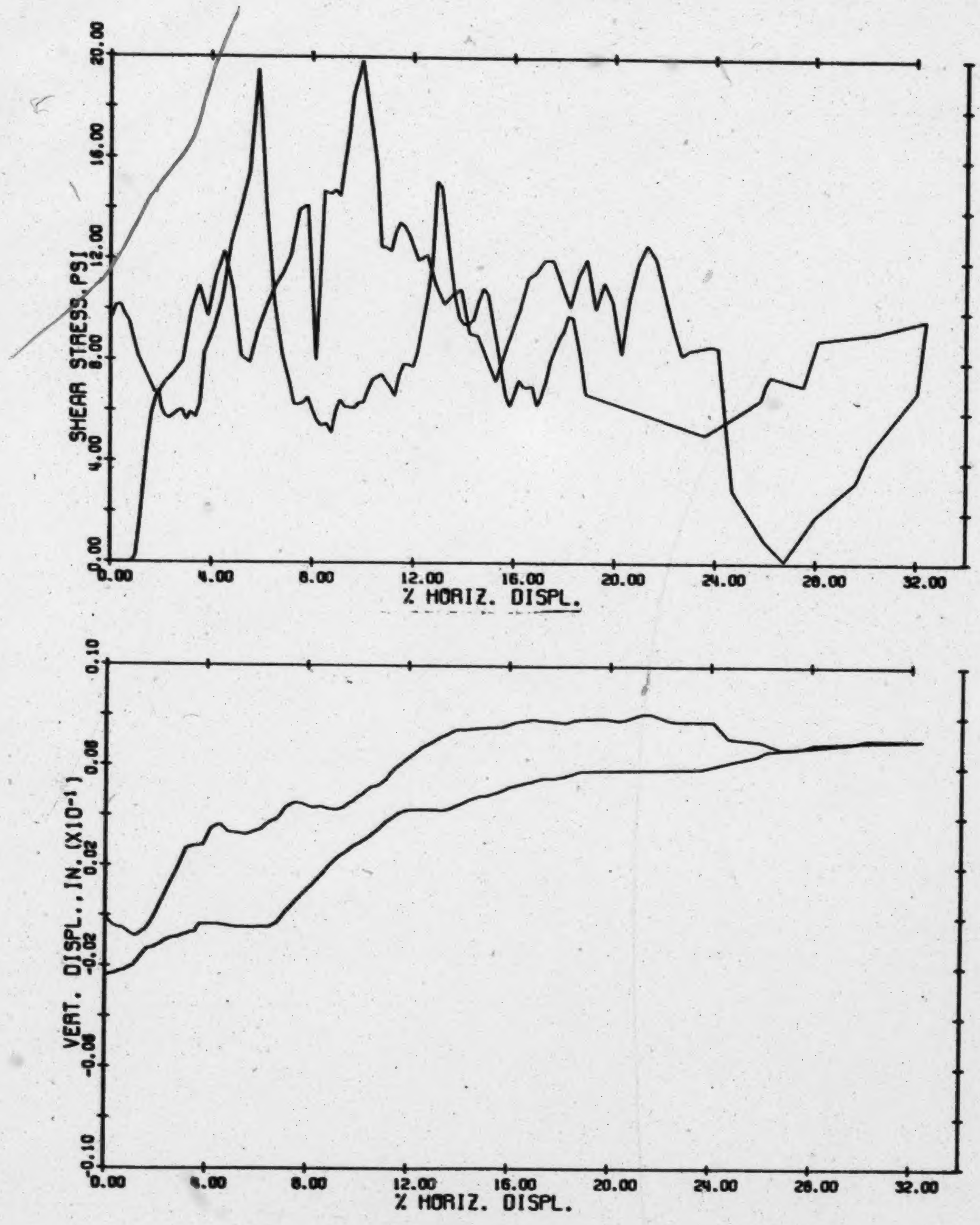

TEST 1-BB14-4, VERT. LOAD=136.32*, AO=3.44SQ. INS.

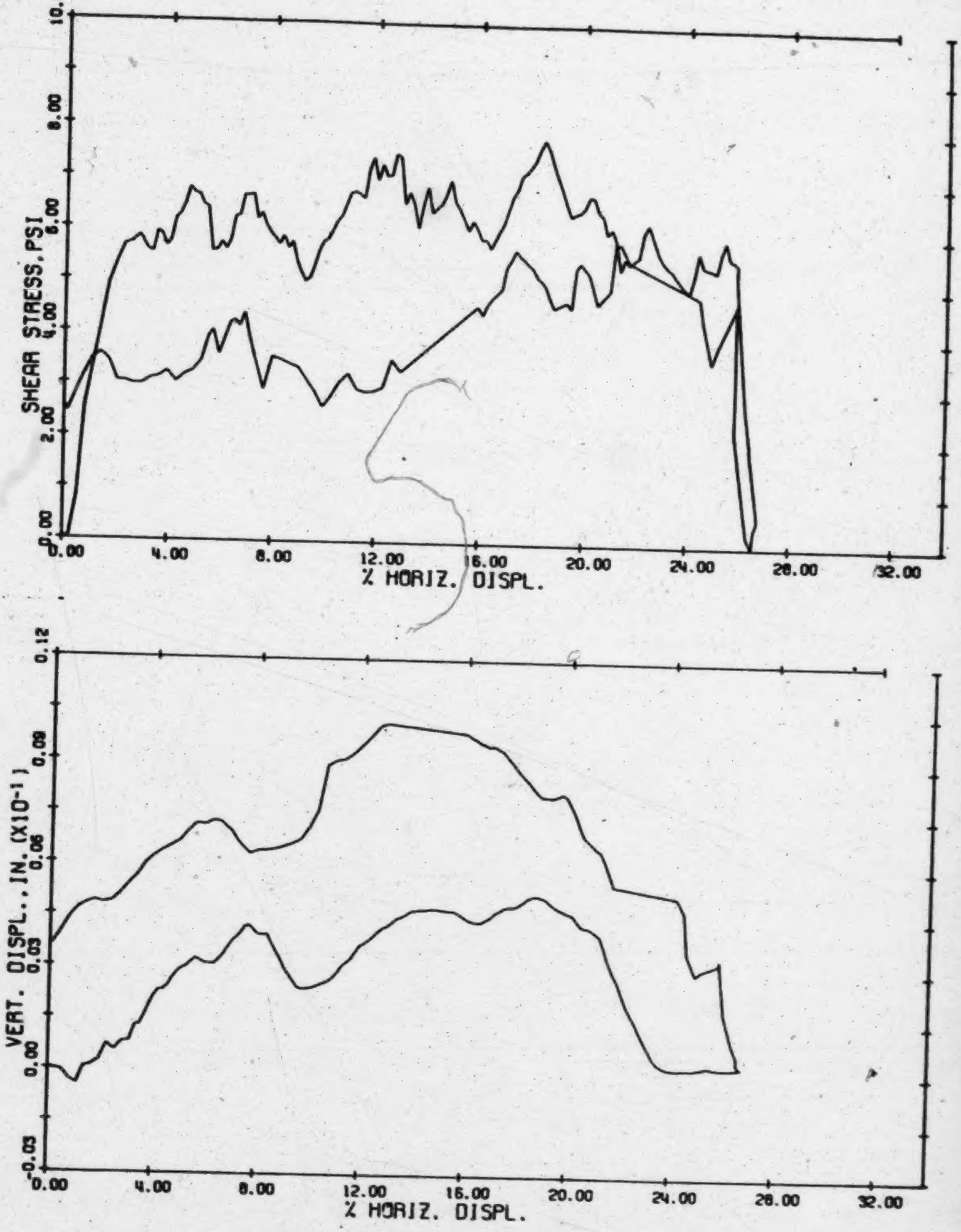

TEST ON 1-BB10, NORMAL LOAD= 16.31*, A0=3.57SQ. IN.

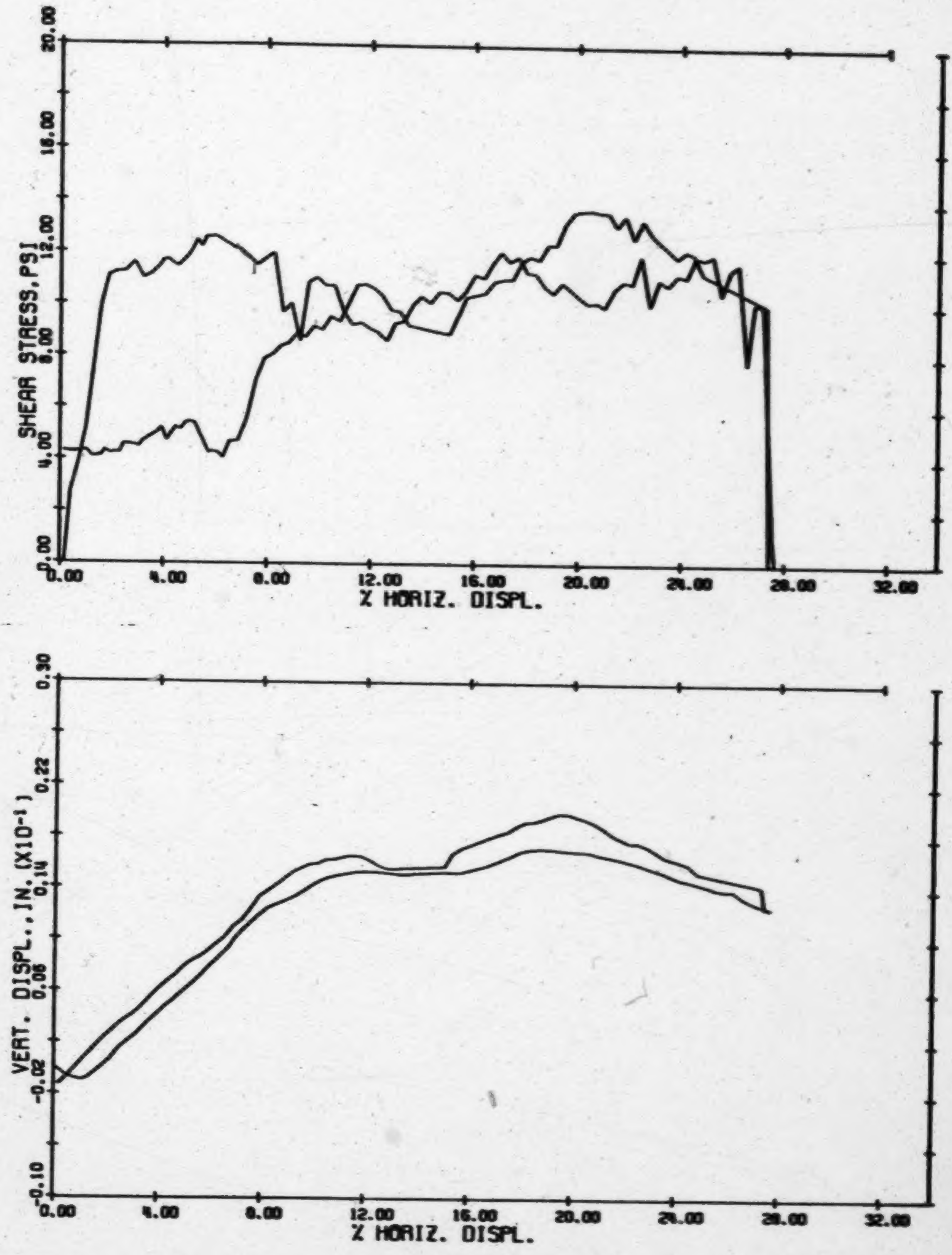

TEST ON 2-BB10,NORMAL LOAD= 31.29*,AO=3.29SQ.IN.

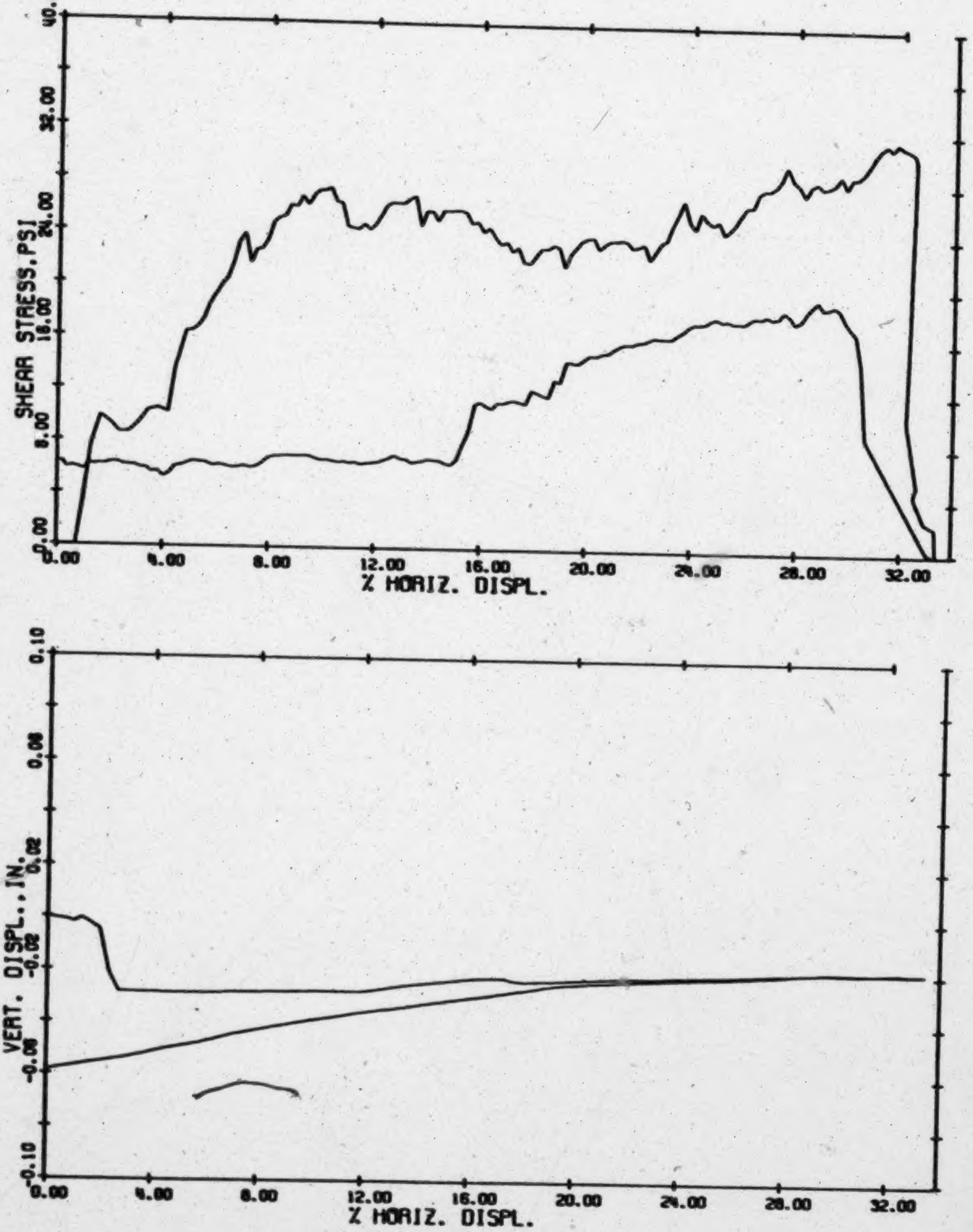

TEST ON 3-BB10,NORMAL LOAD= 56.30#,AO=2.84SQ.IN.

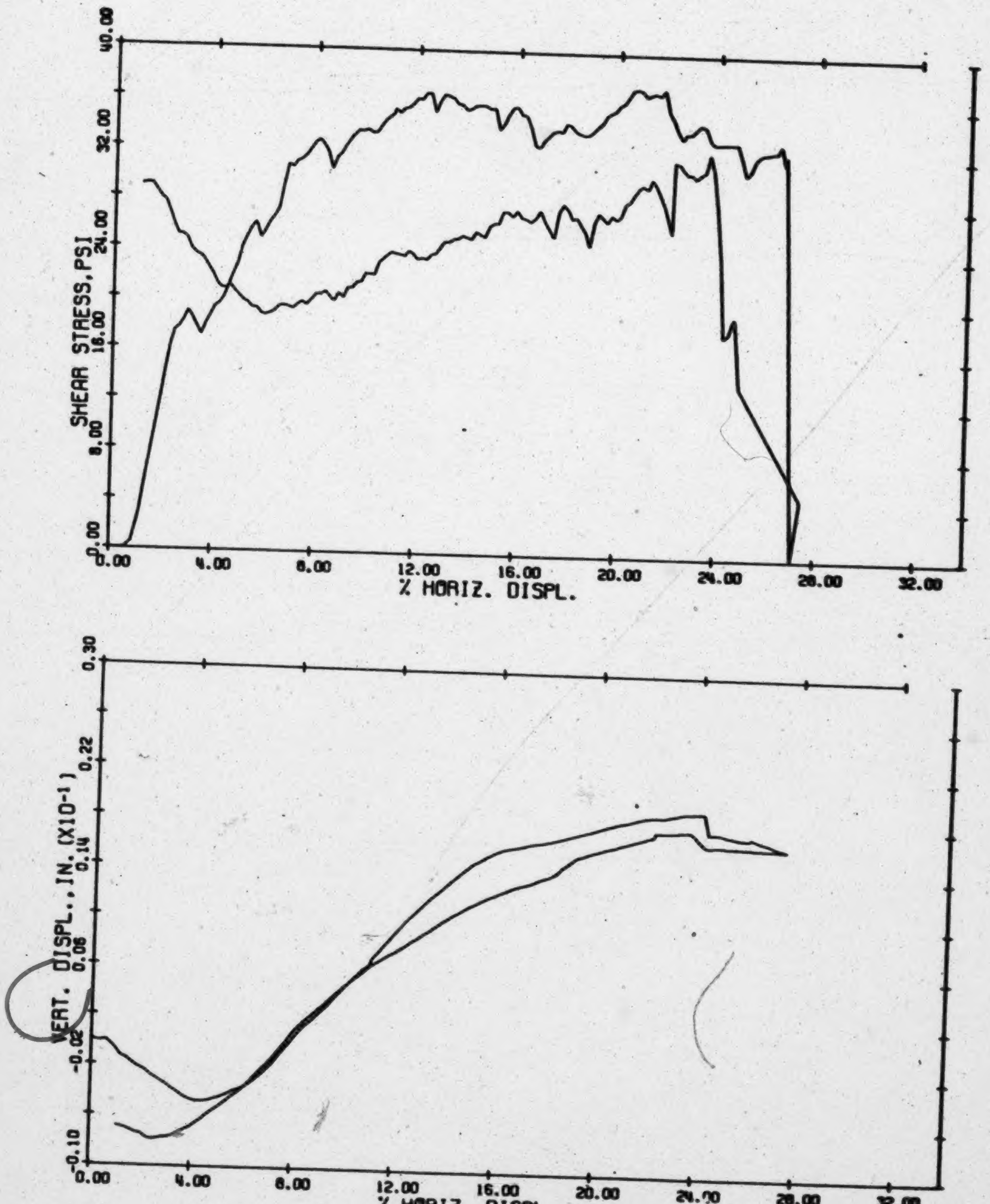

TEST ON 4-BB10,NORMAL LOAD=136.30#,A0=3.50SQ.IN.

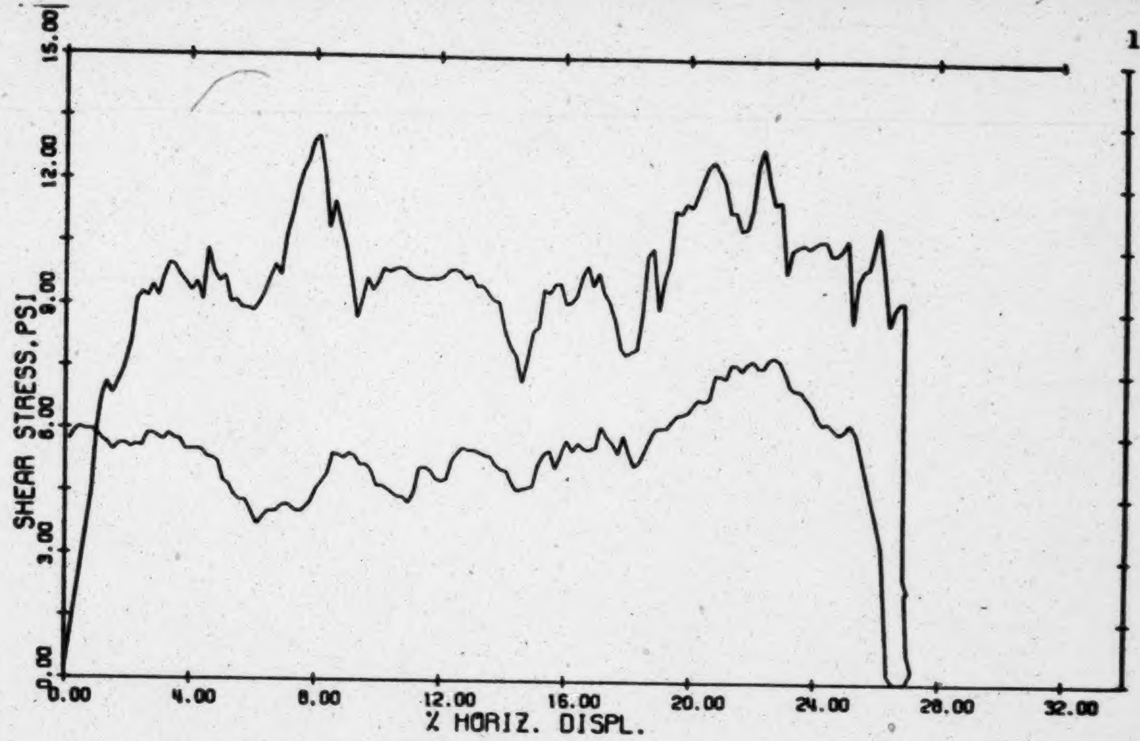

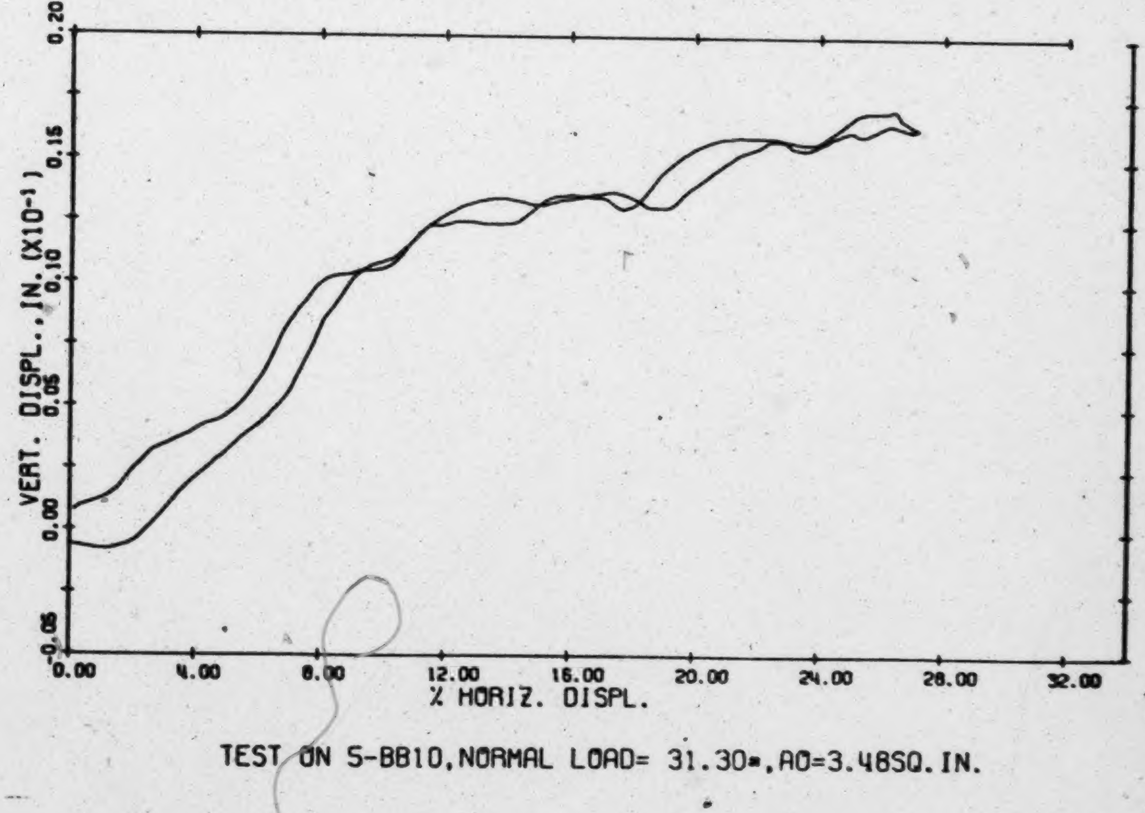

TEST ON S-BB10, NORMAL LOAD= 31.30#, AO=3.48SQ. IN.

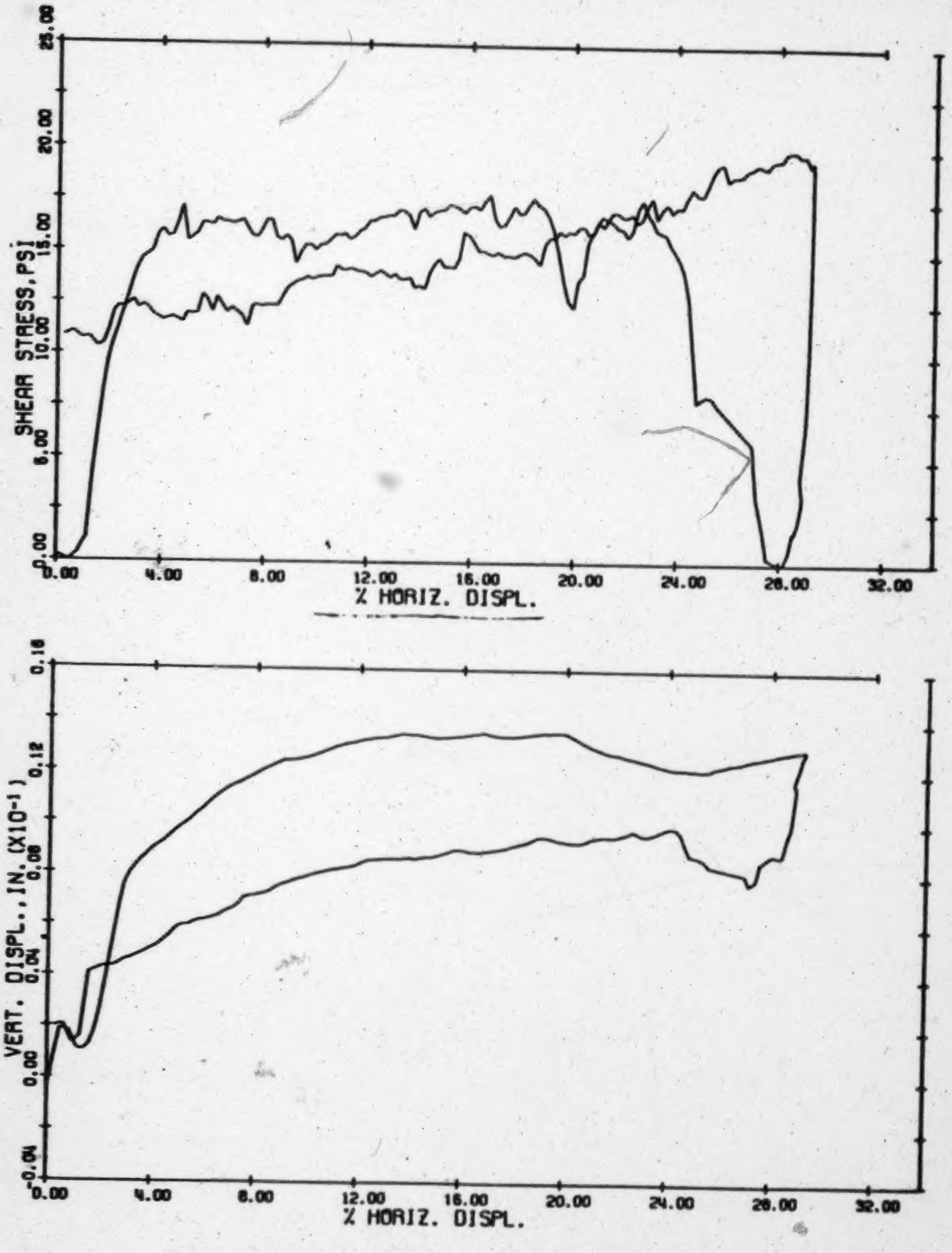

TEST ON 6-BB10, NORMAL LOAD= 51.30*, A0=3.01SQ.IN.

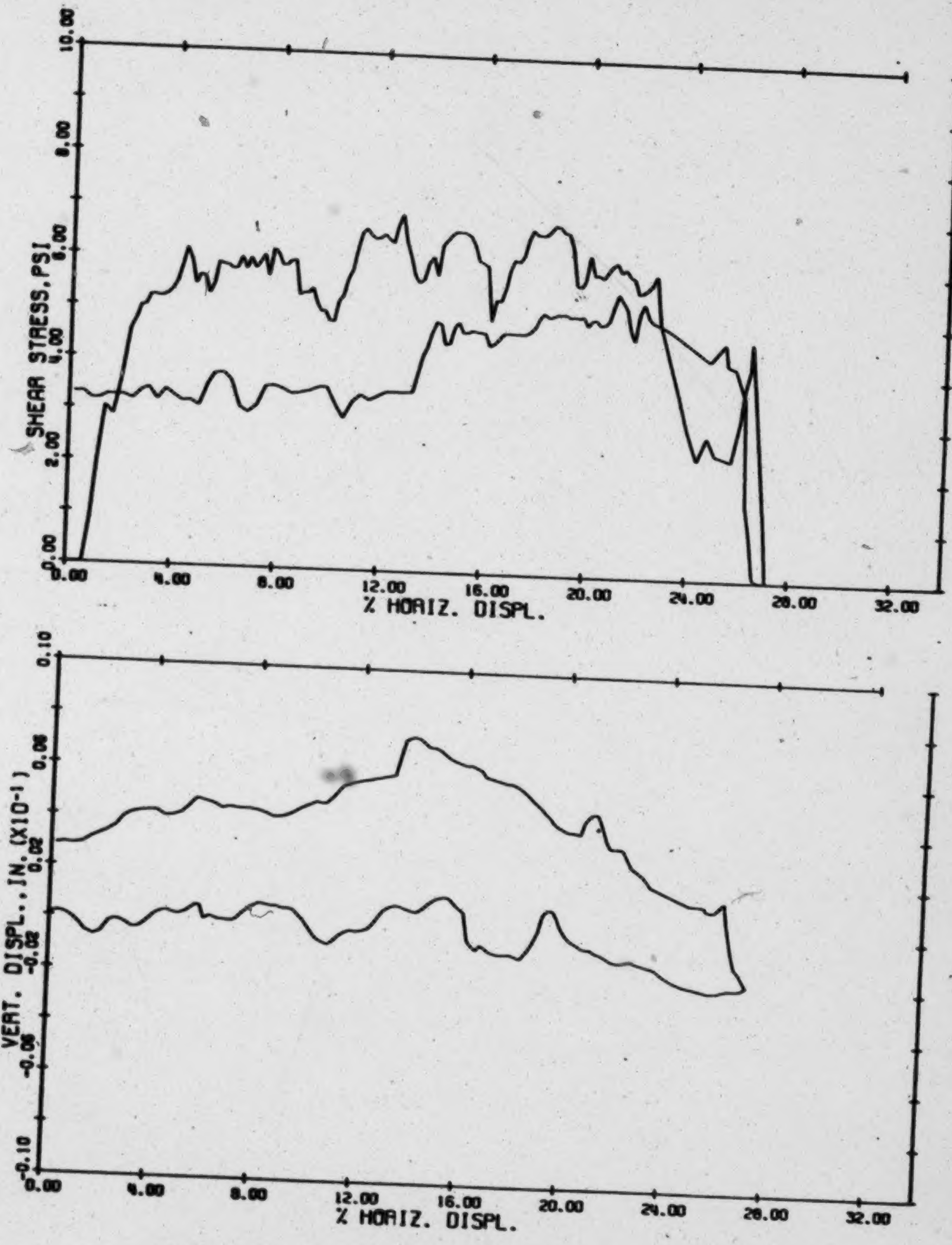

TEST 1-BB10-1, VERT. LOAD= 16.31#, A0=3.57SQ. INS.

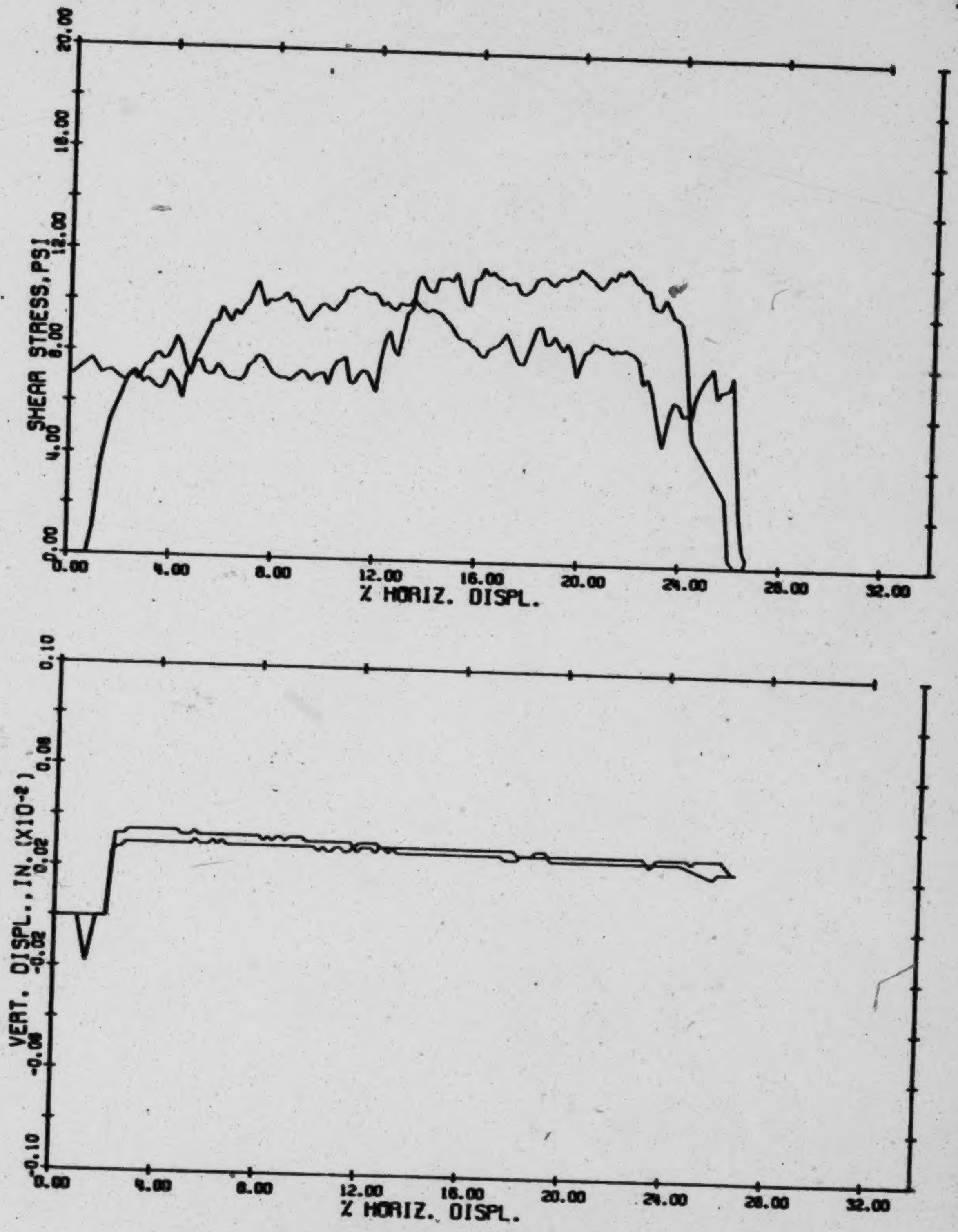

TEST 1-BB10-2, VERT. LOAD= 36.31#, AO=3.57SQ. INS.

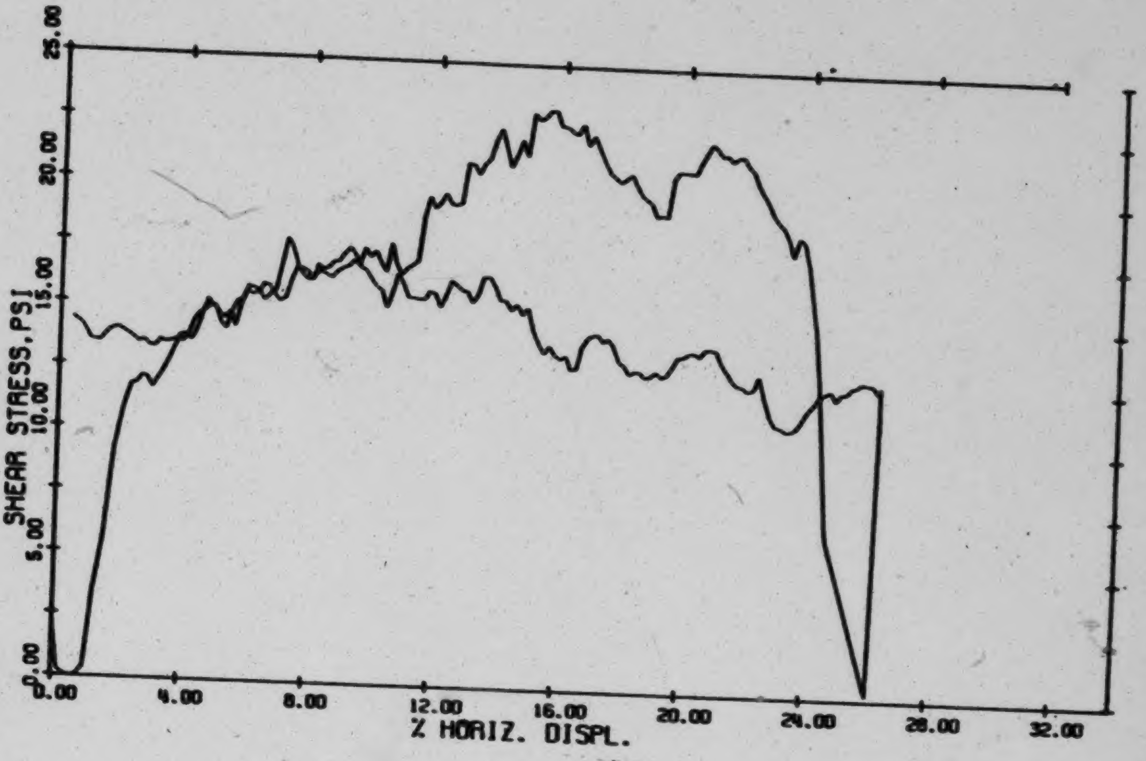

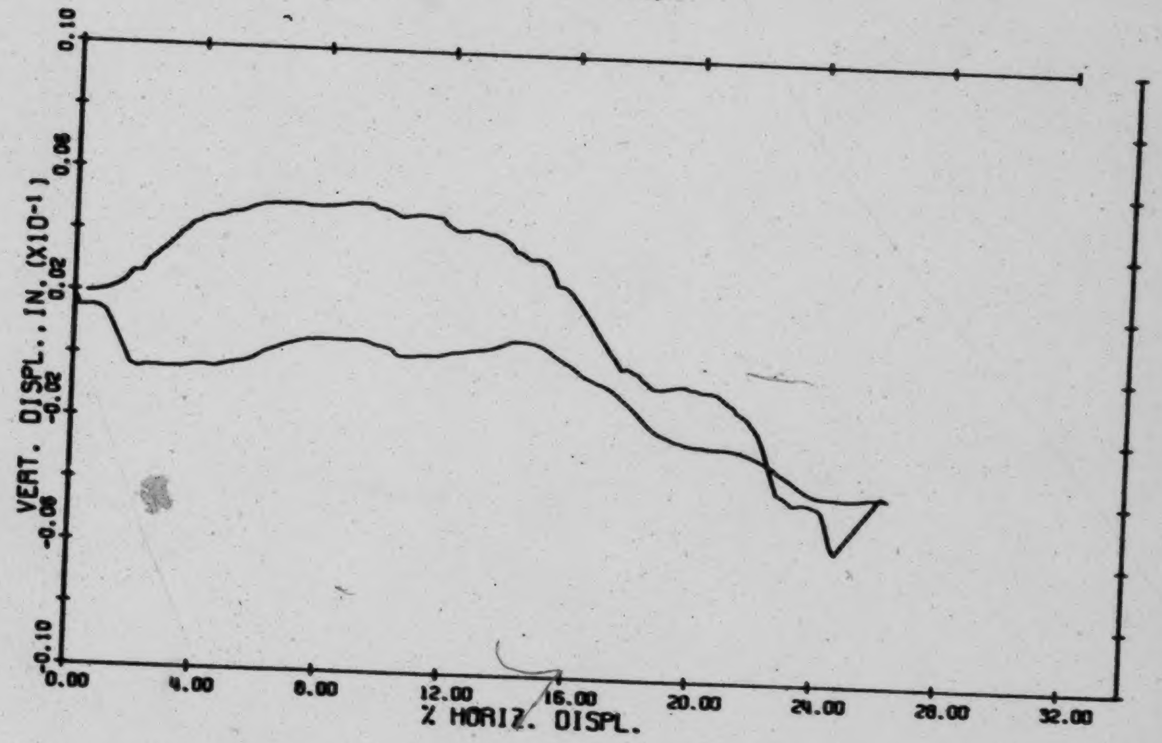

TEST 1-BB10-3, VERT. LOAD= 71.31*, AO=3.57SQ. INS.

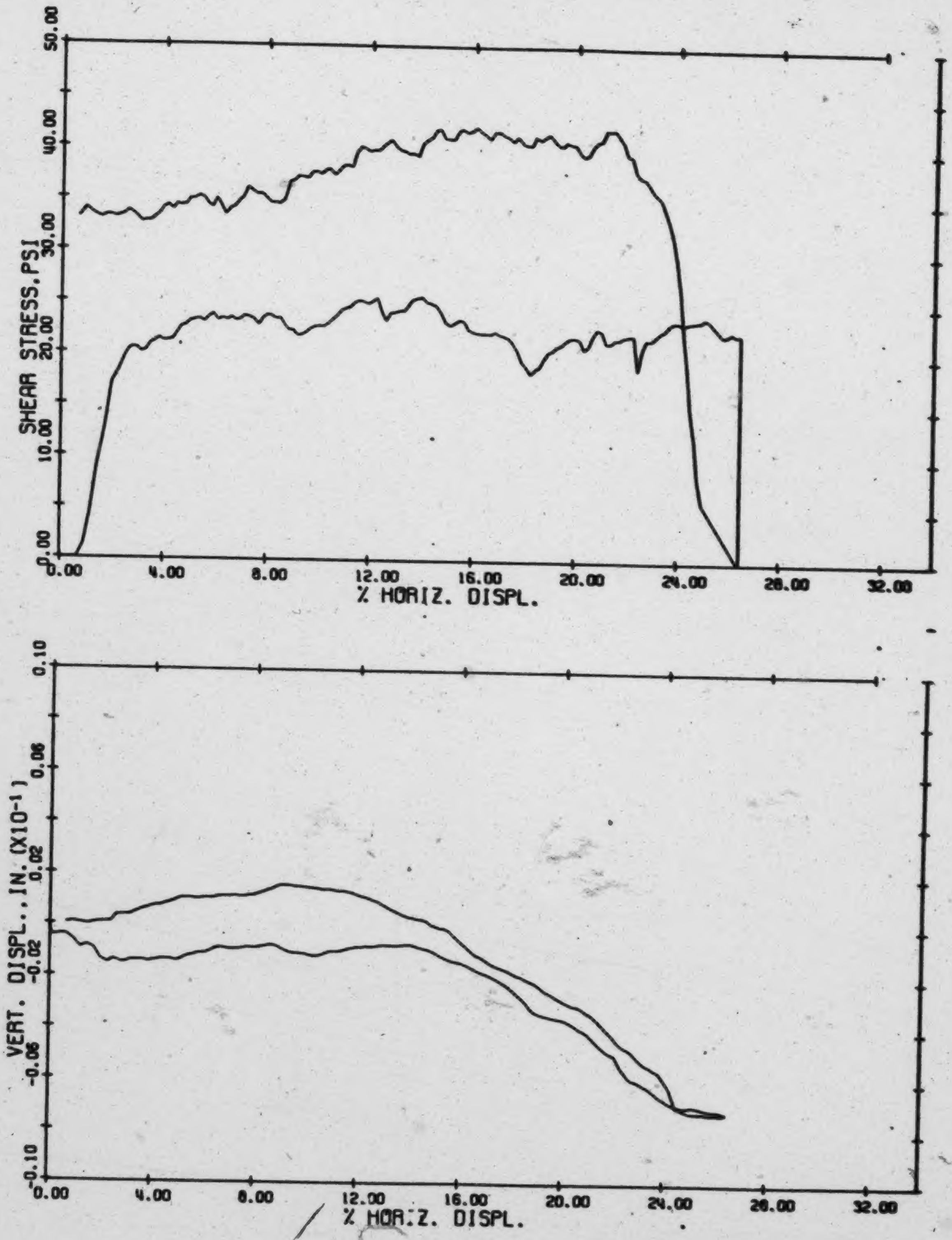

TEST 1-BB10-4,VERT. LOAD=141.31#,AO=3.57SQ. INS.

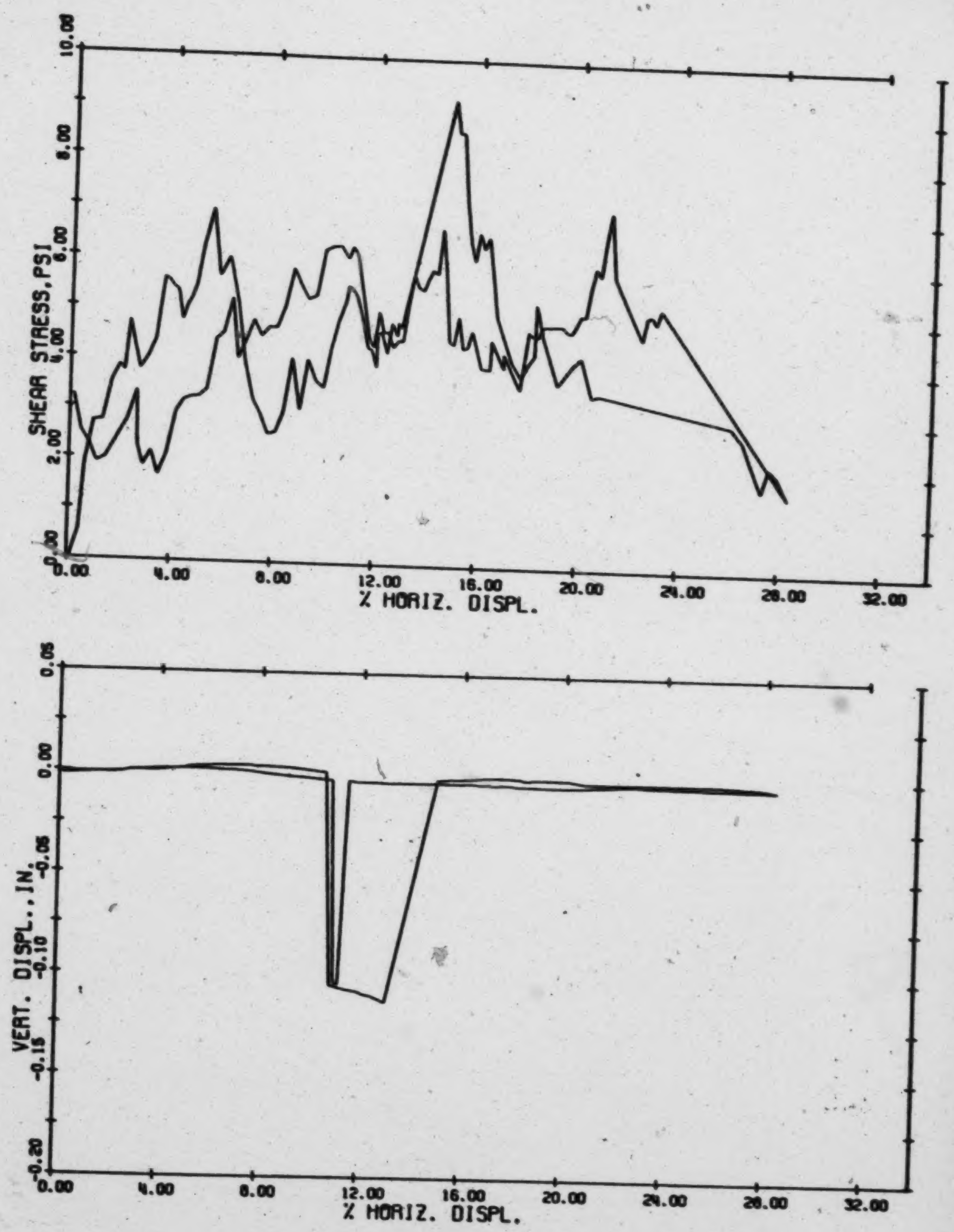

TEST 1-EC12 ,VERT. LOAD= 36.32#,AO=3.51SQ. INS.

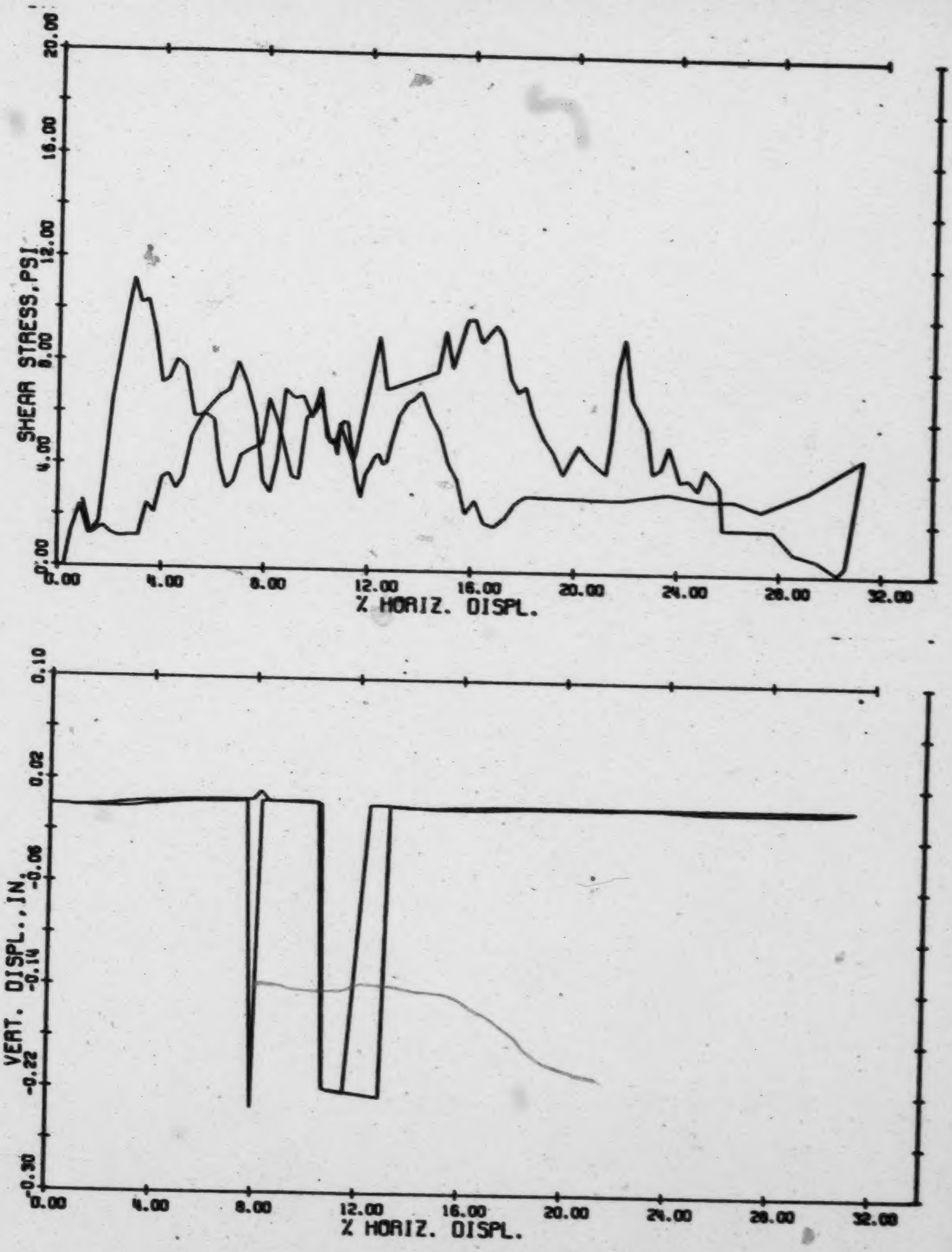

TEST 2-EC12 , VERT. LOAD= 76.36#, A0=3.86SQ. INS.

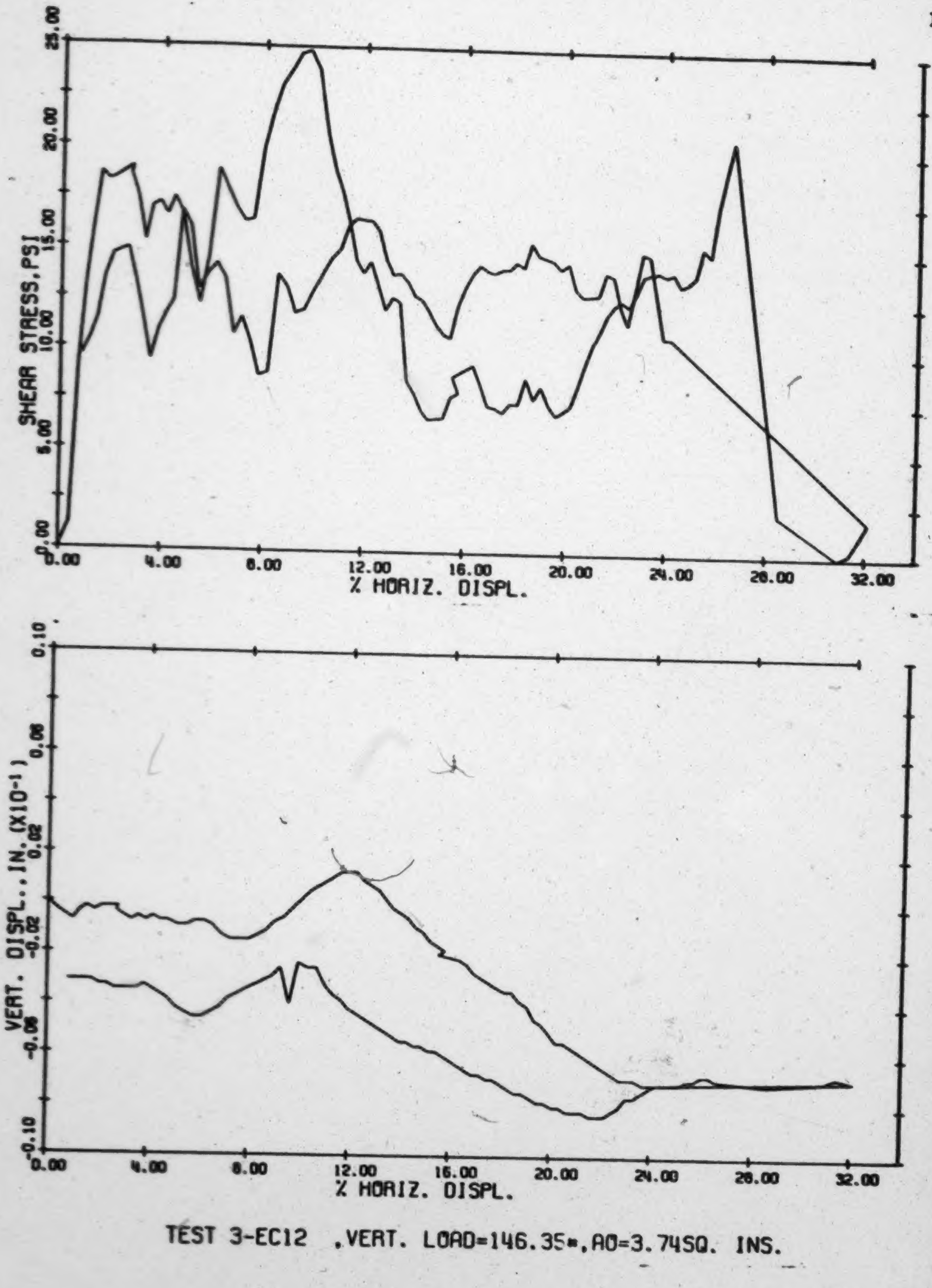

TEST 3-EC12 ,VERT. LOAD=146.35#,AO=3.74SQ. INS.

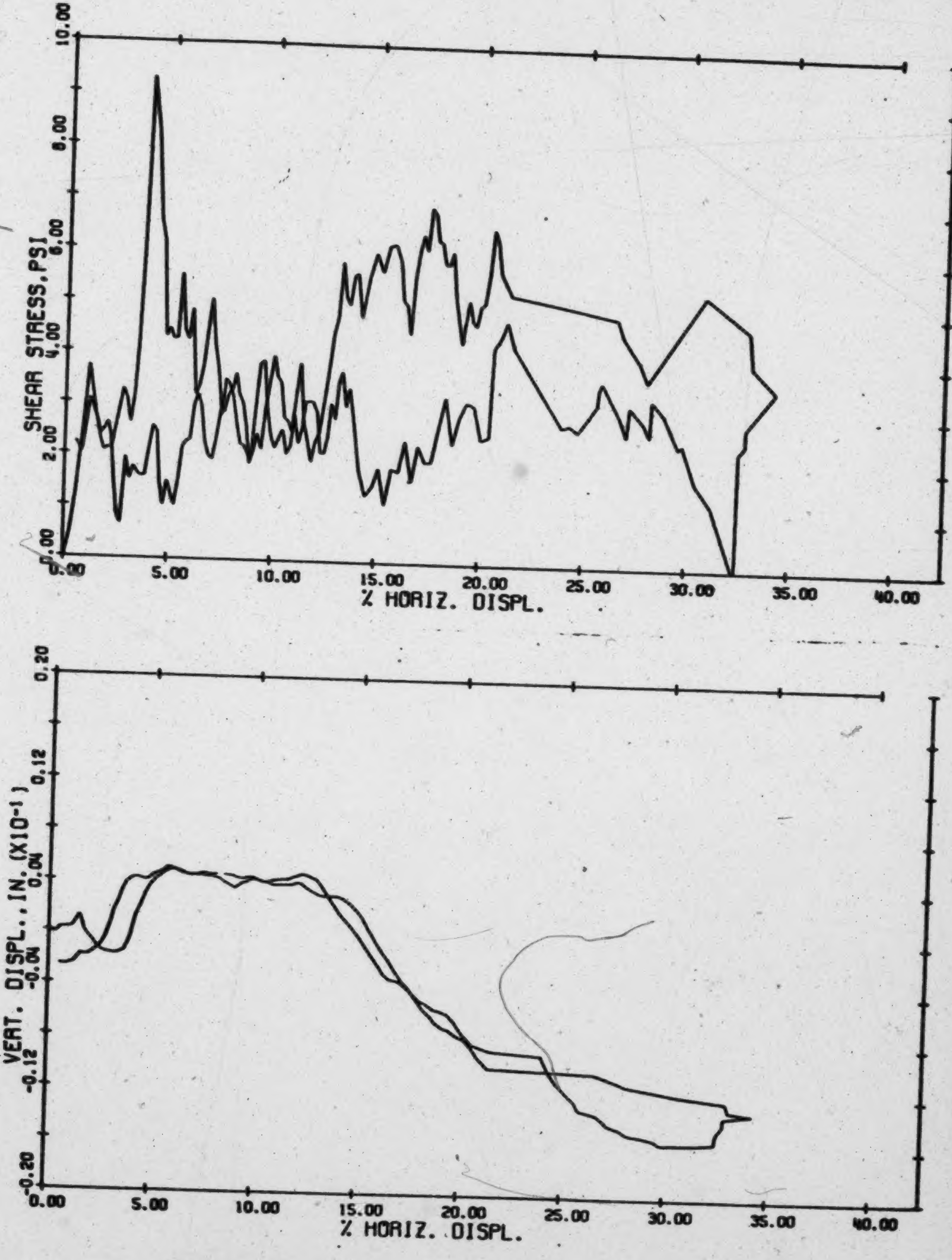

TEST 4-EC12 ,VERT. LOAD= 31.29#,AO=3.33SQ. INS.

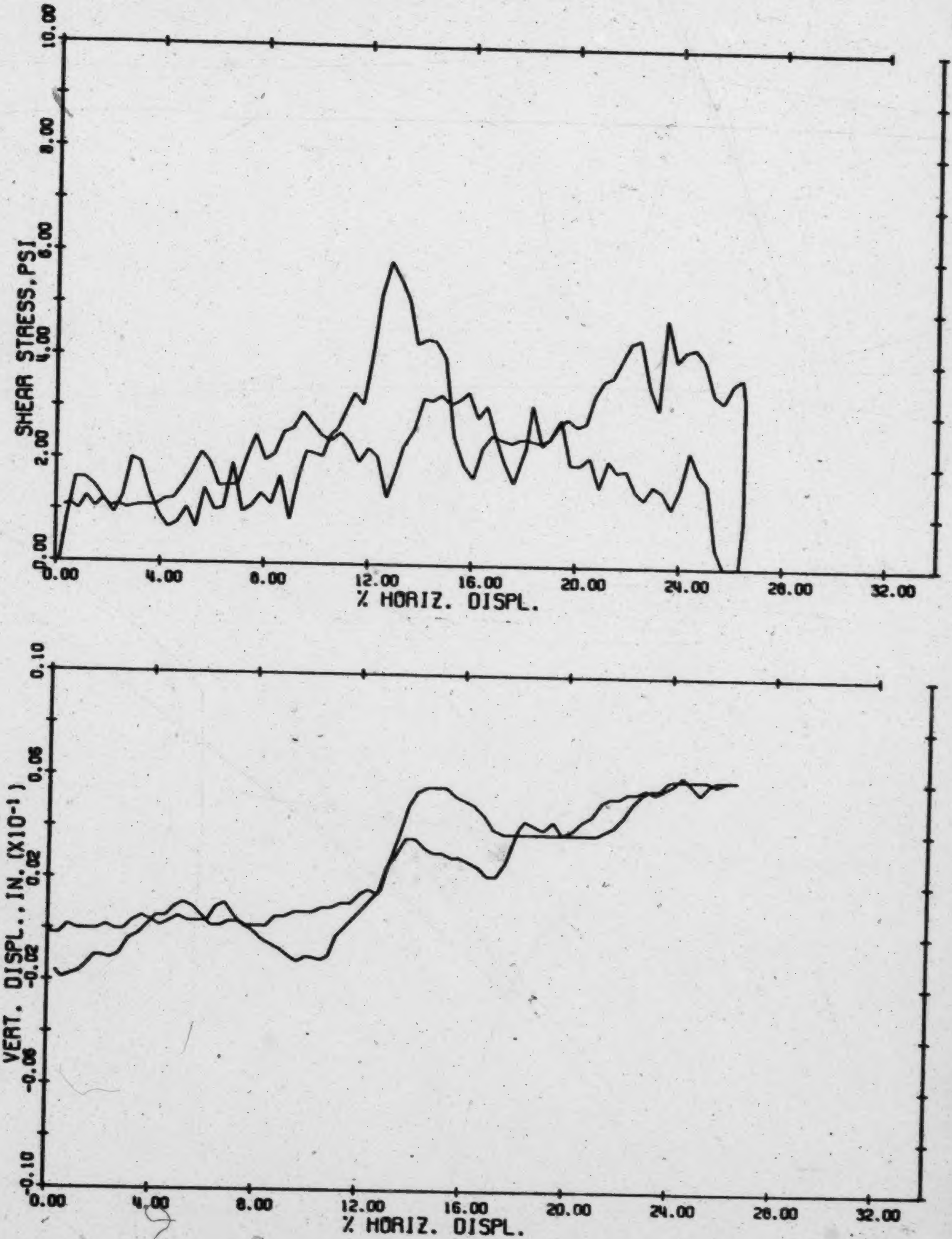

TEST 5-EC12 ,VERT. LOAD= 16.29*,A0=3.64SQ. INS.

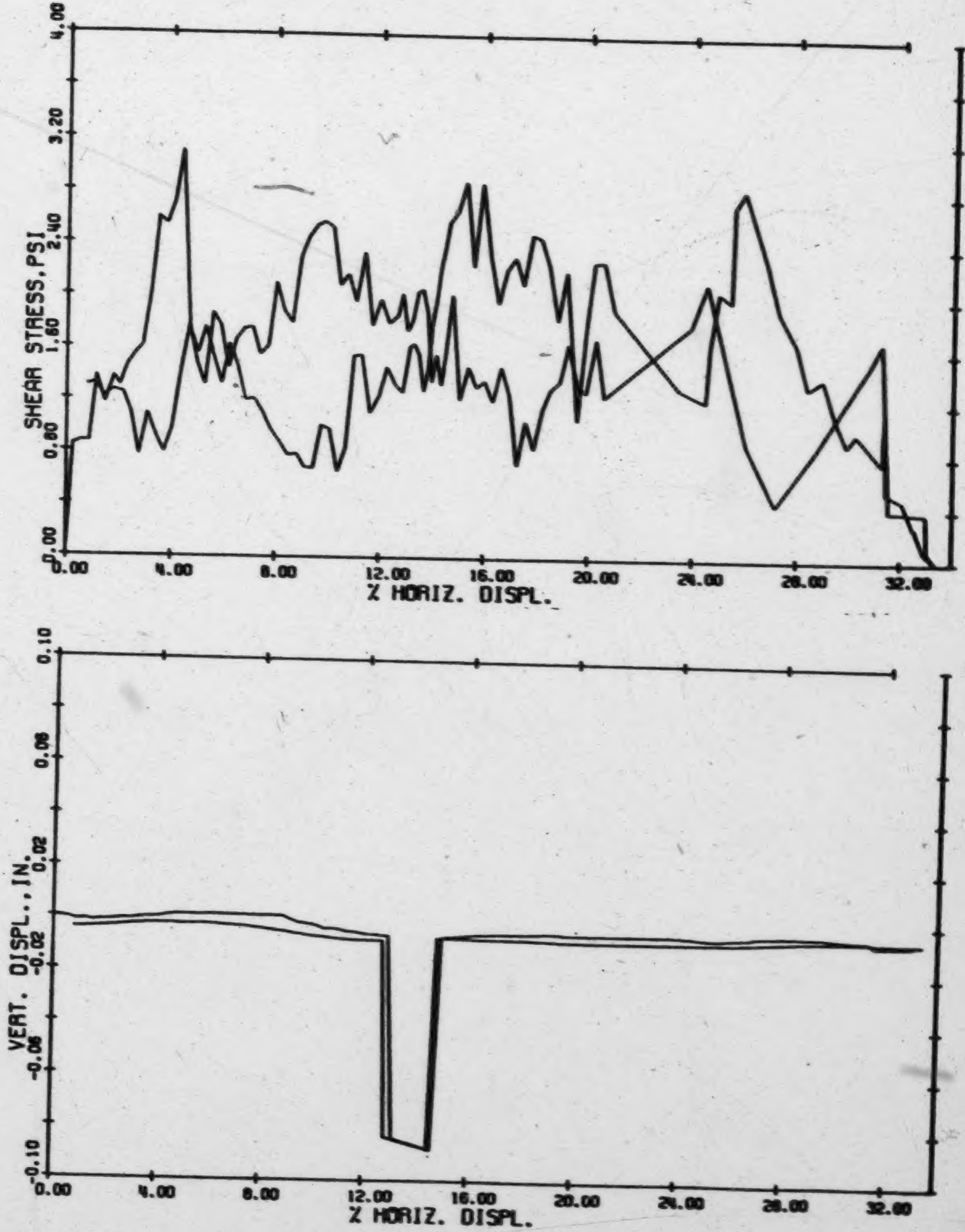

TEST 1-EC12-1, VERT. LOAD= 16.32*, AO=3.51SQ. INS.

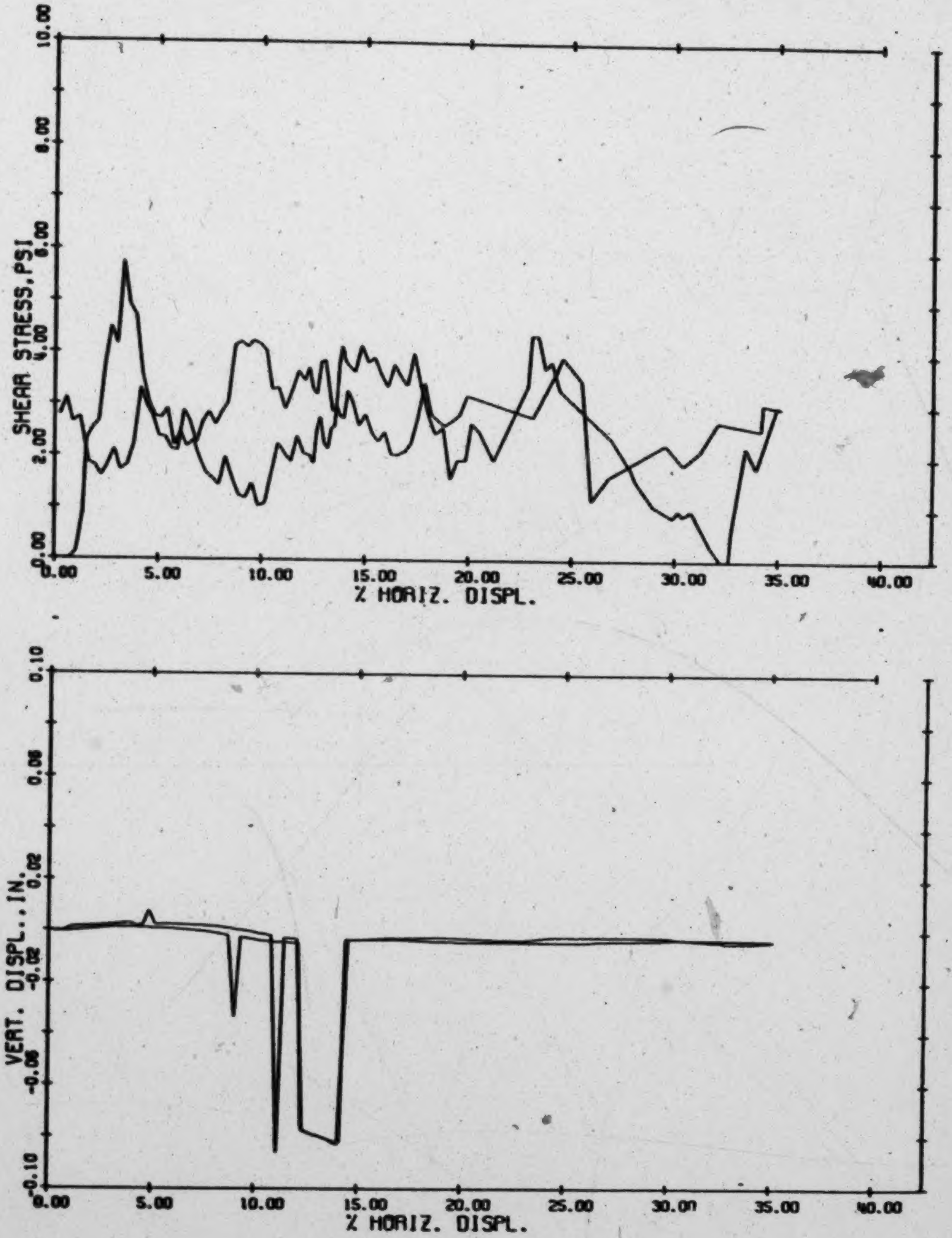

TEST 1-EC12-2, VERT. LOAD= 36.32#, AO=3.51SQ. INS.

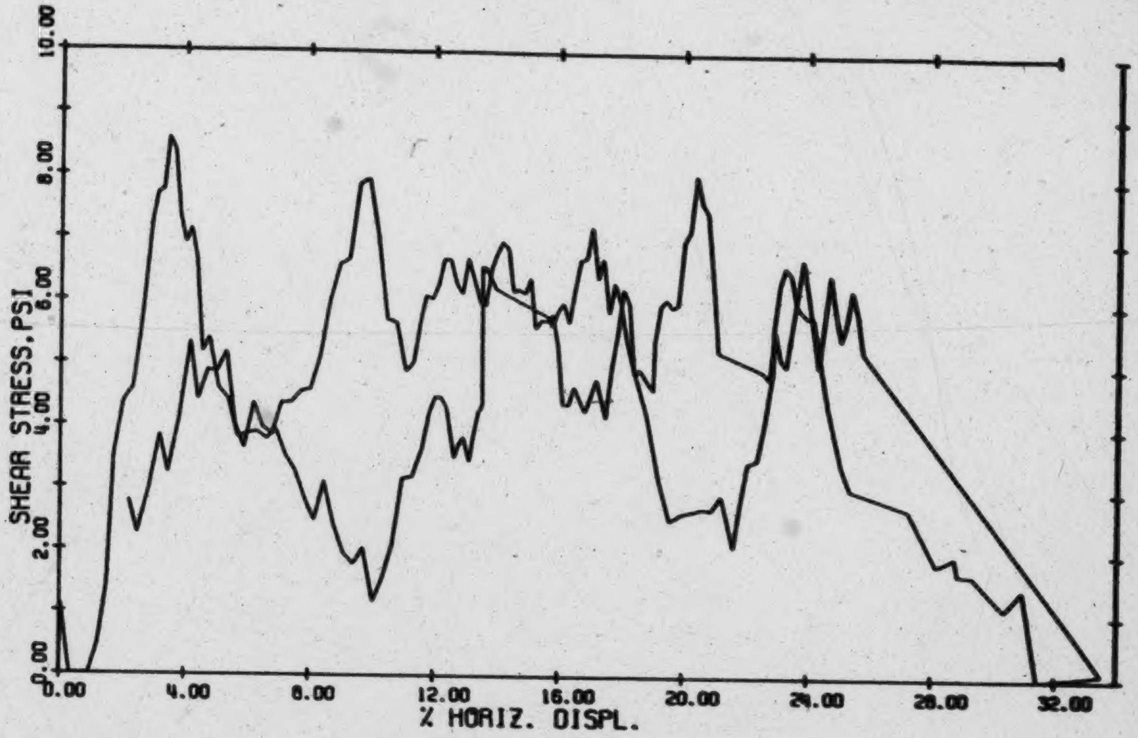

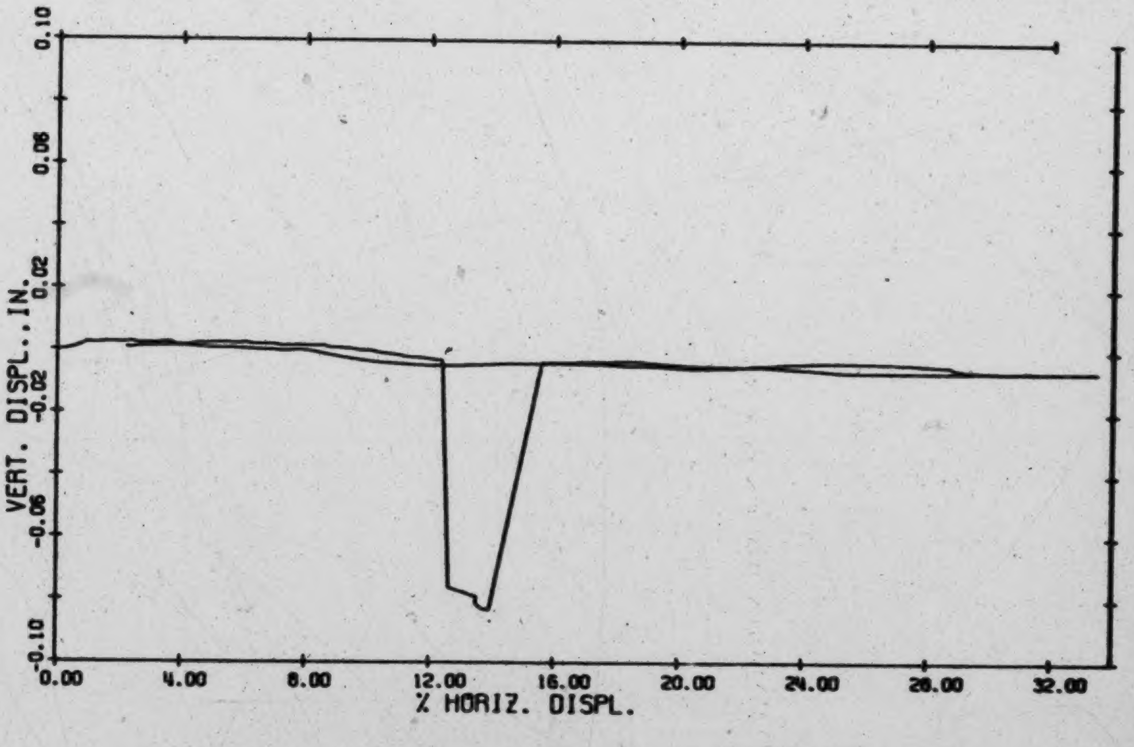

TEST 1-EC12-3,VERT. LOAD= 71.32#,AO=3.51SQ. INS.

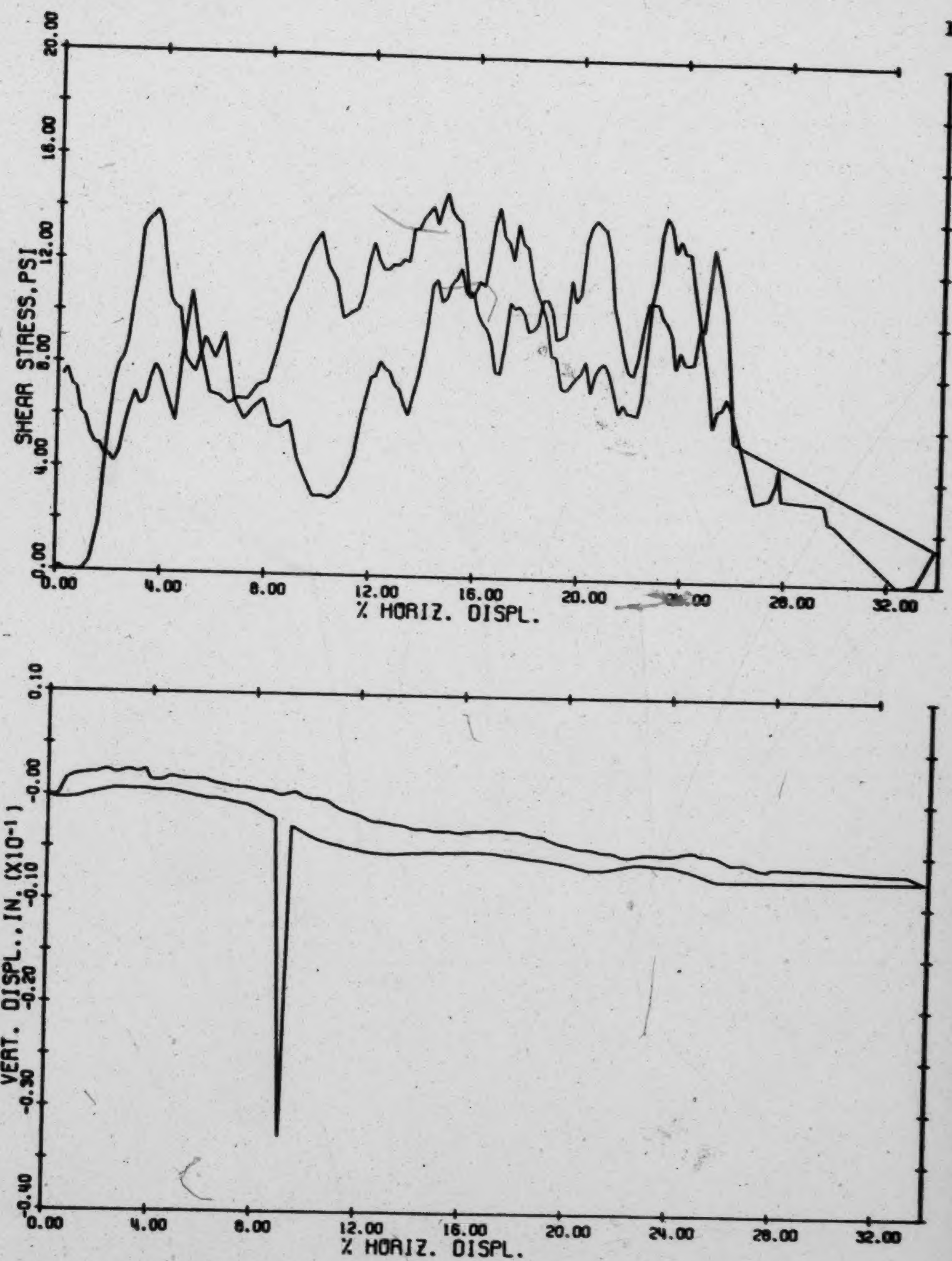

TEST 1-EC12-4, VERT. LOAD=136.32*, AO=3.51SQ. INS.

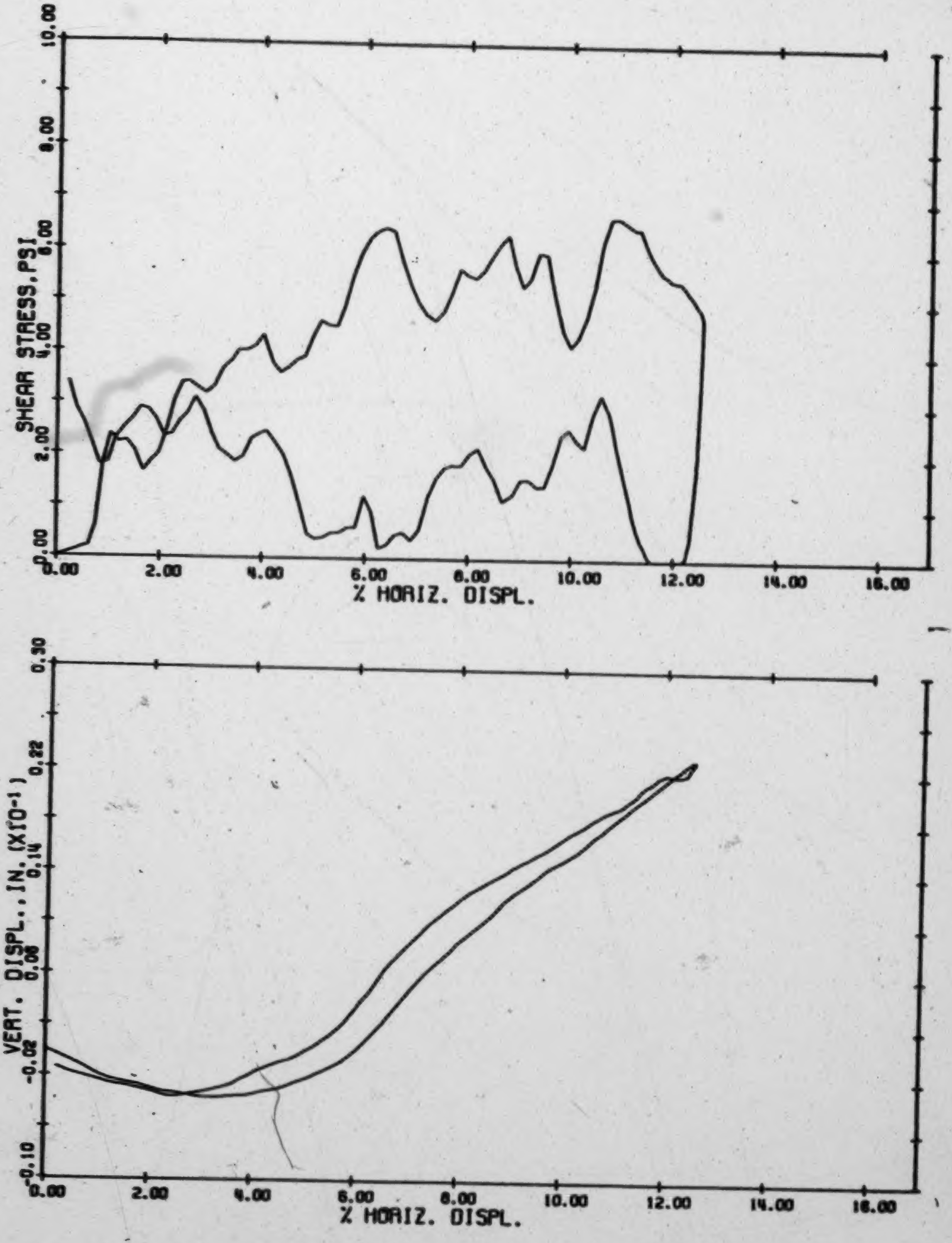

TEST BB12-4 ,VERT. LOAD=155.5#,A0=15.48 SQ. INS.

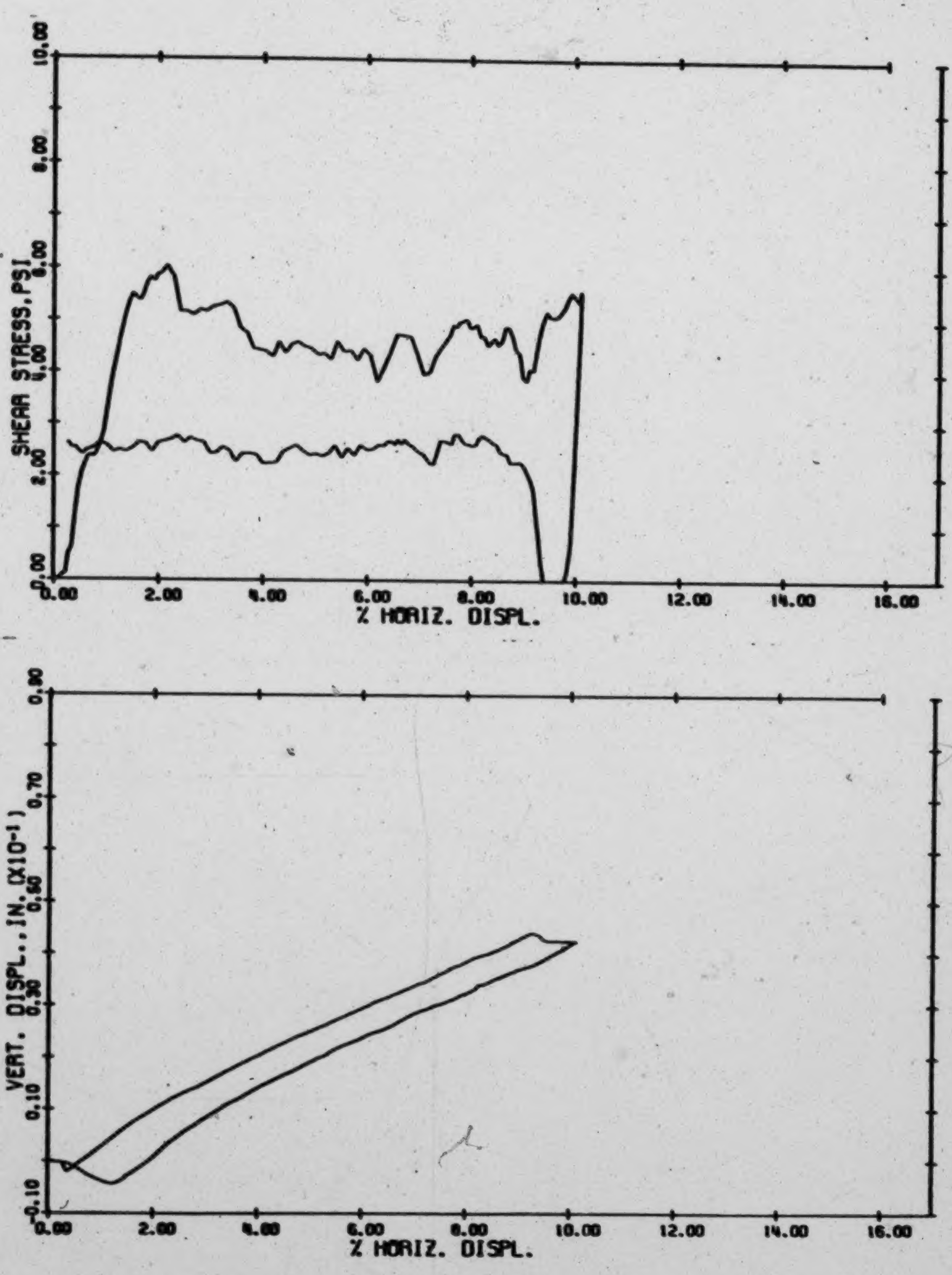

TEST BC3-2 ,VERT. LOAD= 98.6#,AO=19.52 SQ. INS.

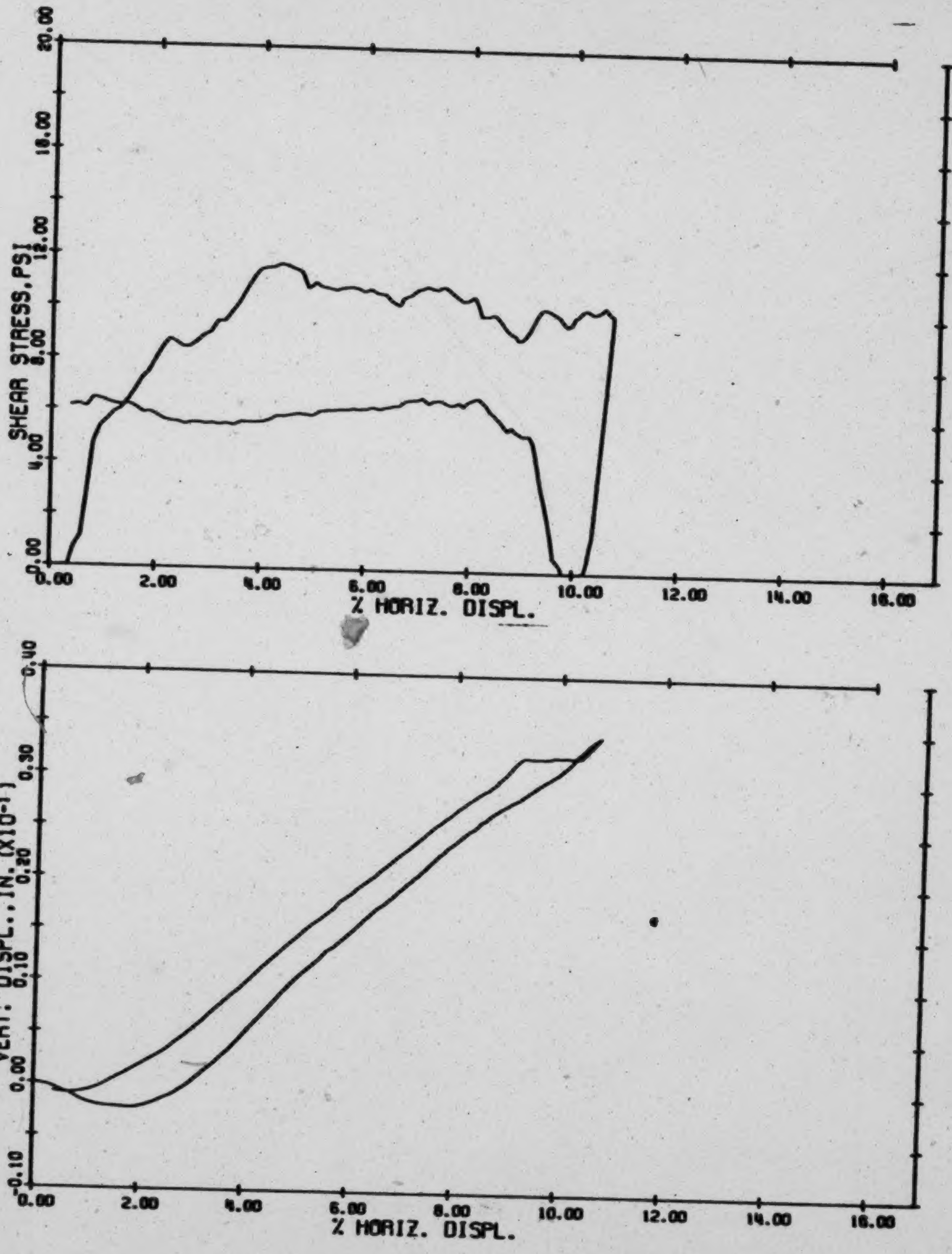

TEST BBS-1 ,VERT. LOAD=181.8#,AO=18.16 SQ. INS.

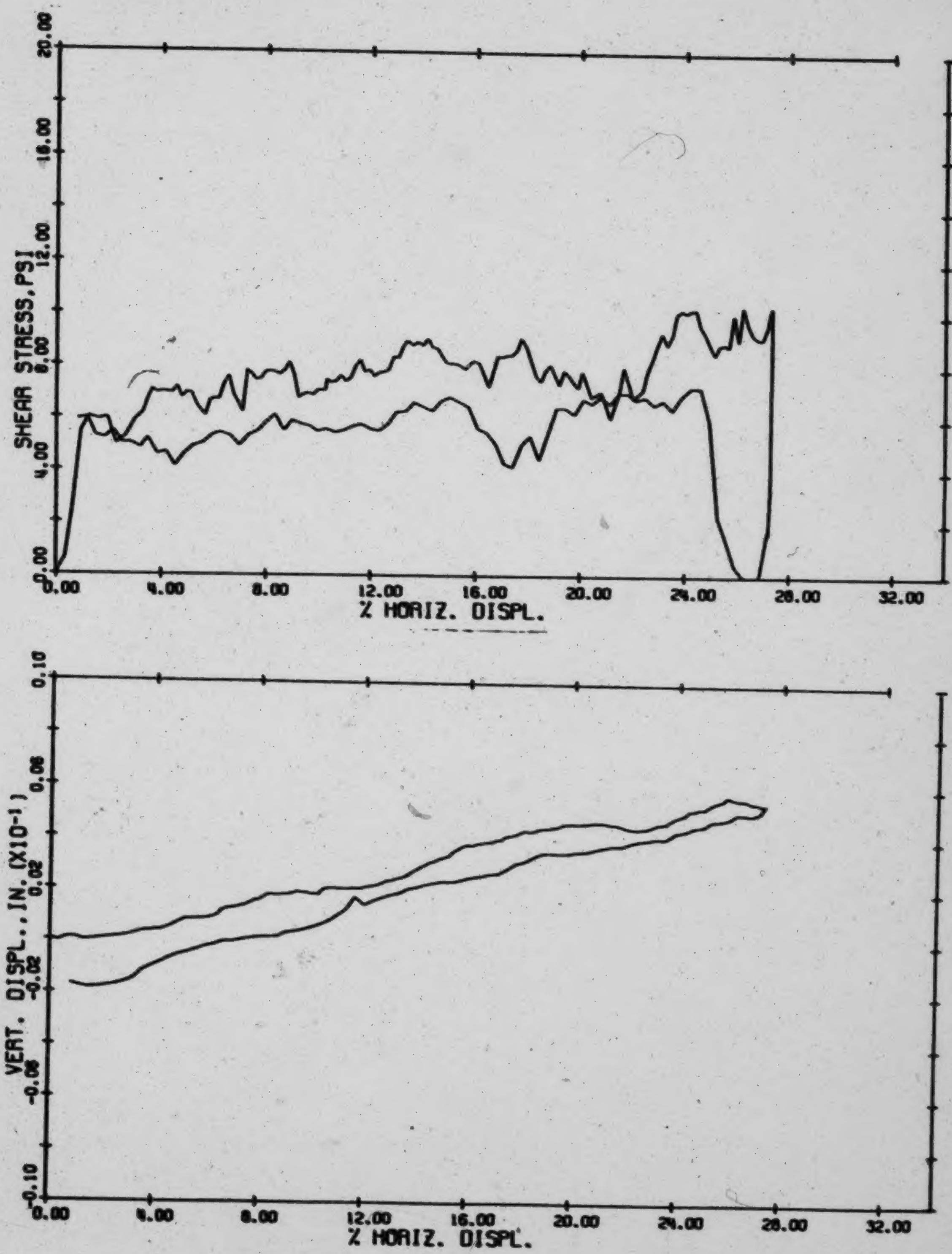

TEST ON 2-8814 WITH MOLYBDENITE REMOVED,N=30.2*

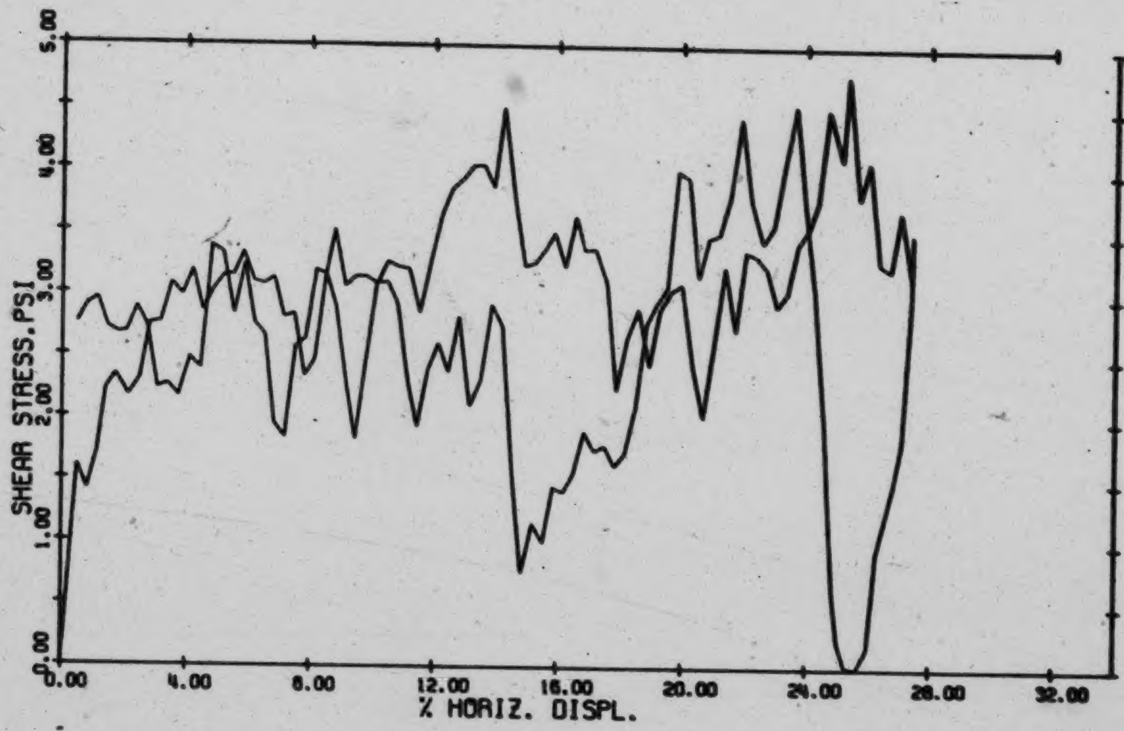

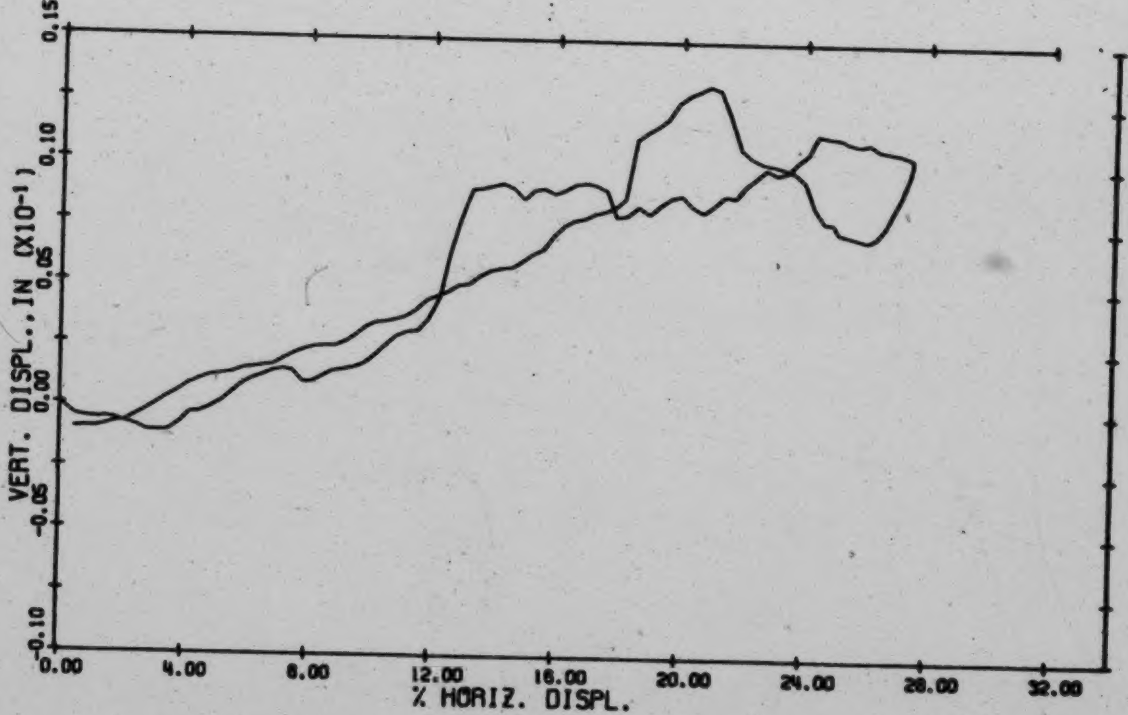

TEST ON 1-BB14 WITH UPPER BOX SUSPENDED, N=25.7*